UC Davis
Working Papers

Title

Summary of Construction Activities and Results from Six Initial Accelerated Pavement Tests Conducted on Asphalt Concrete Pavement Section for Modified-Binder Overlay

Permalink

https://escholarship.org/uc/item/59d8560n

Authors

Bejarano, Manuel O.
Morton, Bruce S.
Scheffy, Clark

Publication Date

2005-08-01

Peer reviewed

eScholarship.org Powered by the California Digital Library
University of California

DRAFT

Summary of Construction Activities and Results from Six Initial Accelerated Pavement Tests Conducted on Asphalt Concrete Pavement Section for Modified-Binder Overlay

Research conducted under Partnered Pavement Research Center Strategic Plan, Goals 4.1, 4.5, and 4.7

Prepared for:
California Department of Transportation

By:

Manuel Bejarano, Bruce Morton, and Clark Scheffy

Pavement Research Center
Institute of Transportation Studies
University of California Berkeley
University of California Davis
August 2005

EXECUTIVE SUMMARY

This report summarizes the activities and data collected during the construction of a pavement section used for investigating the performance of asphalt concrete pavements under accelerated pavement testing. This report also presents the preliminary results of six accelerated pavement tests conducted on the test section.

The pavement section was constructed in September 2001 at the Pavement Research Center, located at the University of California Richmond Field Station. The construction was performed by a highway contractor with the purpose of simulating highway paving operations. Under these conditions, the results from the tests can be translated into predicting the behavior of actual in-service pavements.

The pavement was composed of 90 mm of asphalt concrete, and 410 mm of recycled aggregate base on top of a prepared 200 mm subgrade. The layer thicknesses were designed according to Caltrans design procedures and checked using mechanistic methods to ensure limited rutting in the subgrade.

Preparation and construction of the subgrade, aggregate base, and asphalt concrete were completed according to Caltrans practice. Compaction of the asphalt concrete was controlled based on the maximum theoretical density of the mix.

Average in-situ relative densities for the subgrade and aggregate base were above 95 percent. Average air-void contents in the asphalt concrete layer were between 7 and 10 percent. Average thickness was 79 mm. Asphalt extractions from two samples indicated binder content by weight of aggregate of between 4.3 and 5.7 percent. The target binder content was 5.0 percent.

Deflection testing conducted during the construction of the pavement section showed the effect of the asphalt concrete layer on the behavior of the aggregate base and subgrade layers.

The asphalt concrete provided an increase in confining pressure, which created an increase in the modulus of the aggregate base, as well as an additional cover that reduced the stresses on the subgrade and created an increase in the modulus of the subgrade. The intensive FWD testing conducted on the pavement section also helped identify portions of the section susceptible to premature failure. These areas were subsequently rejected as locations for HVS test sections.

In general, FWD testing indicated that areas of soft subgrade translated into areas of soft or low aggregate base modulus. The FWD testing also revealed the effect of asphalt concrete modulus on the behavior of the aggregate base. The data indicated that aggregate base modulus increased with asphalt concrete modulus.

FWD testing also revealed the effect of temperature on the modulus of the asphalt concrete, which is typical of asphalt concrete layer and important for the interpretation of the performance of asphalt concrete mixes.

The Heavy Vehicle Simulator (HVS) was used to test the asphalt concrete under conditions of accelerated loading. HVS test sites were selected within the constructed test section to evaluate their performance. The results were compared in terms of fatigue cracking, rutting, and surface deflections. Results indicate that the sections tested during the dry/warm season lasted longer than those tested during the wet/cold season.

The performance of the sections seems to have been controlled by the behavior of the aggregate base. Elevated moisture contents in the aggregate base were recorded during the wet/cold months with corresponding FWD results which indicated high aggregate base modulus values for the same period. The results suggest that the modulus of the aggregate base is not a good indicator of performance.

The results of the HVS test sections are being used to analyze the performance of asphalt concrete pavements and to develop performance models for pavement life prediction as defined in Research Goals 4.1, 4.5, and 4.7 in the PPRC Strategic Plan for 2003/2004.

TABLE OF CONTENTS

LIST OF FIGURES

LIST OF TABLES

1.0 INTRODUCTION

This report is the first in a series of reports concerned with the Goal 9 Project (Strategic Plan Task 4.10). The overall purpose of Goal 9 is to investigate the reflection cracking performance of conventional asphalt concrete together with asphalt rubber and other modified binder mix overlays placed over cracked and/or jointed pavements and to develop tests, analysis methods, and design procedures to mitigate this distress mechanism.

The purpose of the test program described herein is to evaluate the performance of mixes containing a conventional asphalt and a number of modified binders subjected to accelerated load testing using the Heavy Vehicle Simulator (HVS). Laboratory fatigue testing of the mixes used in the accelerated pavement test program is included. This field/laboratory test program consists of two phases:

- Phase 1 (completed): included construction of a conventional asphalt concrete pavement consisting of a dense-graded asphalt concrete surface (DGAC), untreated aggregate base (AB), and untreated aggregate subbase (ASB) followed by six accelerated pavement tests using the HVS to induce fatigue cracking in the AC layer.
- Phase 2 (underway at the time of this writing): includes pavement of a series of mixes as overlays to rehabilitate the cracked test sections and subjecting these sections to HVS tests to evaluate rutting and cracking in the overlays. Sections include:
    1. a full thickness (90 mm) Dense Graded Asphalt Concrete (DGAC) overlay
    2. a half thickness (45 mm) Rubberized Asphalt Concrete Type G (RAC-G) overlay
    3. a half thickness (45 mm) Asphalt Concrete Type G-MB4 (RMB4) overlay (with an asphalt rubber binder meeting the requirements for grade MB4)

4. a full thickness (90 mm) Asphalt Concrete Type G-MB4 (RMB4) overlay (with an asphalt rubber binder meeting the requirements for grade MB4)
5. a half thickness (45 mm) Asphalt Concrete Type G-MB-15 (RMB-15) overlay (with an asphalt rubber binder with approximately 15 percent rubber)
6. a half thickness (45 mm) MAC-15 overlay (with an asphalt rubber binder with approximately 15 percent rubber)

In addition, laboratory tests are being conducted to evaluate and compare the properties of the overlay mixes, and to evaluate the effects of construction and mix design variables on their performance. Tests and analyses will include evaluation of fatigue response, rutting, and reflection cracking.

Results of the HVS testing and the laboratory testing are expected to provide 1) comparisons of the performance of the three modified binder (MB) products with ARHM Type G and DGAC control overlays; and 2) a measure of the effects of design thickness on performance of mixes containing the modified binders.

This report describes the results of the Phase 1 study including a summary of construction activities and the six HVS tests on the pavement prior to being overlaid. A timeline of these activities is provided in the following figure:

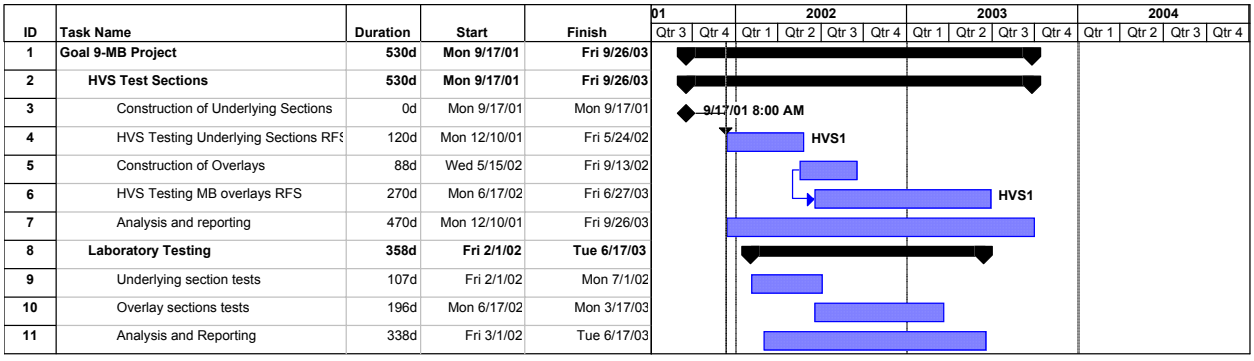

2.0 LAYOUT AND CONSTRUCTION OF THE TEST PAVEMENTS

The site for the project is located at the Pavement Research Center at the University of California Richmond Field Station (RFS). The site is located on Lark Drive between Avocet Way and Building 280. Figure 1 shows the location of the project. Figure 2 shows the layout of the HVS test sections at the test site.

The thickness for the pavement section was designed according to the Caltrans Highway Design Manual chapter 600 using the computer program NEWCON90 (*1*). Design thicknesses were based on a subgrade R-value of 5 and a Traffic Index of 7 (1.0 million ESALs). Design thicknesses are shown in Table 1.

Table 1 Design Thicknesses for Pavement Test Section

Pavement Layer	**Thickness, mm**
Asphalt Concrete	90
Aggregate Base	410
Recompacted subgrade	150

A limited mechanistic analysis was conducted to ensure that rutting from the subgrade rutting would be minimal under HVS trafficking. For the worst case conditions of soft subgrade and cracked asphalt concrete, subgrade deviator stress-to-strength ratios were estimated to be below 0.4 under the 40-kN load and below 0.5 under the 80-kN load. A subgrade deviator stress-to-strength ratio below 0.5 is considered to limit permanent deformation from the subgrade.(*2*) Actual stress-to-strength values may be lower than those estimated under the worst case scenario.

Gallagher and Burke, a local paving contractor, was selected to construct the test pavement. The project was constructed during the period September 14–24, 2001. Appendix A contains the bid document.

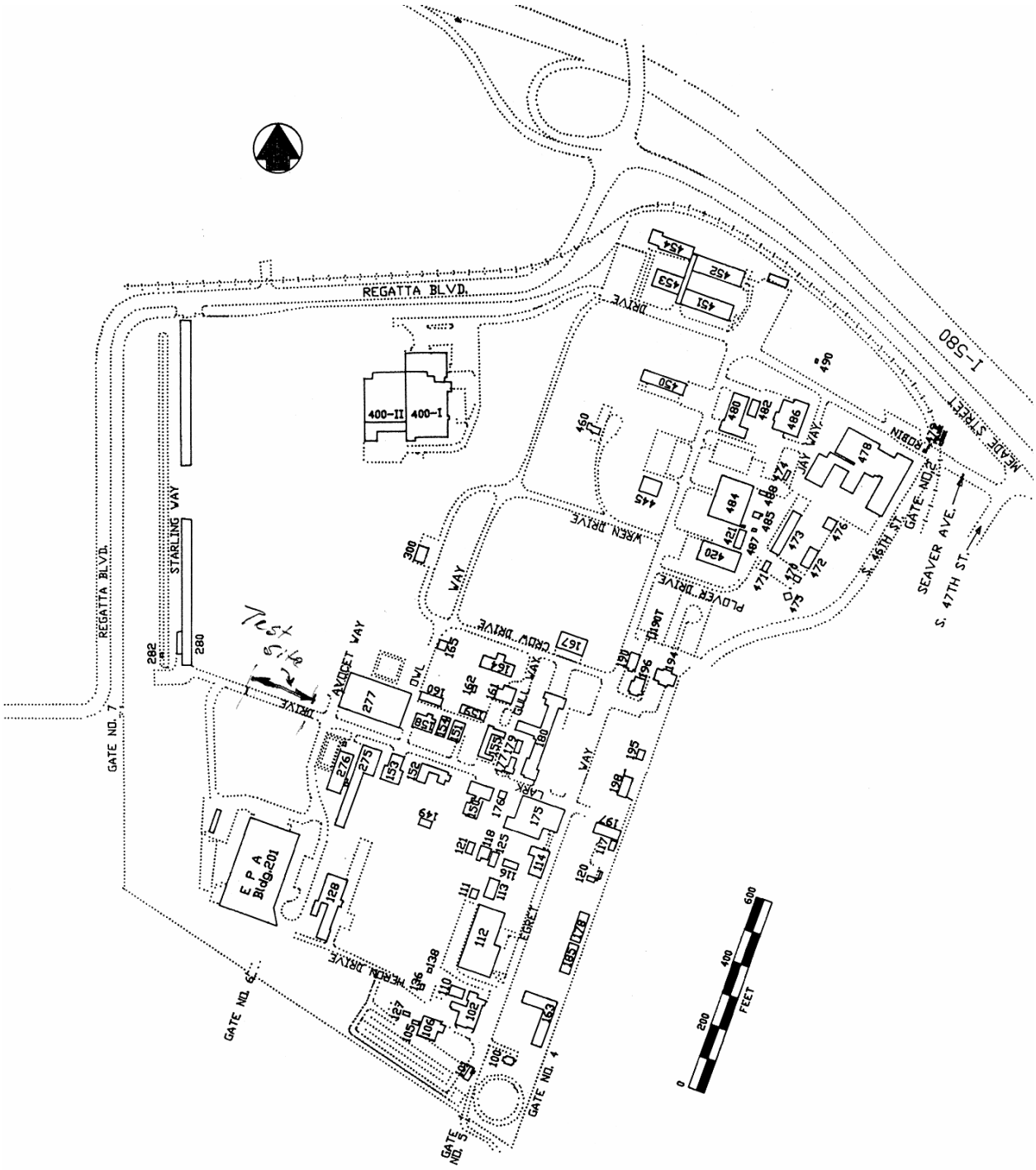

Figure 1a. Project location.

Figure 1b. Project location.

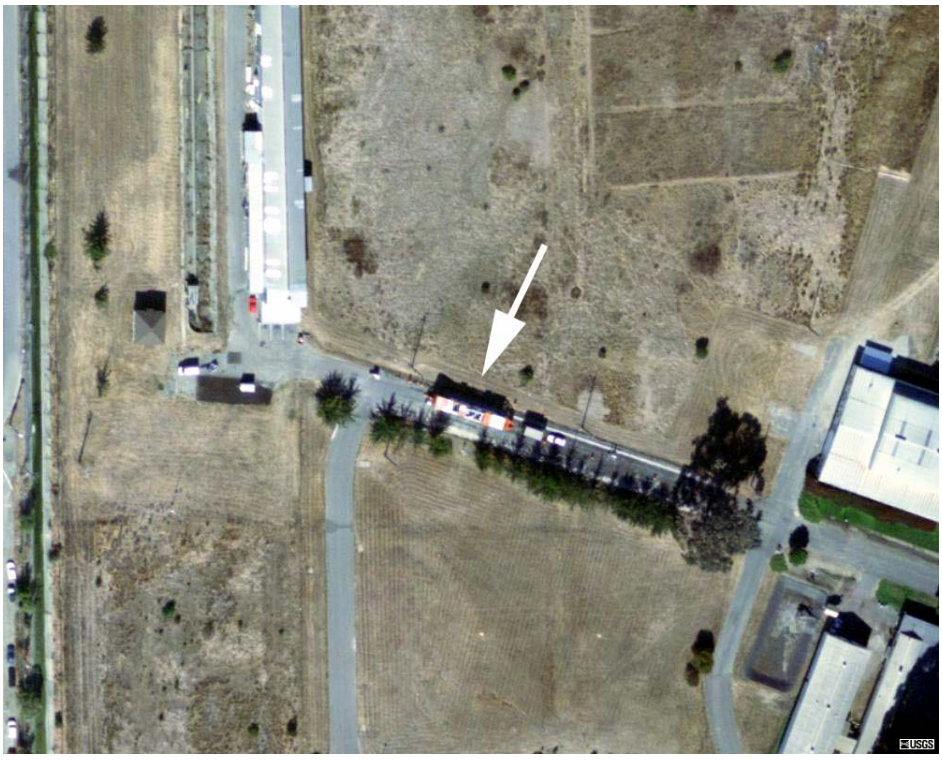

Figure 1c. Project location.

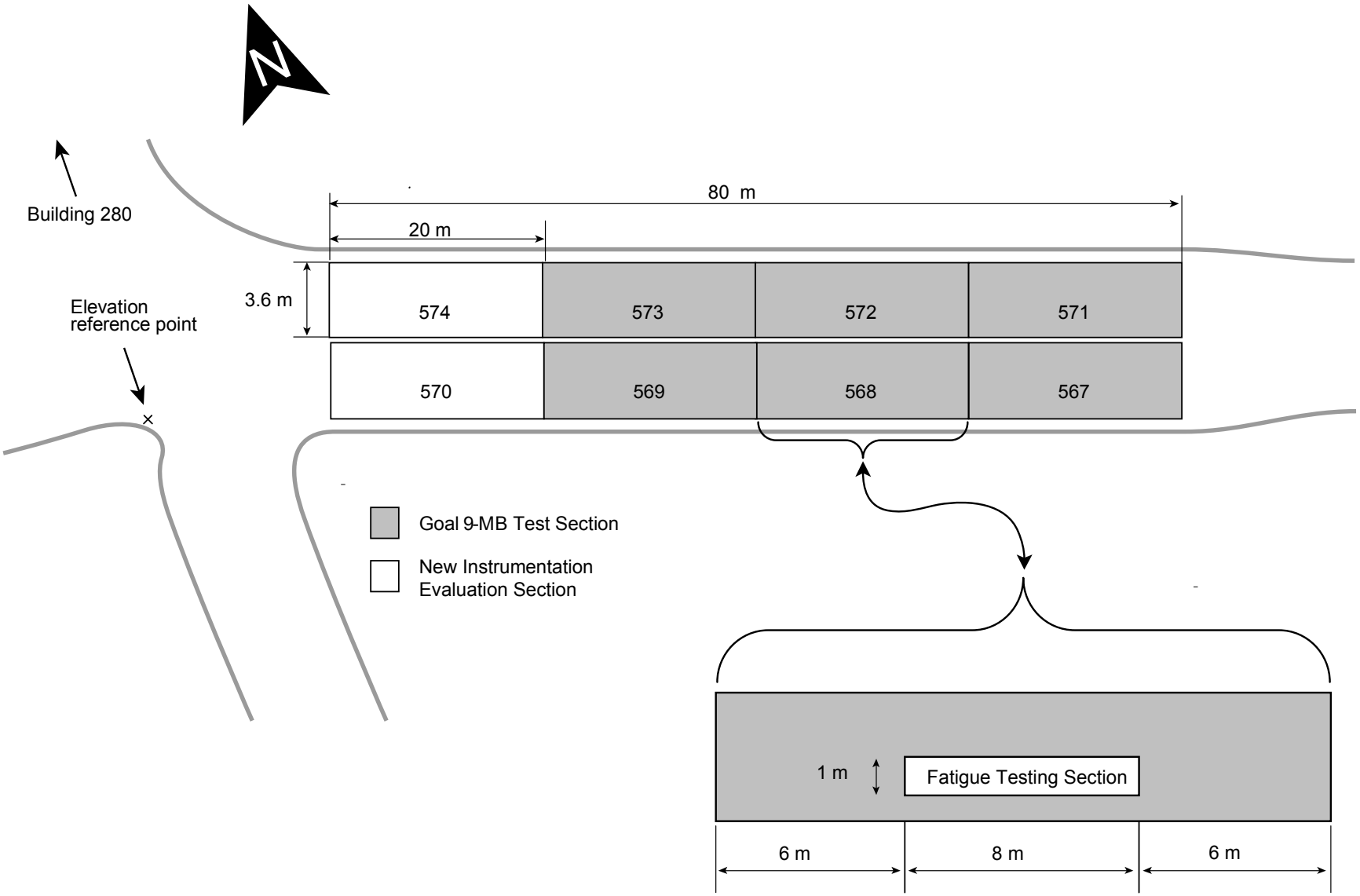

Figure 2. Layout of HVS test sections.

2.1.1 Staking of the Test Pavement

Construction staking of the test pavement was performed by Pavement Research Center (PRC) personnel. Stakes were located along the southern edge of the proposed test pavement at a distance of 3 m from the edge of the pavement at 15-meter intervals. Elevation of subgrade, edge of pavement, final grade elevation, and cross-slope of the test pavement were recorded on each stake. Additional stakes were placed to define the two taper sections at the ends of the test pavement and the positions of instrumentation.

2.1.2 Milling of Existing Aggregate Base and Asphalt Concrete

The existing aggregate base and asphalt concrete layer were milled to a depth of 250 mm, which removed all material to the surface of the subgrade. The ends of the pavement (25 m in length) were tapered to a thickness of 100 mm to remove the existing asphalt concrete (AC), leaving the existing aggregate base (AB) and subgrade in place.

2.1.3 Subgrade Compaction

Following the milling operation, the subgrade was scarified to a depth of 150 mm. Its water content was then modified and remixed to improve workability. The subgrade was graded to uniform cross-slope of 2 percent, compacted with a sheepsfoot roller, and finished with a 20-ton steel wheel roller to remove the surface irregularities formed by the sheepsfoot roller. Relative compaction of the subgrade was determined from field wet densities obtained using a nuclear device and the laboratory maximum wet density of the subgrade according to California Test Methods (CTM) 231 and 216, respectively.(*3*)

The test results indicated the relative compaction did not meet Caltrans specification of 95 percent.(*4*) This was likely due to a water content of approximately 2.5 percent below the

optimum according to CTM 216. To improve the degree of compaction, the subgrade moisture content was adjusted, and it was reworked to a depth of 200 mm and recompacted. This resulted in relative compaction of 97 percent. To limit hauling of in-situ material, the cross slop of the subgrade was increased to 2.25 percent.

2.1.4 Drainage Construction

Although the existing access road had drainage ditches, these were inadequate and poorly maintained. Accordingly, drainage ditches were constructed along each edge of the pavement. Realignment and widening of the road also required the construction of an additional drainage system. This was accomplished by replacing the existing drainage pipe under the road with a larger pipe on a new alignment of the drainage ditch.

2.1.5 Instrumentation of Subgrade

Following compaction of the subgrade soil, seven Time Domain Reflectometers (TDRs) and five pressure cells were installed in the subgrade. The description and locations of these instruments within the test pavement are included in Appendix B.

Six TDRs were placed horizontally at a depth of 50 mm below the subgrade surface while one TDR was positioned vertically at a depth of 200 mm below the subgrade surface. The TDRs were compacted in place using a hand tamper and the wires taken to the edge of the shoulder, and then buried in the subgrade layer to protect them from being damaged by the aggregate trucks and the larger aggregate particles of the compacted base material.

Soil pressure cells were installed in excavations approximately 75 mm in diameter to limit disturbance of surrounding material (Appendix B). The wires for the pressure cells were buried in the subgrade in the same manner as for the TDRs. After installation was complete, the

wires protruding from the edge of the shoulder were sealed in waterproof bags and buried in the shoulder material to protect the instrumentation from moisture and to prevent accidental damage during construction of the aggregate base and asphalt concrete layer.

2.1.6 Aggregate Base Compaction

The aggregate base was constructed from material supplied by the Dutra Materials plant in San Rafael, California in a uniform thickness of 410 mm along the 80-m length of the test sections. The base was placed in three lifts of 150, 150, and 110 mm to achieve a relatively uniform material. Base thickness was varied in the taper sections in order to link the test pavement elevation with the existing pavement elevations.

The base material was compacted at the optimum water content for the maximum wet density according to CTM 216 using a steel drum vibratory roller. Nuclear density testing (CTM 231) was performed on the second and final lifts in order to ensure that Caltrans compaction requirements for Class 2 aggregate base were met. The resulting average relative compaction of the aggregate base was 97.0 percent in the second lift and 98.6 percent for the third lift.

2.1.7 Instrumentation of the Aggregate Base

TDRs and pressure cells were installed during construction. In order to facilitate installation and to limit stand-by time of the contractor, these instruments were positioned at elevations corresponding to the lifts of the aggregate base. Details are contained in the design specifications and bid documentation (Appendix A). A total of seven TDRs were installed during the construction of the aggregate base: six were installed after the first lift and one was installed after the second lift. Positions and locations of the TDRs are shown in Appendix B.

Of the five pressure cells that were installed in the aggregate base, only one pressure cell, designated PC 7 (Appendix B), was installed during the construction of the aggregate base. Due to the increased time required to install pressure cells, those located within 150 mm of the surface of the aggregate base layer were installed after construction of the aggregate base.

The wires of the pressure cells and TDRs installed in the aggregate base were installed and protected in the same manner as those of the subgrade (Section 4.2.4).

After completion of the instrumentation of the aggregate base, Heavy Weight Deflectometer (HWD) testing was performed on the aggregate base. These data have been used to back-calculate the moduli of the pavement layers.

2.1.8 Priming of the Aggregate Base and Installation of Strain Gages

The aggregate base was primed two days prior to paving using a CS-70 binder and the area was closed to traffic. CS-70 was used as a prime for the aggregate base. Once priming was completed, asphalt concrete strain gages were installed in their respective positions using the method specified by the instrument manufacturers. A sand asphalt hot mix was used to secure the strain gages in position and the leads were run to the edge of the shoulder where they were bagged and buried in a similar method to that used in the installation of the pressure cells and TDRs (see Section 4.2.4).

2.1.9 Mix Design

The asphalt concrete (AC) mix design as specified in the bid documentation (see Appendix A), was a 19 mm maximum, medium coarse type A dense graded asphalt concrete with an AR-4000 binder. The mix design, submitted by Dutra Materials, utilized an asphalt content of 5 percent (aggregate basis).

The Theoretical Maximum Specific Gravity of the asphalt concrete mix was 2.462. A binder content of 5 percent per mass of aggregate was selected for the AC. The aggregate source was the Dutra San Rafael Quarry with a blend of sand from Tidewater.

2.1.10 Paving Operation

The AC was placed in two lifts of 45 mm each with a paving width of 3.7 m. Each lift was compacted using a steel drum roller. Density was controlled by means of nuclear density testing. As stated in the bid documentation, the degree of compaction was required to be in the range 92 to 95 percent (air-void content of 5-8 percent) of the theoretical maximum density (California TM 309).

During the paving of the first lift, asphalt concrete was removed from the skip of the paver and spread evenly in a thickness of approximately 20 mm over the strain gages and tamped in place using a hand tamper. The leads of the strain gages were also covered with AC to prevent possible damage to the cords by the paver.

After the first lift was placed and compaction of the AC was accepted, an asphalt emulsion was applied to the surface of the first AC lift. The second lift of AC was then placed and compacted. Some segregation was noticeable at certain locations (most notably at the side of the test pavement adjacent to Building 280) in this layer; fortunately, this occurred outside of the planned HVS testing area.

Average air-void contents in the asphalt concrete were 9.7 and 10.3 percent for the first and second lifts, respectively.

2.1.11 Full Depth Patching

Two days after completion of the test pavement, failure was observed near the edge of the pavement near Test Section 574. The probable reason for this failure was high moisture content in the aggregate base.

Due to the large number of trucks making use of this entrance, the contractor was instructed to patch this section of road. The new 90-mm DGAC layer was removed and the aggregate base re-mixed and allowed to dry before compaction. A 150-mm thick DGAC patch was then paved and compacted to complete the repair.

2.1.12 Shoulder Backing and Completion of Instrumentation

Once the asphalt concrete patch had been placed, the shoulder backing was completed by hand to avoid disturbing the instrumentation cables present in the aggregate base shoulder. Following construction, the buried instrument leads were exposed in the shoulders of the test pavement, combined at each location of instrumentation, bagged, and secured to stakes. This operation was performed to place the ends of the instrument leads above the water level to protect them from moisture damage during potentially heavy rains.

3.0 PRELIMINARY MATERIAL TESTING

A number of tests were conducted during and after construction of the pavement test section to characterize the pavement materials and the subgrade.

3.1 Air-Void Content and Thickness of Asphalt Concrete Layer

Nuclear density measurements and extracted cores were obtained to determine the air-void content distribution in the asphalt content layer after construction. The data were also used to establish a relationship between nuclear test and laboratory test air-void contents. Laboratory air-void contents were determined on extracted cores according to Caltrans 308 and AASHTO T-166 test procedures at locations where nuclear readings were obtained. Acceptance was based on AASHTO T-166 test results. Figure 3 shows the relation between Caltrans 308 and the nuclear device air void data to AASHTO T-166 air void data. As shown in the figure, the average measured air-void content difference between AASHTO T-166 and the nuclear device was 4.6 percent.

Figure 4 shows a relative frequency and cumulative histogram for the asphalt concrete air-void content in the dense graded asphalt concrete. A wide range of air voids with more than one peak value is evident in Figure 4. More than one data distribution can be found over the range of measured air voids. This may be due to the presence of segregated areas on the asphalt concrete mat observed during construction. These areas were primarily caused by the asphalt mix in the hopper of the paver cooling while waiting for the next truck to deliver hot asphalt concrete mix to the site. Because the cooled mix in the paver was not completely remixed with the new hot mix, proper compaction of the cooled mix was not possible. As a result, some areas have high air voids. These segregated areas were excluded from consideration when selecting the sub-sections for accelerated pavement testing.

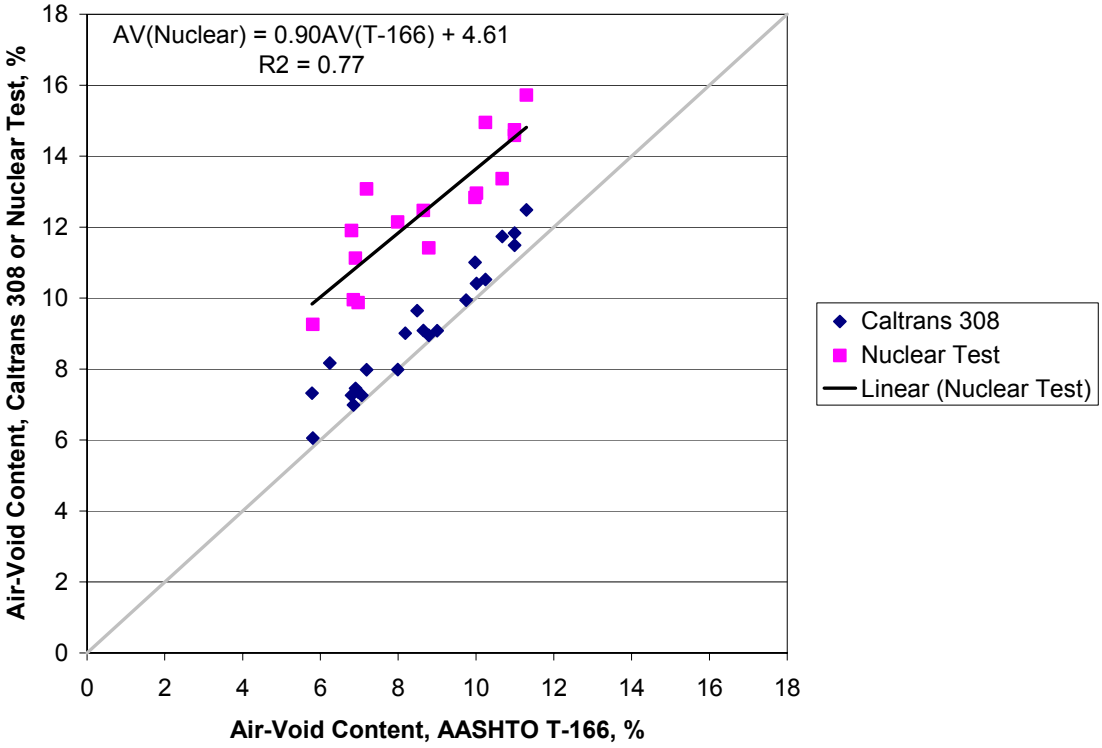

Figure 3. Relationship between Caltrans 308 and nuclear device air-void content measurements to AASHTO T-166 air-void content measurements.

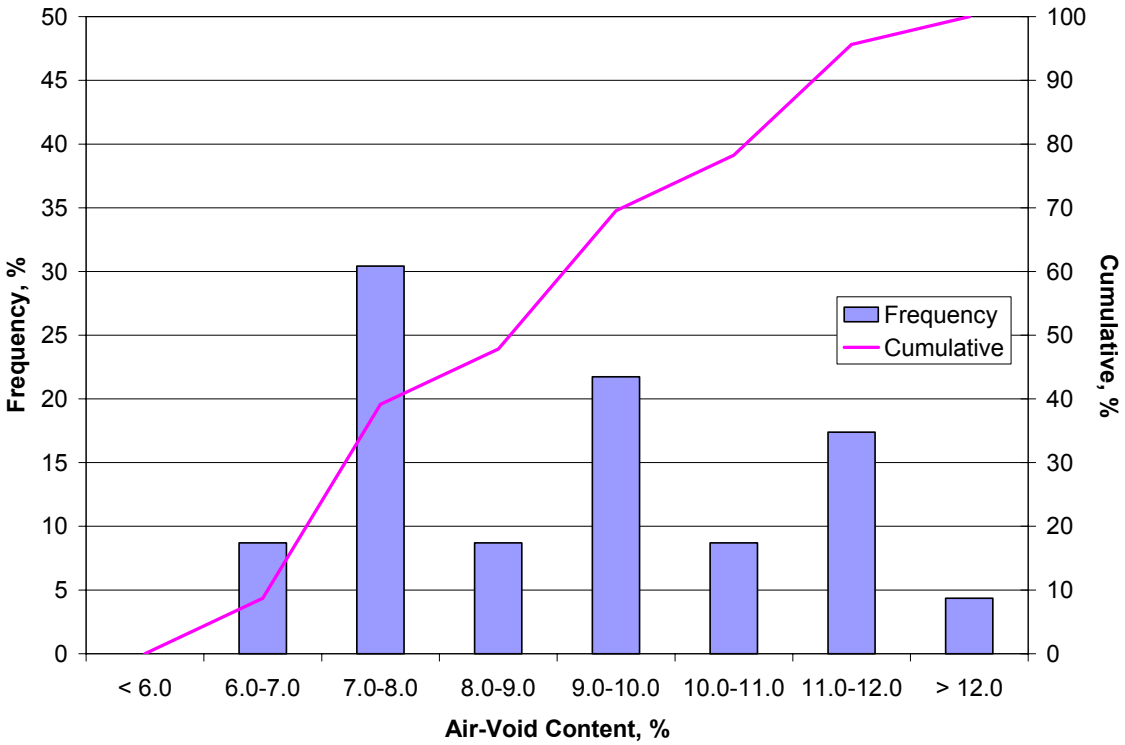

Figure 4. Air-void content relative frequency and cumulative histogram.

The distribution of air voids along the project is critical for the evaluation of the accelerated pavement tests since the air void contents of the mixes have a significant impact on the fatigue performance of asphalt concrete layers. The average air-void content in the compacted asphalt concrete layer was 9.1 percent with a standard deviation of 1.8 percent. This average excludes air-void contents in the segregated areas. Figure 5 shows the distribution of air voids in the pavement section based on AASHTO T-166. The distribution of air voids in the mix indicates that high air-void contents were usually obtained near the shoulder.

Extracted cores also were used to determine the distribution of asphalt concrete thickness along the test section. Figure 6 shows the relative frequency and cumulative histogram for the asphalt concrete thickness. The data show that about 76 percent of the asphalt concrete cores are between 70 to 90 mm thick. The average thickness along the pavement section was 79.0 mm with a standard deviation of 9.9 mm. The design thickness for this project was 90 mm.

Figure 7 shows the distribution of the pavement thicknesses across the whole section. Distribution of thickness along the project can also influence the fatigue and rutting performance of the test sections. An increase in pavement thickness increases the service life of the pavement by reducing the tensile strain at the bottom of the asphalt concrete, thereby increasing the fatigue performance of the asphalt concrete. Increased thickness also reduces the state of the stresses in the unbound layers, which improves the rutting performance of the granular base and subgrade.

3.2 Asphalt Extraction and Gradations

Asphalt binder extractions and aggregate gradations were obtained from two loose mix samples to check in-place mixtures. The binder contents of the samples were 4.34 and 5.69 percent (aggregate basis). Target binder content was 5.0 percent. Figure 8 summarizes aggregate

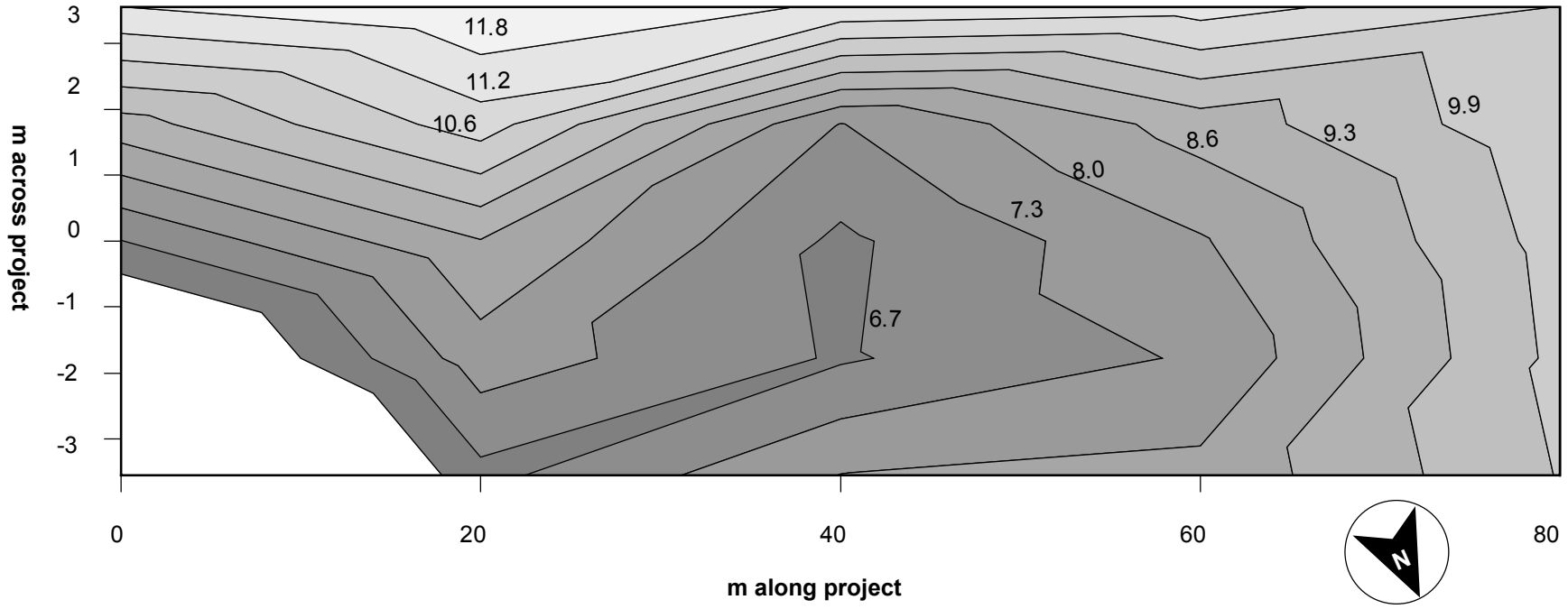

Figure 5. Air-void distribution in asphalt concrete layer along the project.

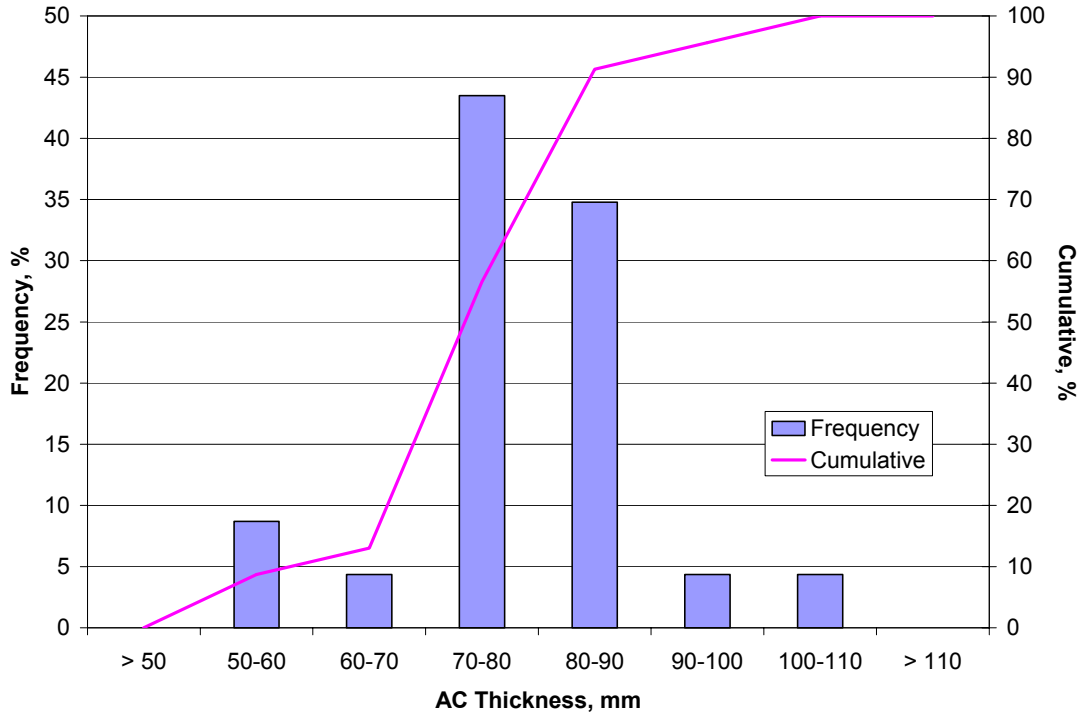

Figure 6. Relative frequency and cumulative histogram for AC thickness.

gradations for the two samples and for the mix gradation used in the mix design. Sample 1 appears to be within the specification but sample 2 seems to be slightly finer than the specification. There is not enough information to perform a statistical evaluation of the impact of binder content and mix gradation on the performance of pavements. However, these two parameters may have an influence on air-void contents of the compacted mix.

3.3 Dynamic Cone Penetrometer Testing of Unbound Materials

Figure 9 summarizes Dynamic Cone Penetrometer (DCP) tests in terms of DCP penetration rates in the aggregate base and subgrade along the pavement section. These were obtained after construction of the aggregate base and asphalt concrete layers. DCP tests were performed at the same 17 locations where AC cores were extracted. Average penetration rates

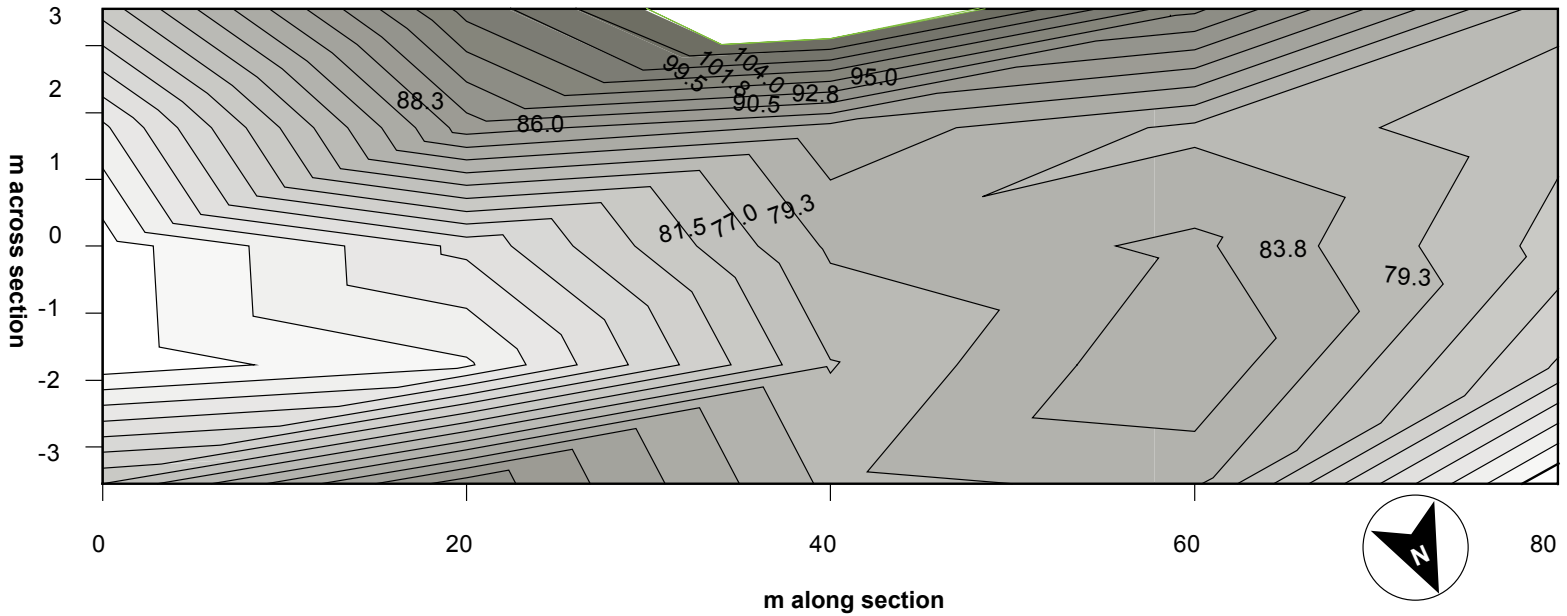

Figure 7. Distribution of asphalt concrete thickness across pavement section.

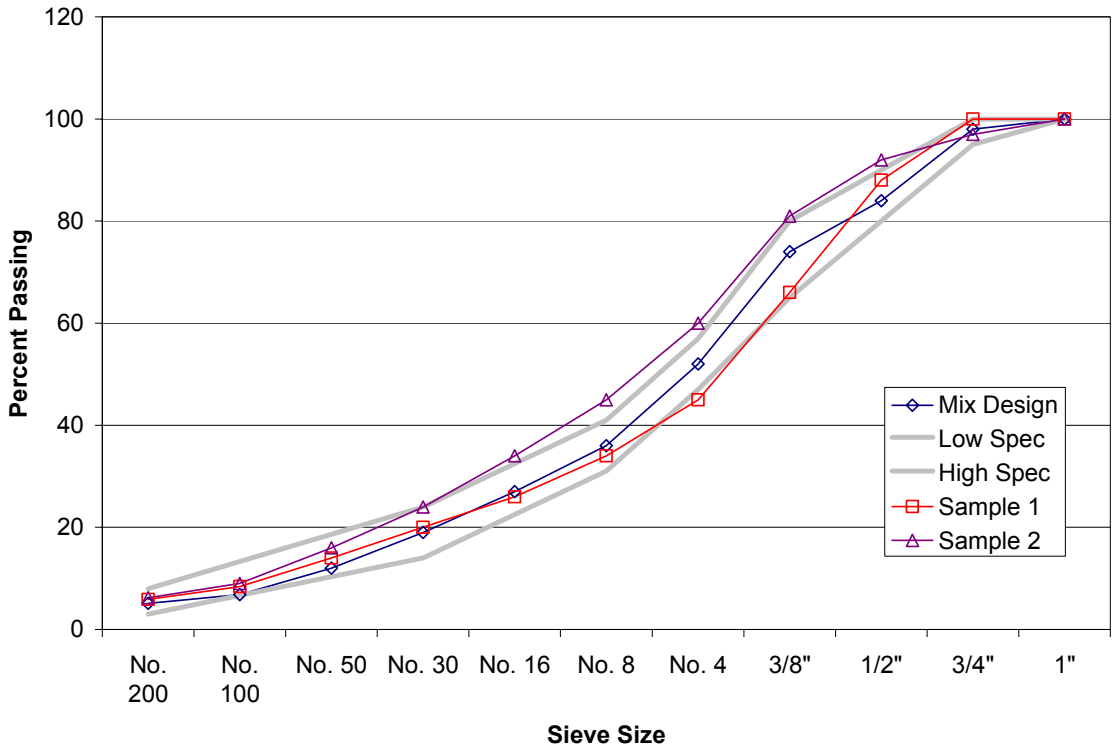

Figure 8. Asphalt concrete mix gradations.

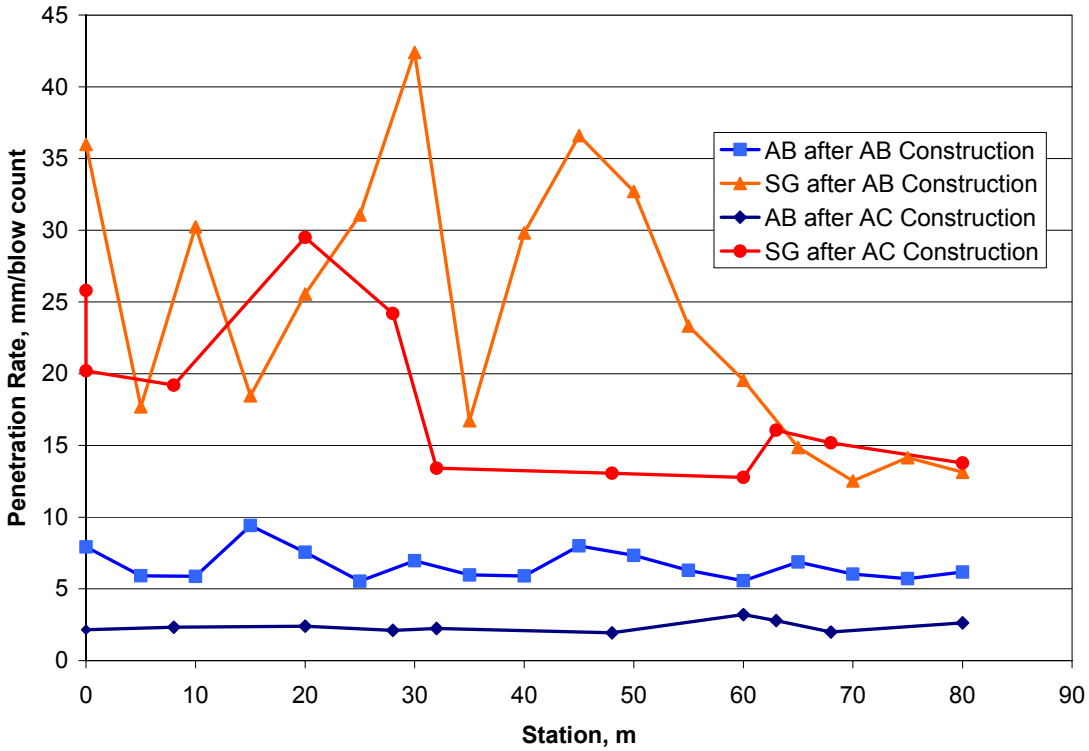

Figure 9. DCP data for unbound materials.

for the aggregate base and subgrade before placing the asphalt concrete were 6.4 and 23.4 mm/blow with standard deviations of 1.0 and 9.0 mm/blow. After placing the asphalt concrete layer, the average penetration rates in the aggregate base and subgrade were 2.4 and 17.8 mm/blow with standard deviations of 0.4 and 5.4 mm/blow.

The DCP tests obtained after the asphalt concrete layer was placed were conducted five months after completion of the project. The decrease in penetration rates over this period indicate a significant strengthening of the aggregate base over time. Strengthening of the subgrade is observed at most test locations, with dramatic increases observed near stations 30 and 45. Increased strength of the subgrade may have resulted from compaction occurring during construction.

Aggregate base thicknesses along the pavement section were estimated from DCP data at the point where the slopes of the penetration rates of the aggregate base and subgrade intersect. The average thickness of the aggregate base is 375 mm with a standard deviation of 47 mm (design thickness is 410 mm). Figure 10 shows aggregate base thickness along the pavement section. The data indicate a difference between the thickness obtained before and after placing the asphalt concrete. The results are not conclusive at this point because they were obtained at different locations.

3.4 Unbound Materials Classification

The aggregate base (AB) met gradation specifications for aggregate base Class 2. While visual evaluation of the material indicated that it contained more than 50 percent recycled material including pieces of used bricks, asphalt concrete, and portland cement concrete (upper limit of 50 percent for Class 2 material), subsequent lab testing showed that the material met or exceeded the requirements for Class 2 AB.

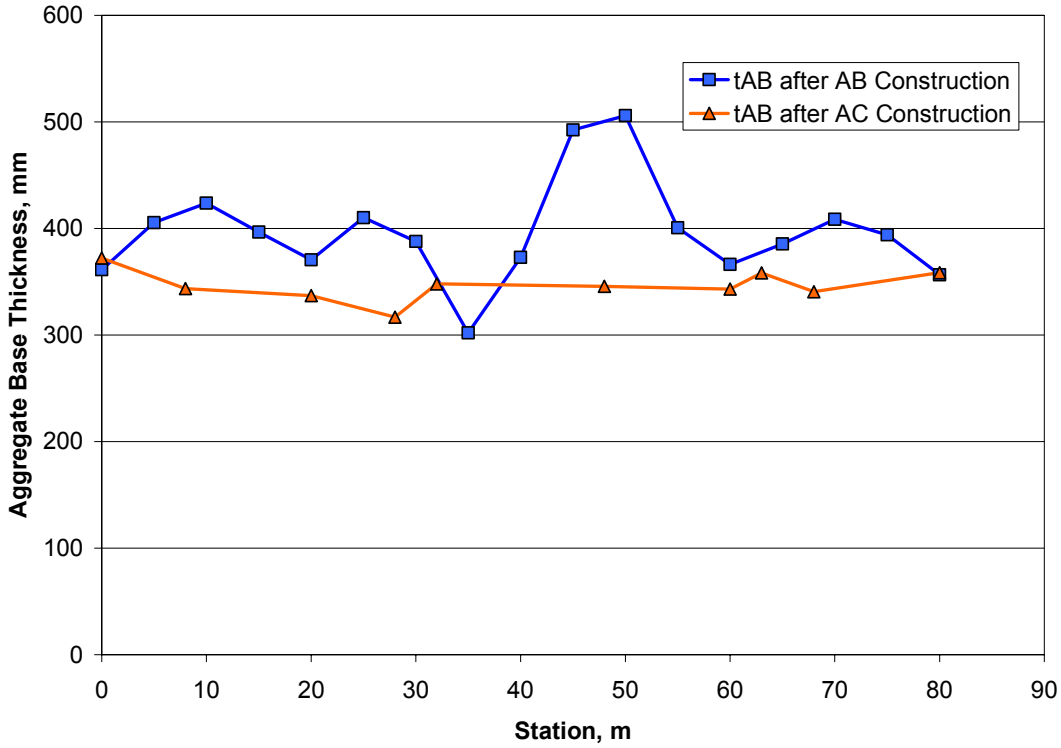

Figure 10. Thickness of aggregate base estimated from DCP measurements.

The subgrade, a dark brown clay, is classified as a lean clay (CL) with Atterberg limits as follows: 1) liquid limit, 38 to 42 percent, and 2) plasticity index, 20 to 27.

3.5 Falling Weight Deflectometer Tests

FWD testing was conducted at various stages during construction to study the effect of the subsequent overlay on the behavior of the pavement. This included tests on the consolidated subgrade, aggregate base, and asphalt concrete layers. FWD tests were conducted along 5 lines of testing parallel to the roadway centerline:

Location	Description	
1.3 S	along a line 1.3 m south of centerline	} south lane
2.3 S	along a line 2.3 m south of centerline	
CL	along centerline	
1.3 N	along a line 1.3 m north of centerline	} north lane
2.3 N	along a line 2.3 m north of centerline	

Moduli of the pavement layers were calculated from deflections using the back-calculation program ELMOD 5.0 (*5*), a program using Odemark's transformation of a layered system and Boussinesq's equations.

3.5.1 FWD Testing on the Subgrade during Construction

Results of FWD tests on top of the cohesive subgrade are not included since shear failure occurred in the subgrade under the loading plate.

3.5.2 FWD Testing on the Aggregate Base

FWD testing was conducted on top of the aggregate base using 22.2- and 40-kN loads. Back-calculated moduli under the 40-kN load for the aggregate base and subgrade are presented in Figures 11 and 12, respectively. Significant variability was observed in the moduli of both layers. The average modulus for the aggregate base was 125 MPa with a standard deviation of 48 MPa, while the average modulus for the subgrade was 38 MPa with a standard deviation of 25 MPa. Relative frequency and cumulative histograms for moduli of the aggregate base and subgrade are presented in Figures 13 and 14, respectively. At this stage, the calculated modulus of the aggregate base is lower than representative values for similar California aggregate base materials. The smaller value is likely due to absence of confinement provided by the AC surface course.

3.5.3 FWD Testing on the Asphalt Concrete

FWD testing was conducted on the surface of the asphalt concrete layer after construction at loads of 22.2, 40, and 60 kN. Back-calculated moduli for the asphalt concrete, aggregate base, and subgrade for the 40-kN load are presented in Figures 15, 16, and 17 respectively. Substantial

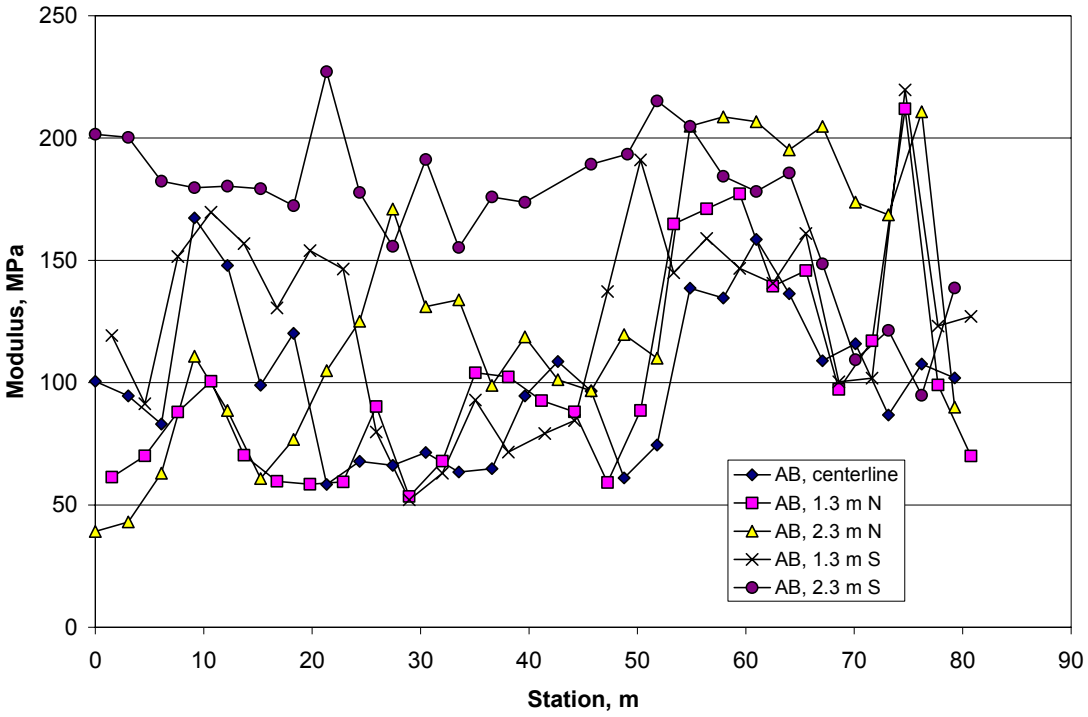

Figure 11. Modulus of aggregate base from FWD testing on aggregate base.

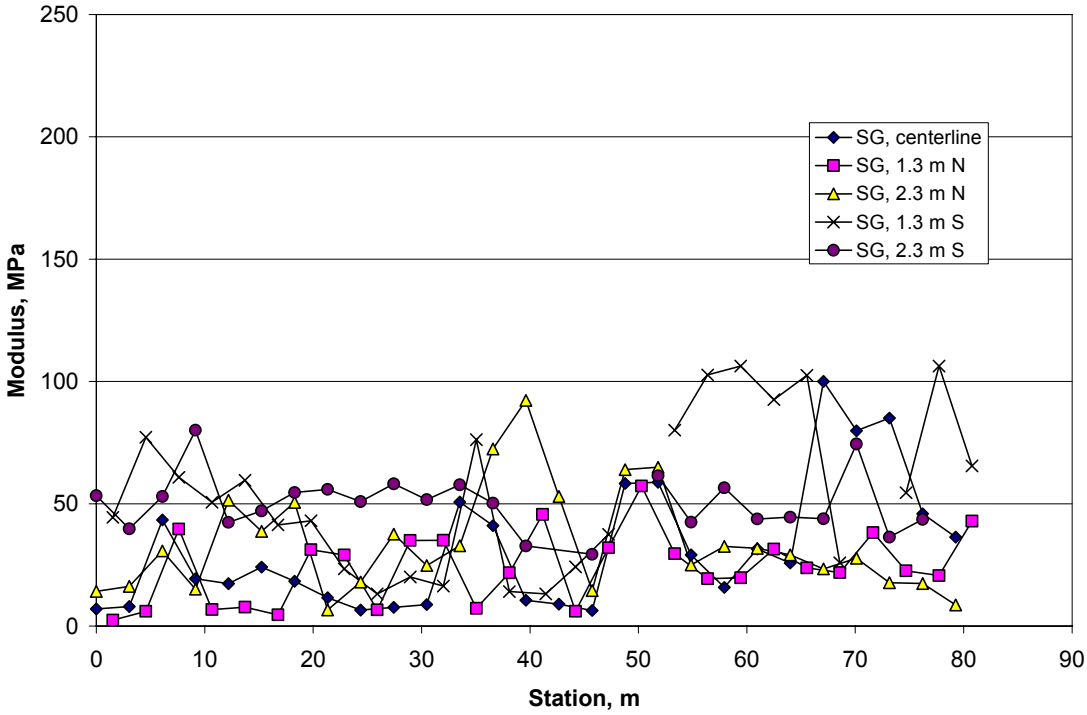

Figure 12. Modulus of subgrade from FWD testing on aggregate base

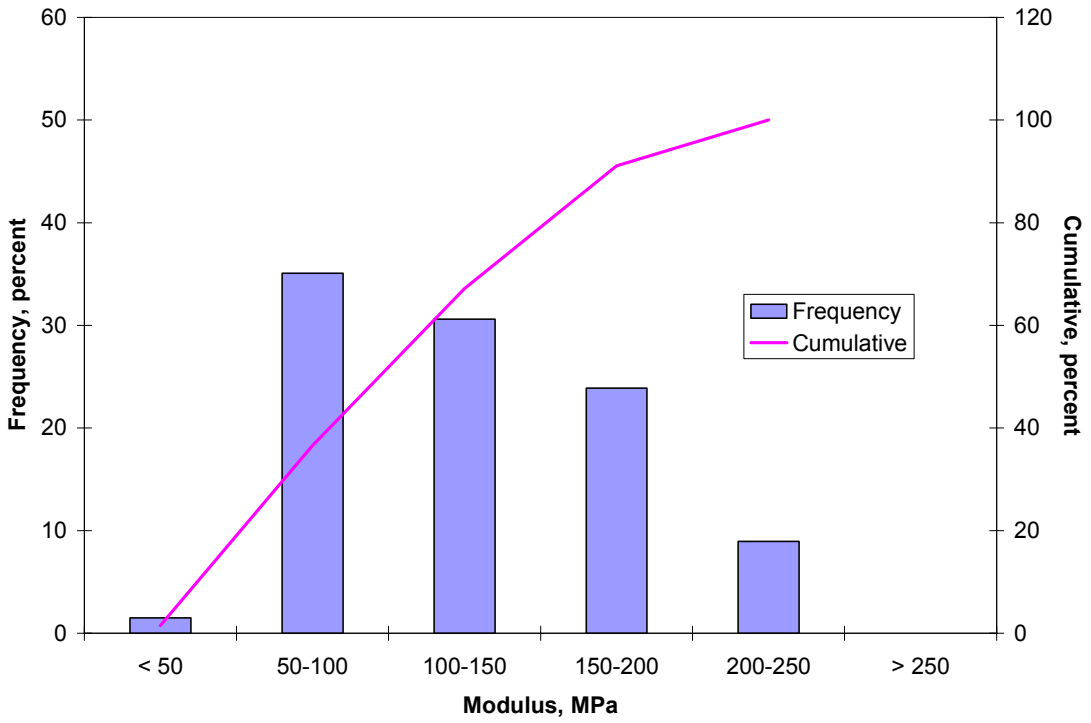

Figure 13. Relative Frequency and Cumulative Histogram for Base Modulus

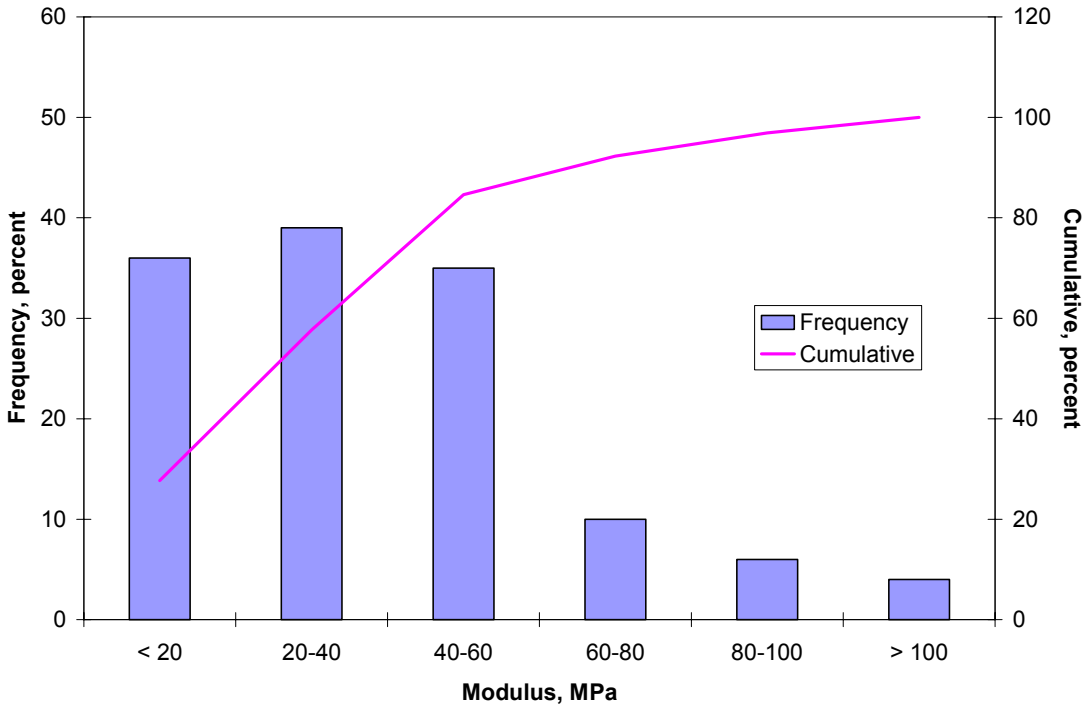

Figure 14. Relative Frequency and Cumulative Histogram for Sugrade Modulus

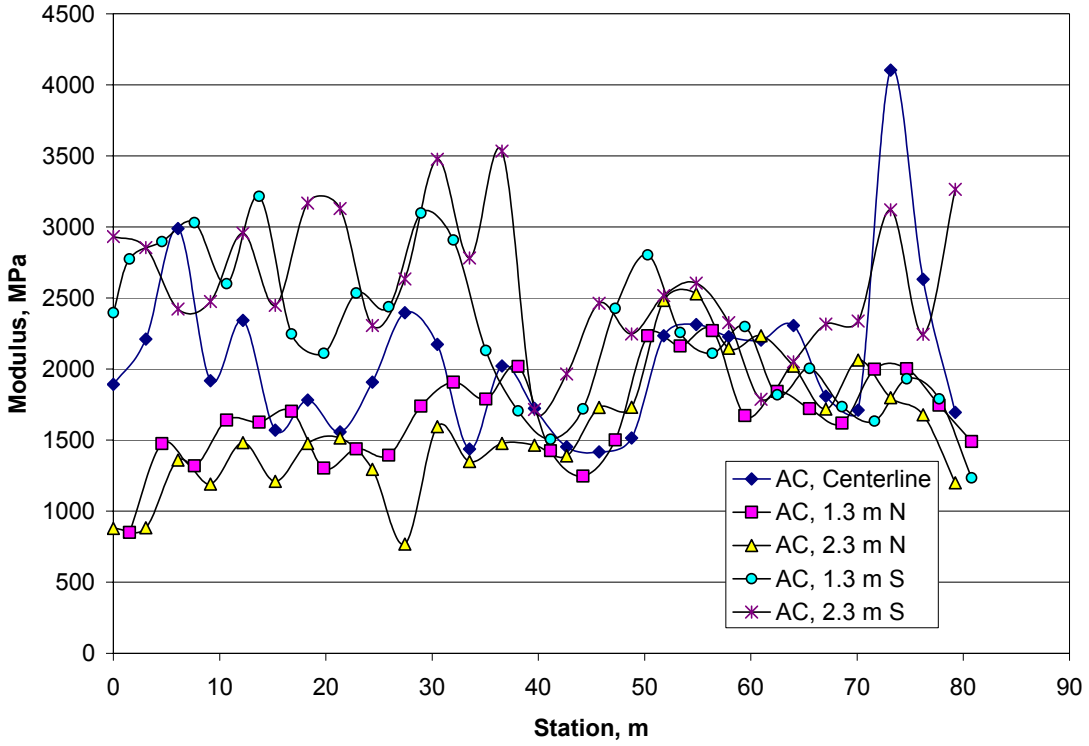

Figure 15. Back-calculated modulus of asphalt concrete from FWD on asphalt concrete layer.

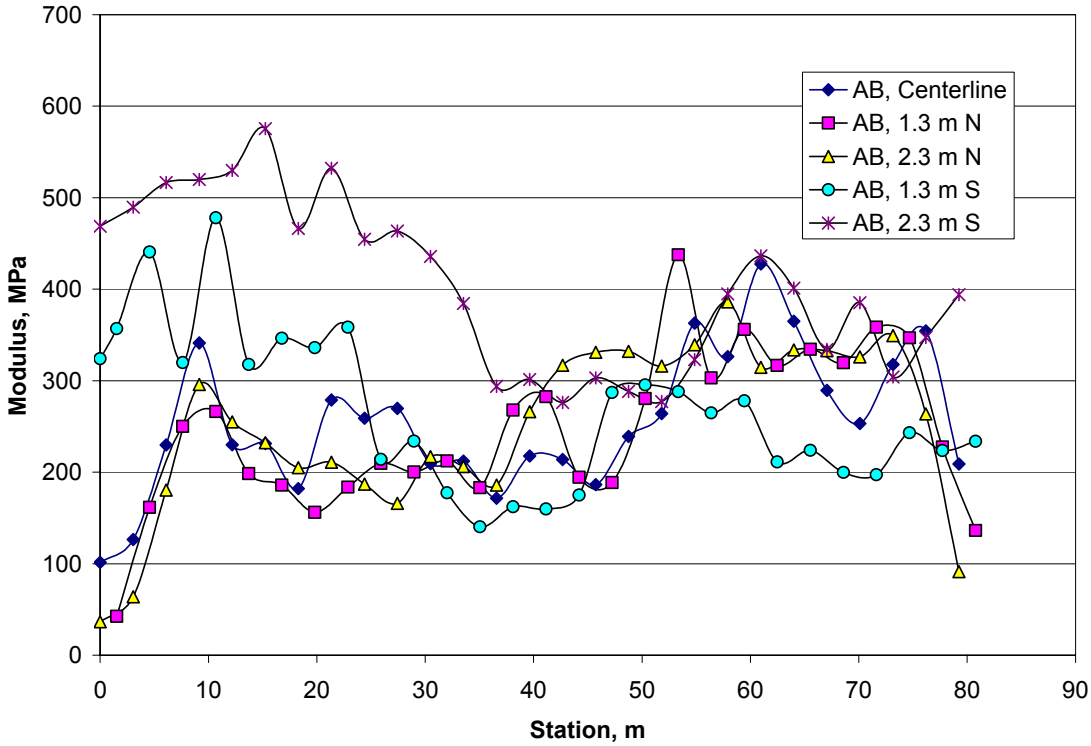

Figure 16. Modulus of aggregate base from FWD on asphalt concrete layer.

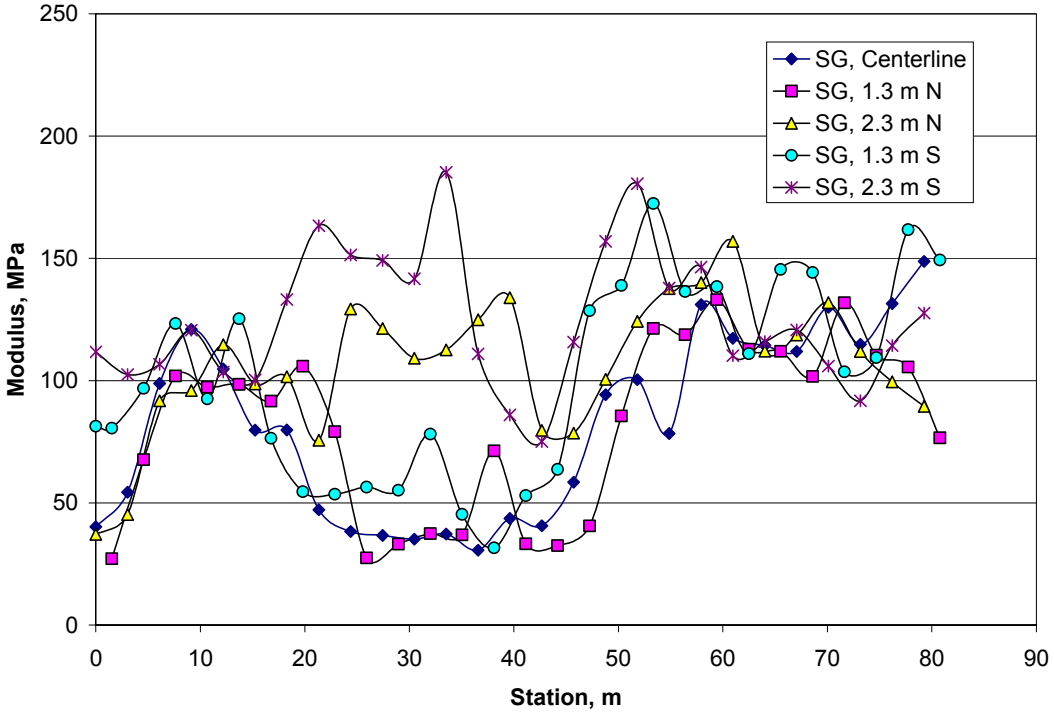

Figure 17. Modulus of subgrade from FWD on asphalt concrete layer.

variability in modului was observed for the pavement layers and the subgrade. Table 2 summarizes the statistics for the moduli. Averages and standard deviations are based on data from all five lines.

Table 2 Summary of Moduli of Pavement Layers and the Subgrade

Layer	Average Modulus, MPa	Standard Deviation, MPa
Asphalt Concrete	2035	602
Aggregate Base	284	104
Subgrade	99	37

3.5.3.1 Effect of Asphalt concrete on Unbound Materials

Direct comparison of the moduli of the unbound materials before and after construction of the asphalt concrete layer indicates an increase in the unbound layer moduli (see Figures 11

and 16, and Figures 12 and 17). The average moduli increased 127 percent and 160 percent for the aggregate base and subgrade, respectively.

The observed trend of increased moduli is reasonable. The aggregate base modulus increase is likely due to the confinement provided by the asphalt concrete layer and to added densification resulting from the compactive effort applied to the asphalt concrete. Increase in the subgrade modulus results from additional cover provided by the asphalt concrete layer and stiffening of the aggregate base, which combine to reduce the level of stresses on the subgrade, which in turn results in an increase in the modulus of fine-grained cohesive soils like the CL material at this site.

3.5.3.2 Modulus of Asphalt Concrete

Figure 18 presents relative frequency and cumulative histograms for the back-calculated moduli obtained along the centerline as well as the north and south lanes of the test pavement section. As seen in this figure, higher moduli were generally obtained along the south lane of the pavement section. A summary of modulus values appears in Table 3.

Table 3 Summary of Average AC Modulus along Pavement Section

Parameter	**FWD Measurements**			
	North	**South**	**Centerline**	**Average of all three test lines**
Average, MPa	1625	2425	2057	2035
Standard Deviation, MPa	394	527	566	602

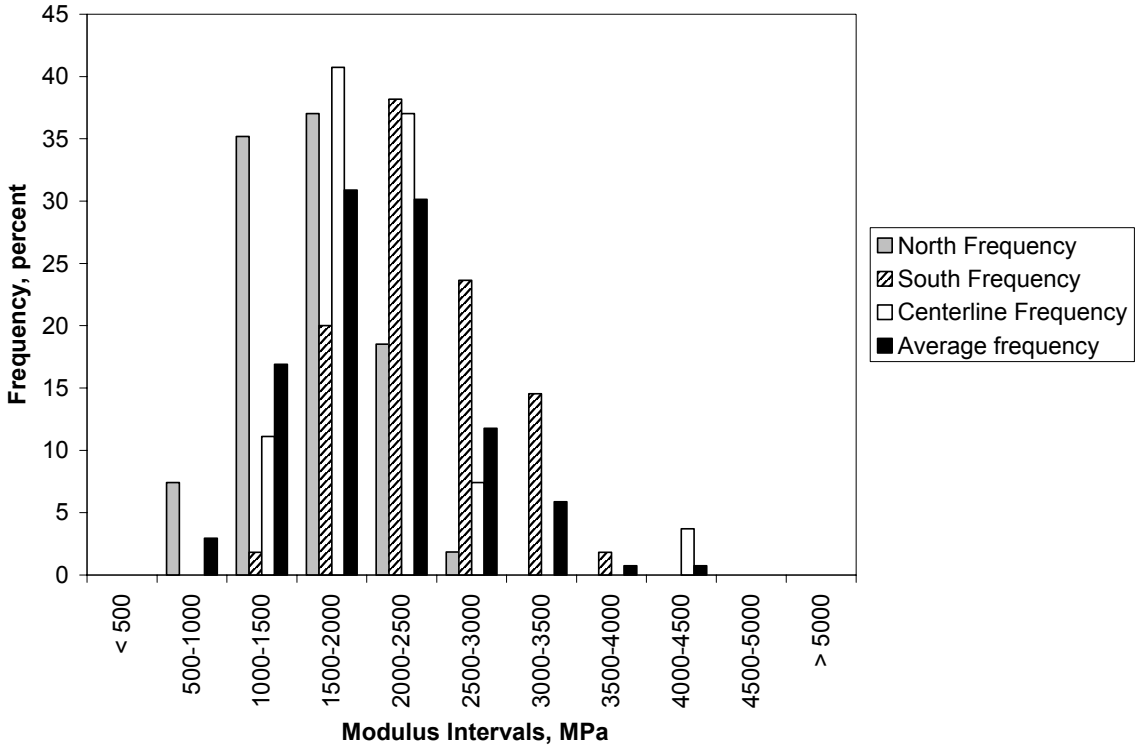

Figure 18a. Relative frequency of AC modulus.

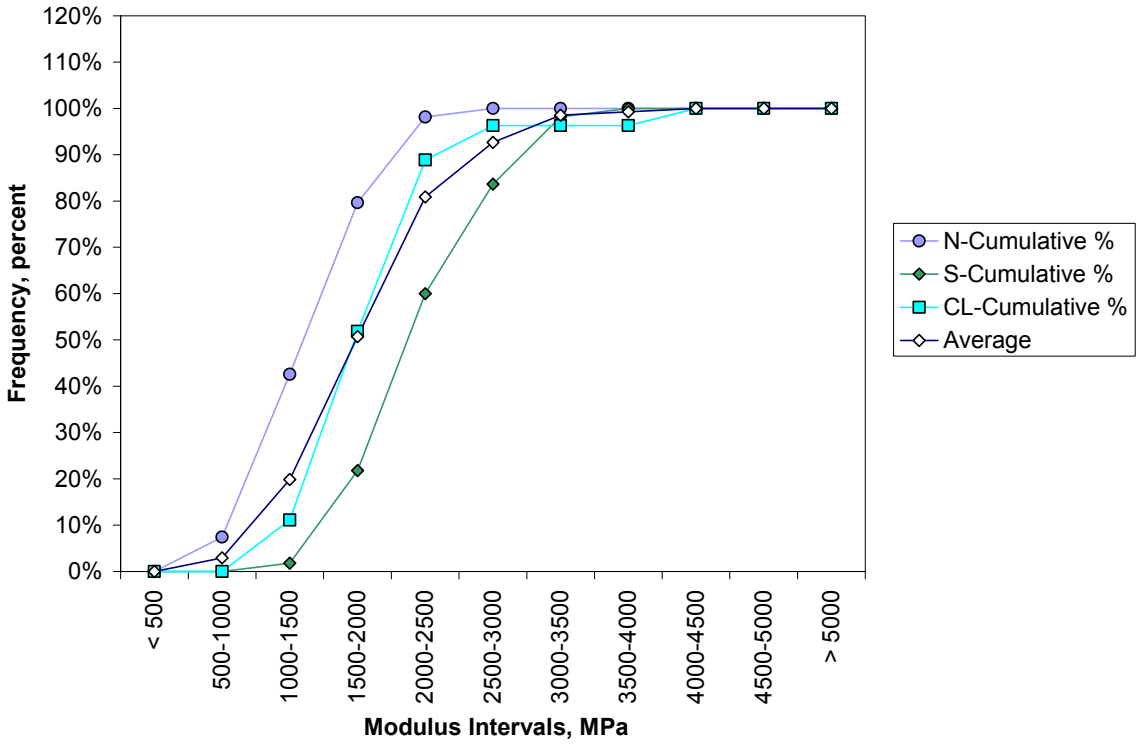

Figure 18b. Cumulative histogram of AC modulus.

Distribution of the asphalt concrete moduli along the pavement section is shown in Figure 19. Darker areas indicate higher modulus values. The distribution shown in Figure 19 corresponds with the location of the segregated areas along the section. This distribution of moduli will be of assistance in analyzing the performance of the six sub-sections subjected to HVS loading.

3.5.3.3 Modulus of Aggregate Base

Figure 20 presents the relative frequency and cumulative histogram of aggregate base moduli along the pavement section obtained from the back-calculation procedure. Results suggest that the first area may consist of two populations of moduli with values of approximately 250 MPa and 350 MPa. As seen in Figure 20, the high modulus values are on the northbound lane between stations 0 and 30 m. Table 4 provides a summary of aggregate base moduli at these different locations across the section.

Table 4 Summary of Aggregate Base Moduli along Pavement Section

Parameter	**FWD Measurements**			
	North	**South**	**Centerline**	**All**
Average, MPa	247	334	254	283
Standard Deviation, MPa	87	110	76	103

Figure 21 shows the distribution of aggregate base modulus along the pavement section. In the figure, darker color indicates higher aggregate base modulus.

3.5.3.4 Modulus of Subgrade

The average modulus of the subgrade was 98 MPa with a standard deviation of 37 MPa. Relative frequency and cumulative histogram are shown in Figure 22. As shown in Figure 17, a

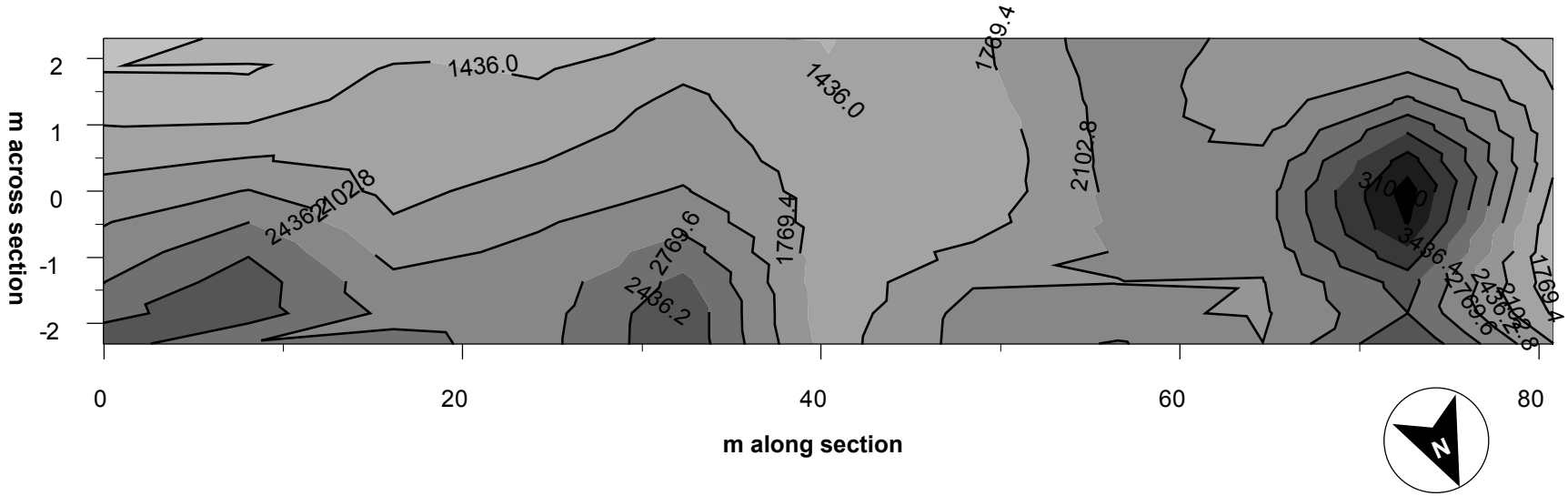

Figure 19. Distribution of AC moduli along the pavement section.

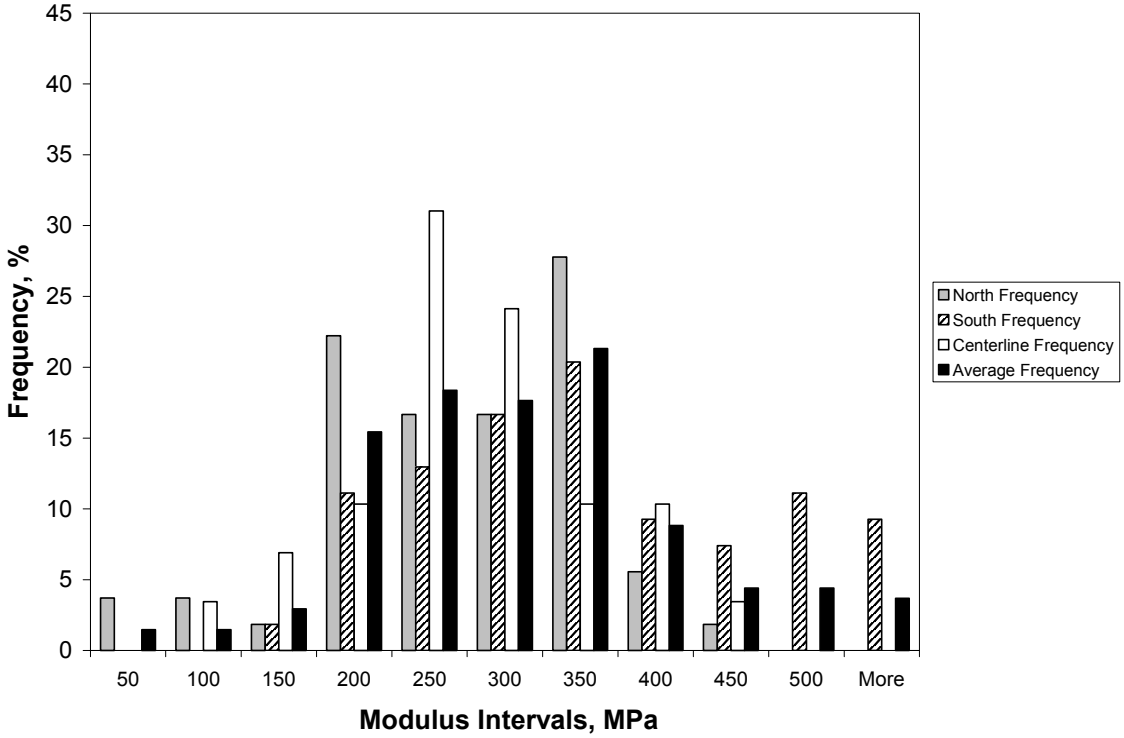

Figure 20a. Relative frequency of base layer modulus.

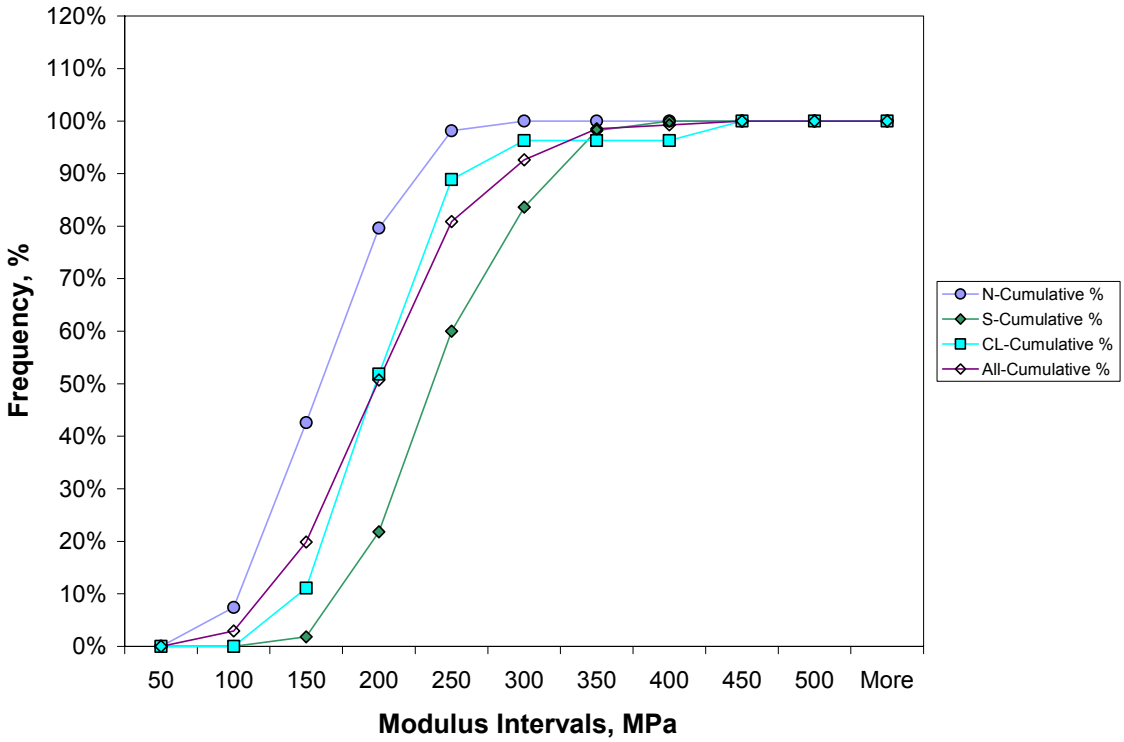

Figure 20b. Cumulative histogram of base layer modulus.

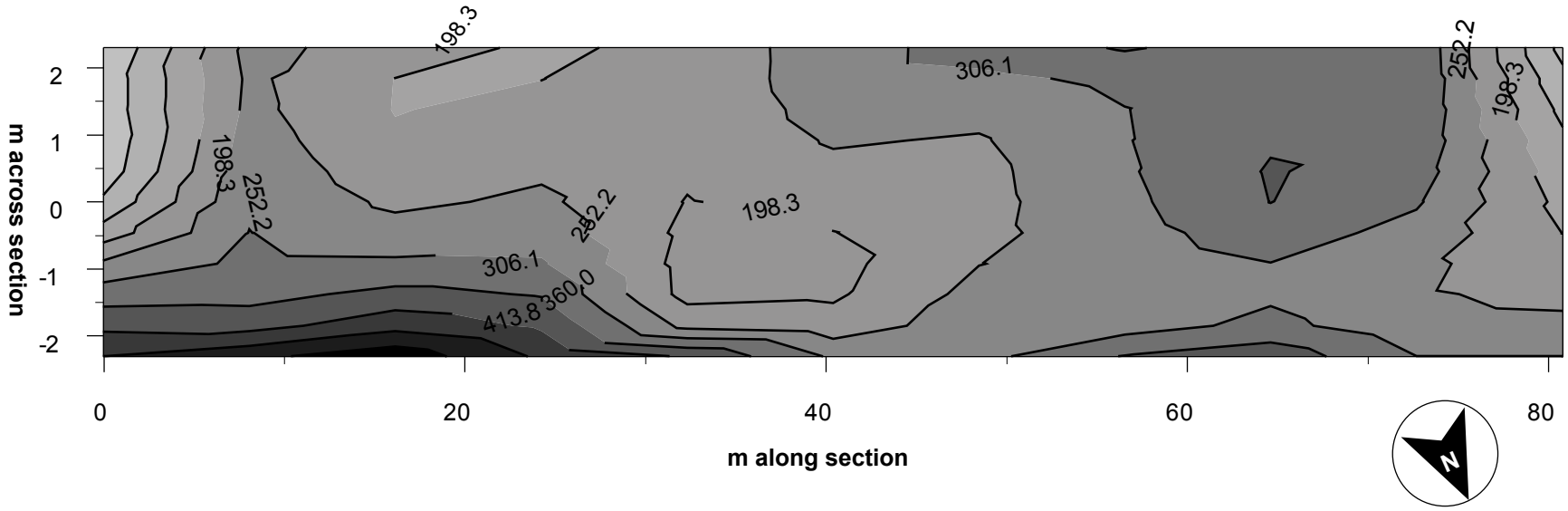

Figure 21. Distribution of aggregate base moduli along pavement section.

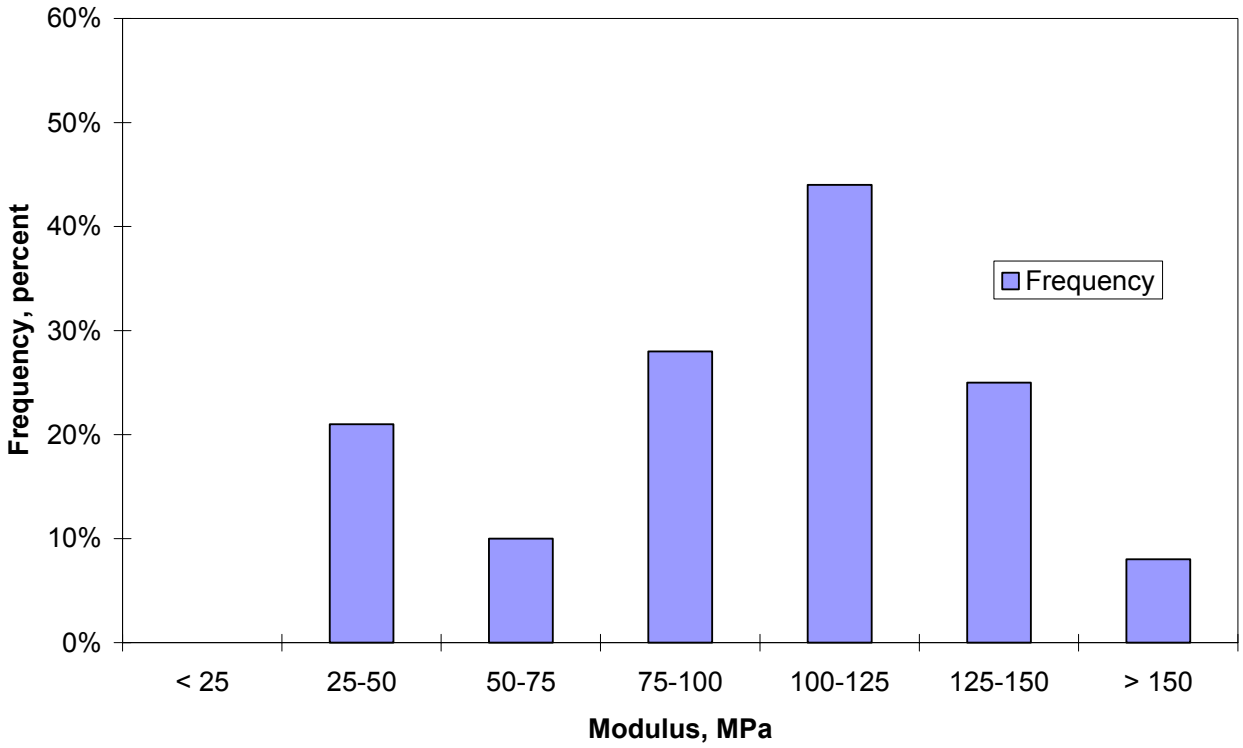

Figure 22a. Relative frequency of subgrade modulus.

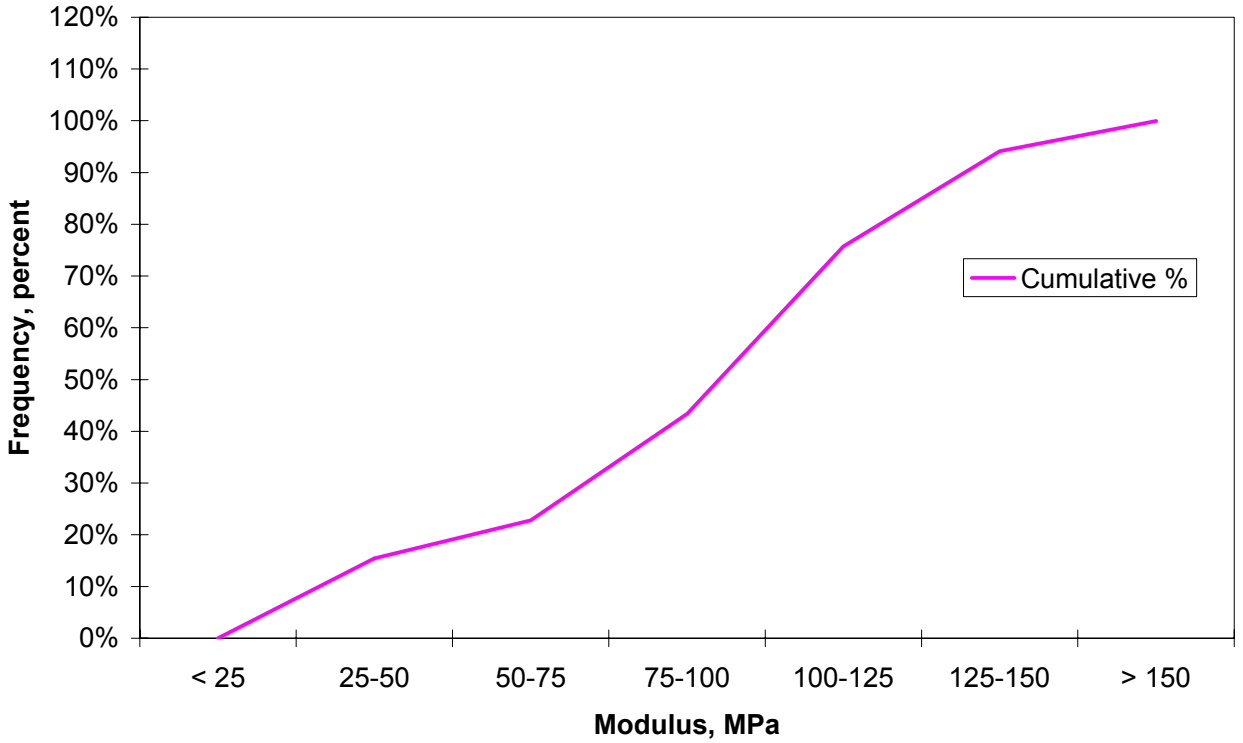

Figure 22b. Cumulative histogram of subgrade modulus.

weak subgrade (lower modulus) was observed between Stations 20 and 50 m in the southbound lane (test lines 1.3 and 2.3 m). While the reason for the low subgrade modulus in this area is not clear, based on observations during construction the subgrade in this area was compacted at high moisture content (to the right of the line of optimums). Compaction in this region induces dispersed particle orientation in this type of soil. This, in turn, results in higher resilient deformations (low resilient modulus) than if compaction occurs to the left of the line of optimums (lower moisture content).

A comparison of Figures 21 and 23 shows that low aggregate base moduli and low subgrade moduli were observed in the same locations. Direct comparison of these two parameters (see Figure 24) indicates that, after construction, the modulus of the aggregate base is related to that of the subgrade. This observation is particularly important for aggregate base construction because a stiffer subgrade enables the aggregate base to reach a higher density than does a weaker subgrade.

3.5.4 Phase 1 FWD Testing

FWD testing was conducted at various times during Phase 1 of HVS testing to monitor changes in the modulus of the bound and unbound layers over time.

3.5.4.1 Deflections

Center plate deflection data (D_0) collected from October 2001 to May 2003 along the five lines of FWD testing at a nominal load of 40 kN are presented in Figure 25 and Table 5. FWD testing was conducted every ten feet along the five test lines with the purpose of studying the effect of climate on pavement stiffness. The data do not include the damage produced by accelerated pavement testing on the six HVS sections.

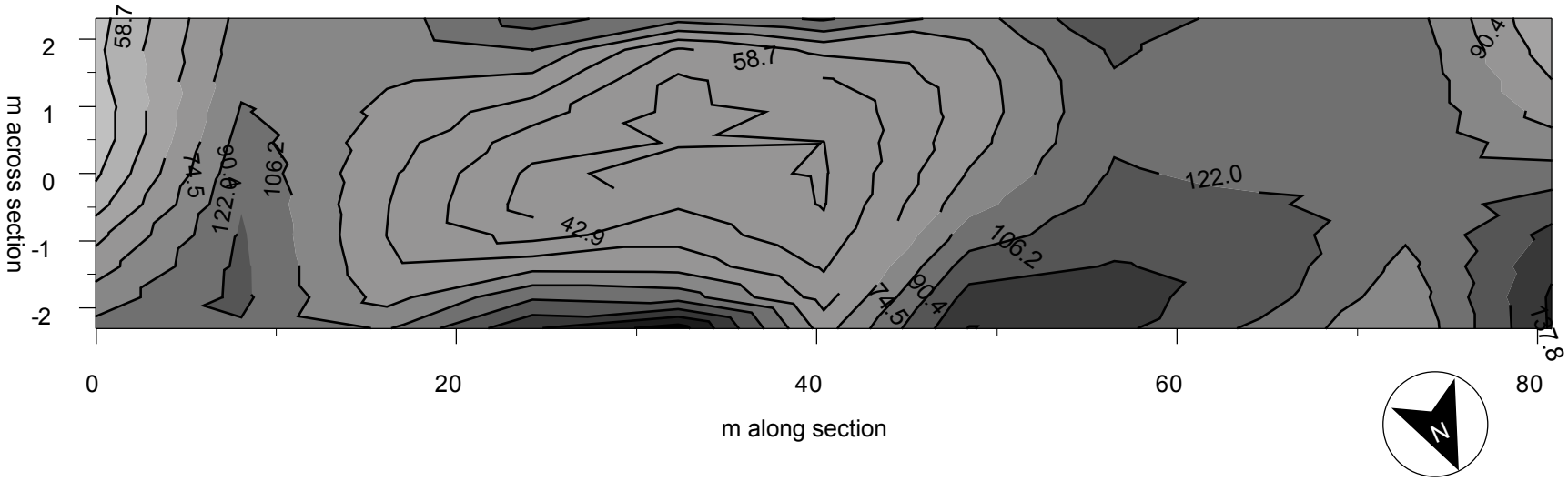

Figure 23. Distribution of subgrade moduli along pavement section.

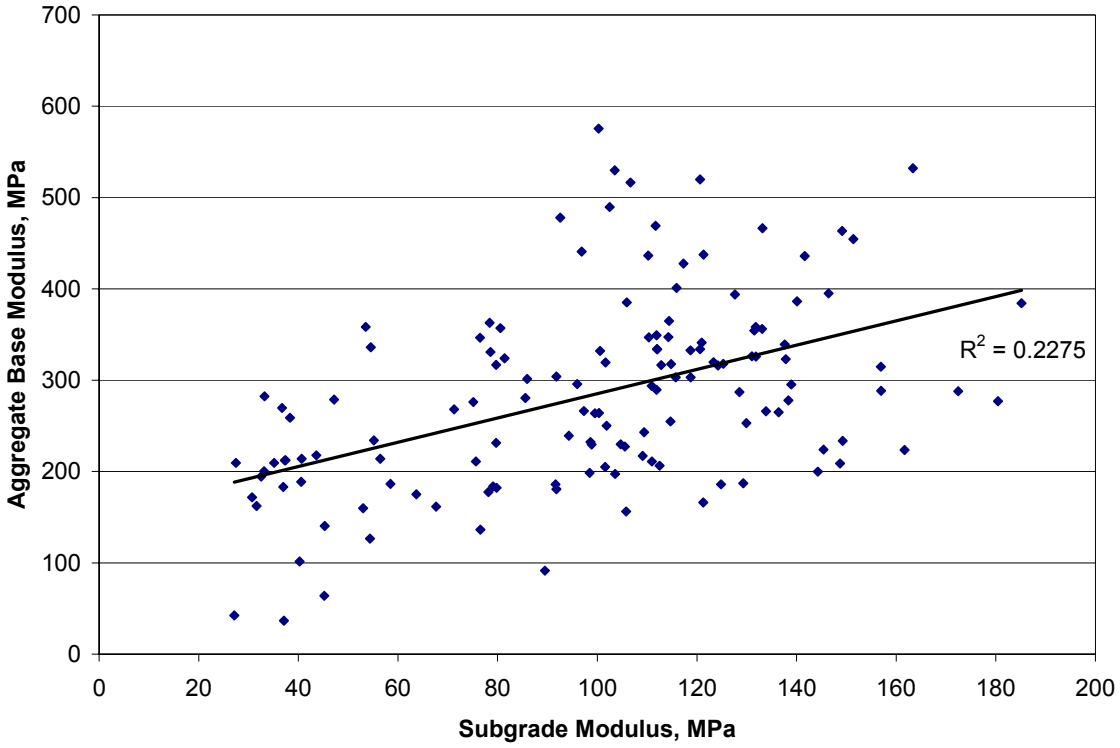

Figure 24. Comparison of subgrade and aggregate base moduli.

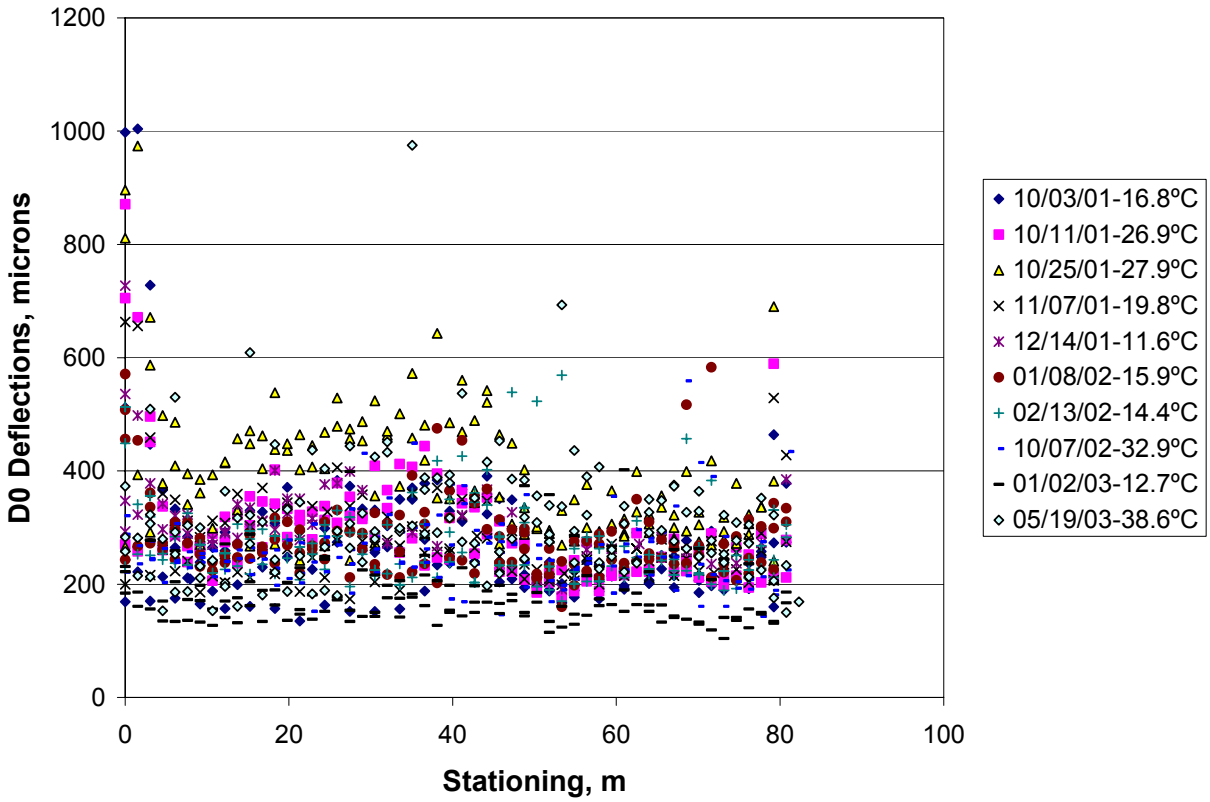

Figure 25. FWD deflections at the load plate (D0) along the pavement section.

Table 5 Average FWD Deflections by Date

Station (m)	Average D0 Deflections by Date										
	10/3/2001	**10/11/2001**	**10/25/2001**	**11/7/2001**	**12/14/22001**	**1/8/2002**	**1/9/2002**	**2/13/2002**	**10/7/2002**	**1/2/2003**	**5/19/2003**
10-20	263	306	397	279	313	261	274	262	240	180	280
20-30	276	324	415	286	346	273	274	274	258	193	290
30-40	282	331	424	277	277	305	230	264	284	179	381
40-50	285	287	411	274	339	312	251	309	263	185	322
50-60	204	211	306	223	231	244	214	261	236	186	333
60-70	224	238	322	242	271	293	236	249	277	191	305

Note: Stations 0-10 and 70-80 are not shown since they lie outside the area trafficked by the HVS

In addition, the data suggest that the subgrade between approximately Stations 17 m and 50 m may be somewhat less stiff than the sections of subgrade from Stations 0 to 17 m and Stations 50 to 70 m (on either side within the boundaries of the various test sections.

3.5.4.2 Back-Calculated Moduli

Moduli were calculated from FWD deflections using the computer program ELMOD 5.0.(*5*) This program uses Odemarks's transformation of a layered system and Bousinessq's equations to calculate pavement layer moduli. A non-linear subgrade and no bedrock were assumed in the back-calculations. Results of the back-calculations are summarized in Figure 26 for average layer moduli along the north and south lanes. In Figure 26, Y-bar errors indicate one standard deviation from the average value.

Figure 26 shows a rapid increase in moduli of all the pavement layers and the subgrade from September 2001 to December 2001. The increase is particularly significant for the asphalt concrete and the aggregate base. The change in asphalt concrete modulus with time is typical and expected for asphalt concrete layers. However, the decrease in unbound layer moduli during the 2003 summer period does not coincide with expected results. It would be expected that the measured aggregate base stiffness moduli would increase because the AC is less stiff and the stresses are higher. It is possible that the confining effect of the AC was less significant due to its reduced stiffness, thereby resulting in the decrease in the AB moduli. The lower moduli of the subgrade is likely a result of increased moisture content from the wet season.

Figure 27 shows the variation of asphalt concrete modulus with pavement temperature for the north and south lanes. Pavement temperatures were estimated from air temperatures using Bell's equation. The data show an increase in modulus with low temperatures, which is typical behavior for asphalt concrete layers. On average, the data indicate that for a given pavement

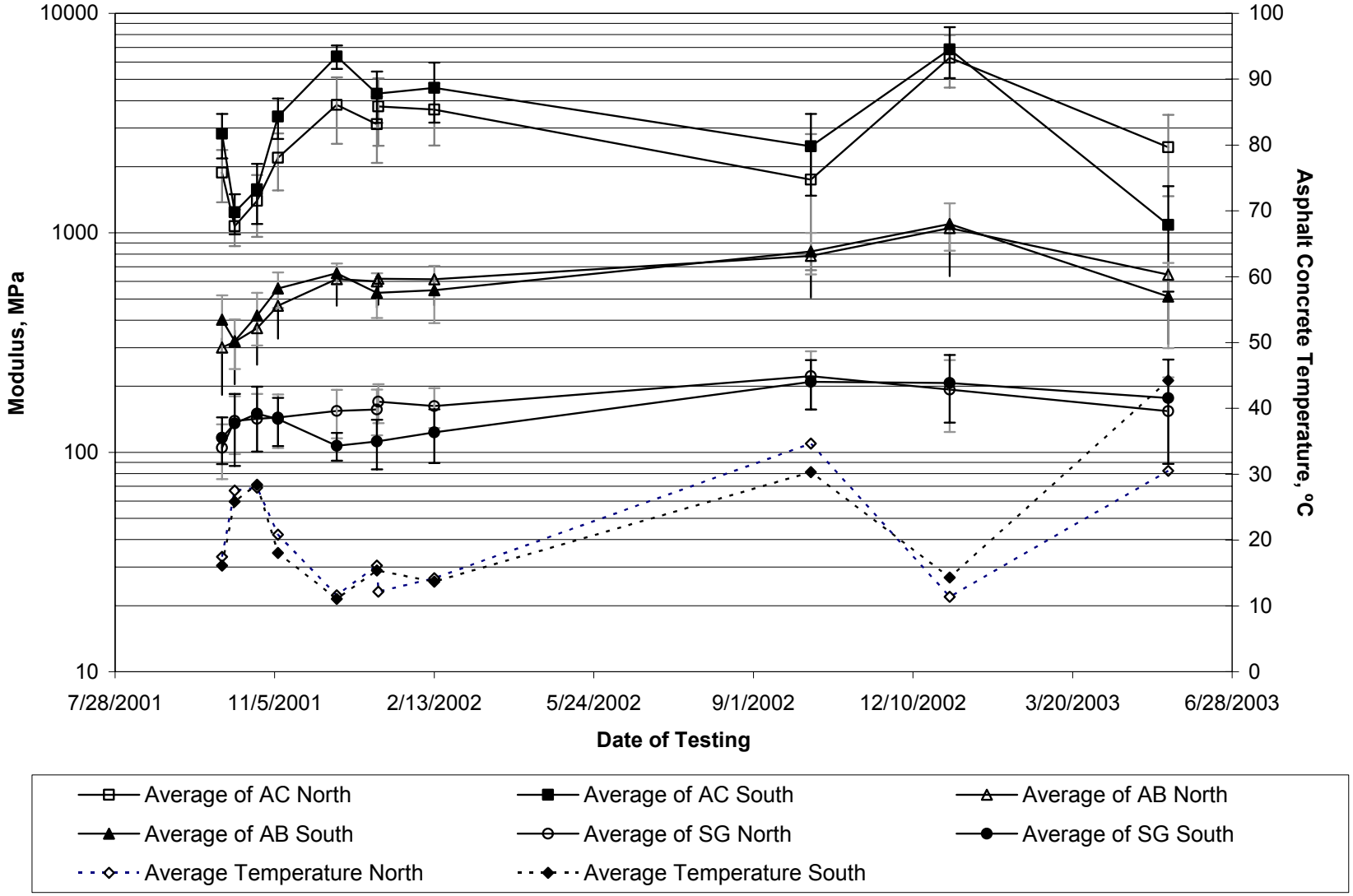

Figure 26. Summary of back-calculated moduli for pavement section.

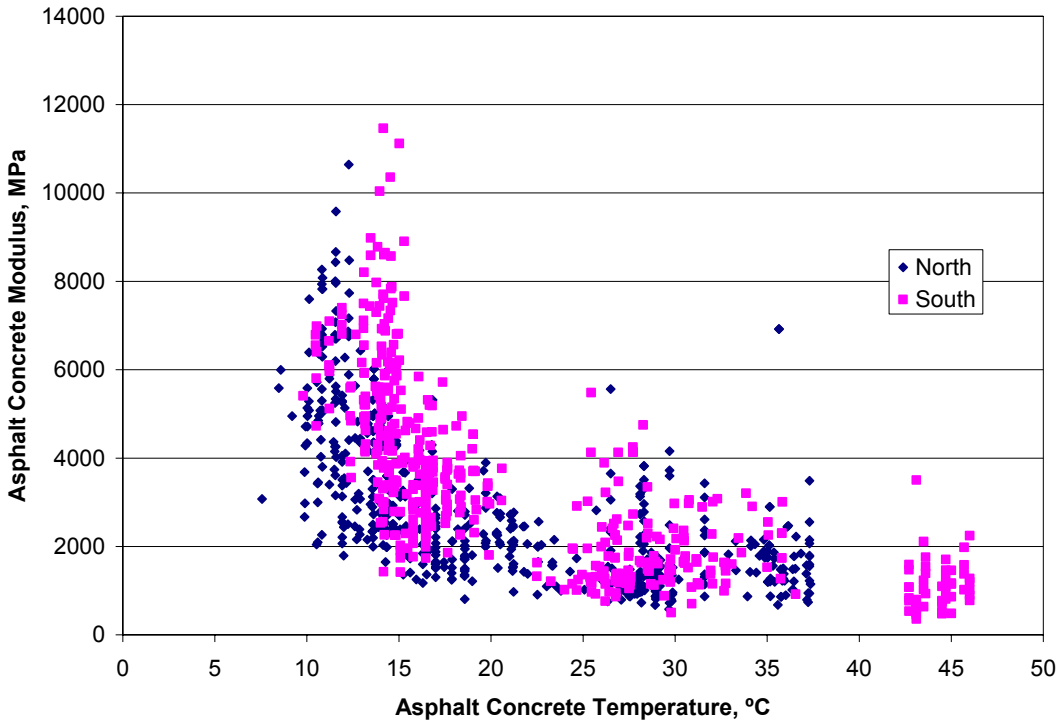

Figure 27. Effect of temperature on modulus of the asphalt concrete layer.

temperature, moduli of the asphalt concrete in the south lane are higher than those in the north lane. This is more evident in Figure 28, which shows average asphalt concrete moduli along the two pavement section lanes. Difference in moduli between the sections occurs mainly in the first 50 m of the section.

As noted earlier, the behavior of the aggregate base does not follow expected trends, i.e., an increase in stiffness with increase in stress (e.g., sum of principal stresses). For example, Figure 29 shows aggregate base modului versus asphalt concrete modului. Laboratory repeated load triaxial compression tests indicate that aggregate base materials increase in stiffness with increase in confining pressure. It is possible that increase in asphalt concrete moduli result in increased confining pressures in the aggregate base layer, resulting in increased aggregate base stiffness moduli.

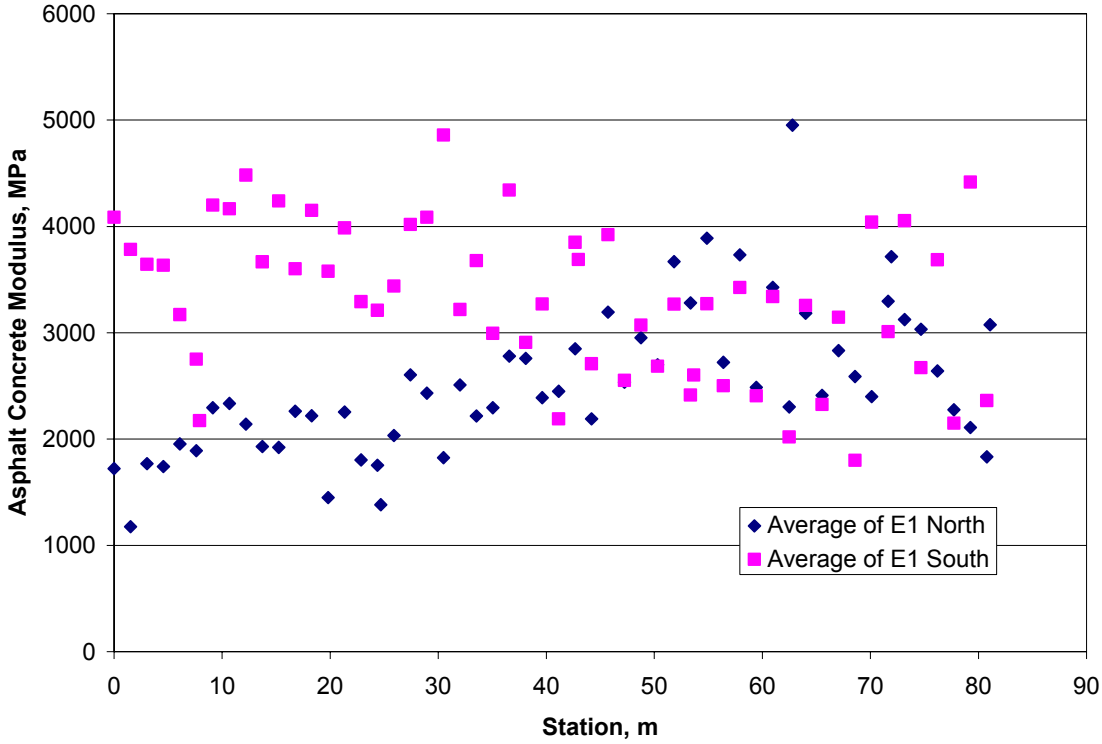

Figure 28. Variation of asphalt concrete moduli along the pavement section.

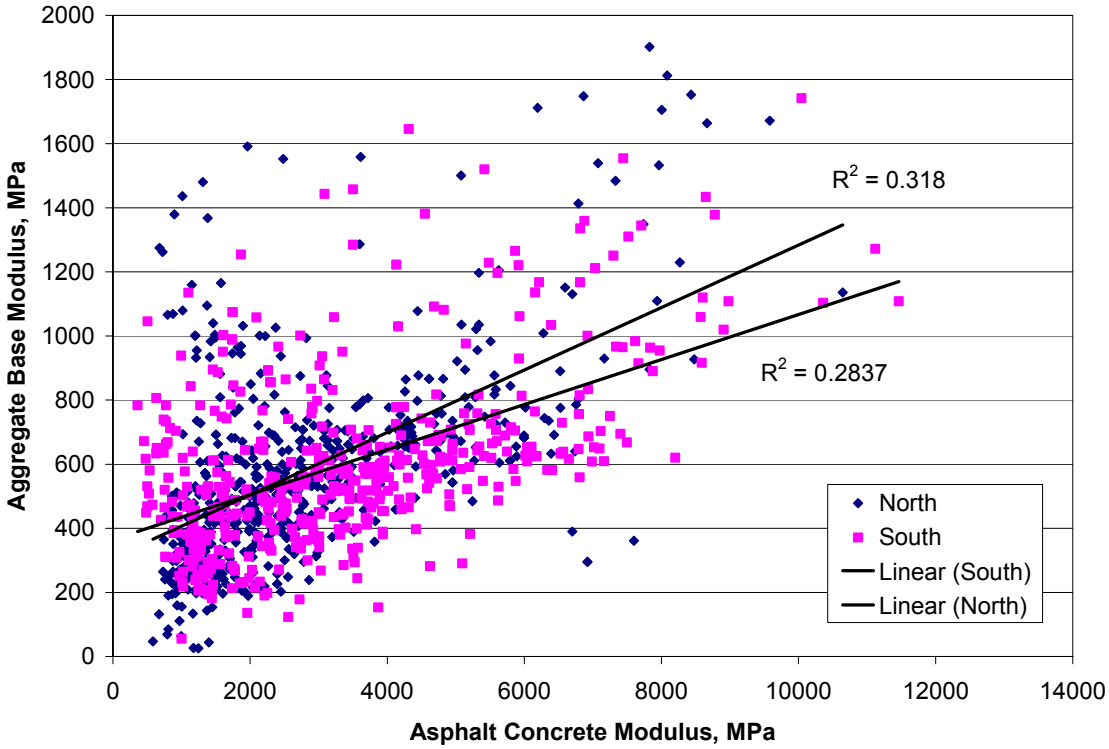

Figure 29. Variation of aggregate base modulus with asphalt concrete modulus.

Effects of subgrade stiffness moduli on aggregate base moduli are shown in Figure 30. These trends follow expected results and are relative to the inability of the untreated aggregate base to accommodate tensile stresses as reported by the Shell investigations.(*7*) These investigations suggested modular ratios between base and subgrade materials in the range 2 to 3.

Average variations of the aggregate base and subgrade moduli presented in Figures 31 and 32 support at least to a reasonable degree, this observation by the Shell investigation.

Figure 33 shows precipitation and moisture content in the unbound materials over time. Water content is presented as a relative number due to the errors in the absolute measurements. However, overall fluctuations and trends in the relative moisture content were correct. The precipitation and subgrade moisture contents exhibited a significant offset: peak moisture contents were recorded seven months after peak monthly precipitation and one month after the last rainfall. This offset between precipitation and measured moisture content could be due to poor subgrade drainage. On the other hand, the precipitation and aggregate base display typical trends with the rate of moisture content decrease lower than the rate of moisture content increase.

Figure 35 shows a decrease in subgrade moisture content and modulus during the months of May and June 2003. This pattern is expected because fine grained soils are affected significantly by moisture content. Figures 34 and 35 indicate variations of base and subgrade modulus and moisture content with time. The effect of moisture content on the aggregate base somewhat contradicts experience for the period of data collected. Figure 34 shows an increase in moisture content in the aggregate base and is associated with an increase in the aggregate base modulus; usually one expects a decrease in stiffness with increase in water content. As discussed earlier, factors such asphalt concrete modulus variations may have a more significant effect on the aggregate base modulus than moisture content.

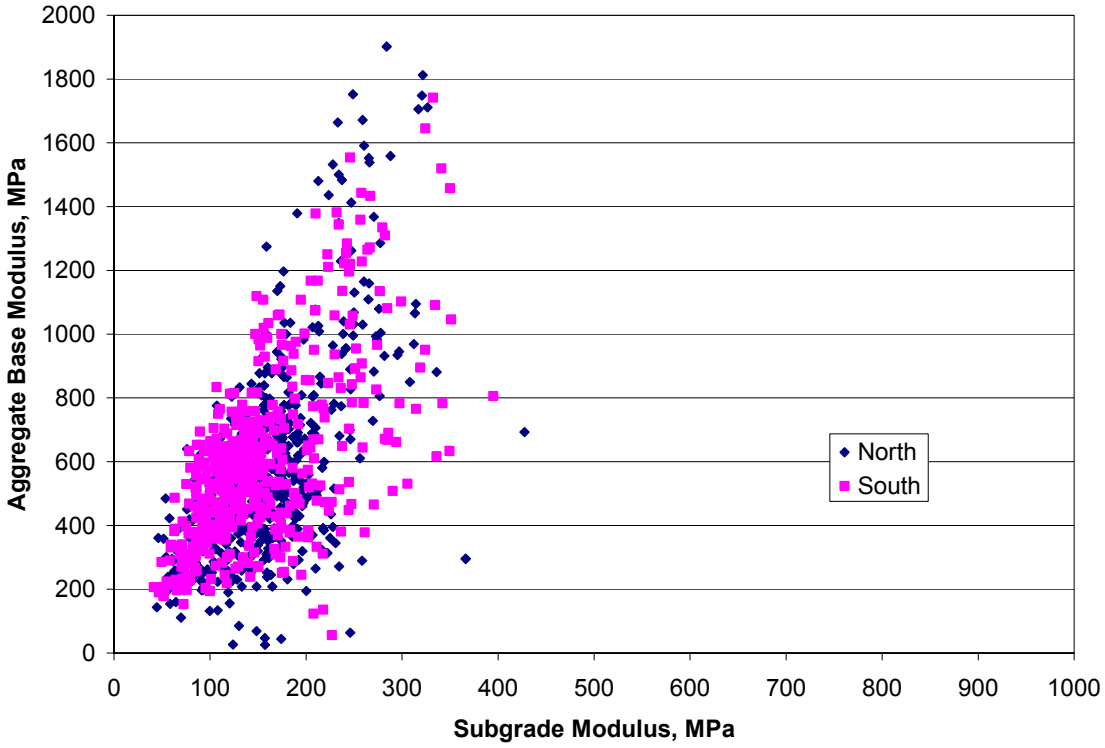

Figure 30. Variation of aggregate base modulus with subgrade modulus.

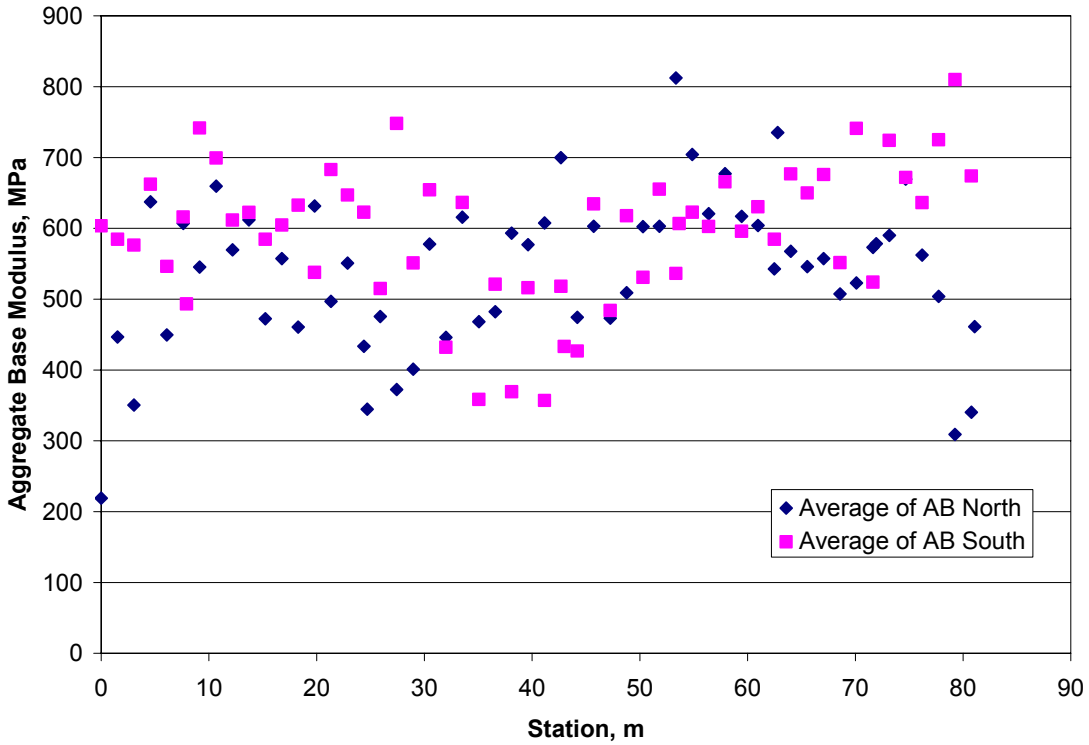

Figure 31. Average aggregate base modulus along the pavement test section.

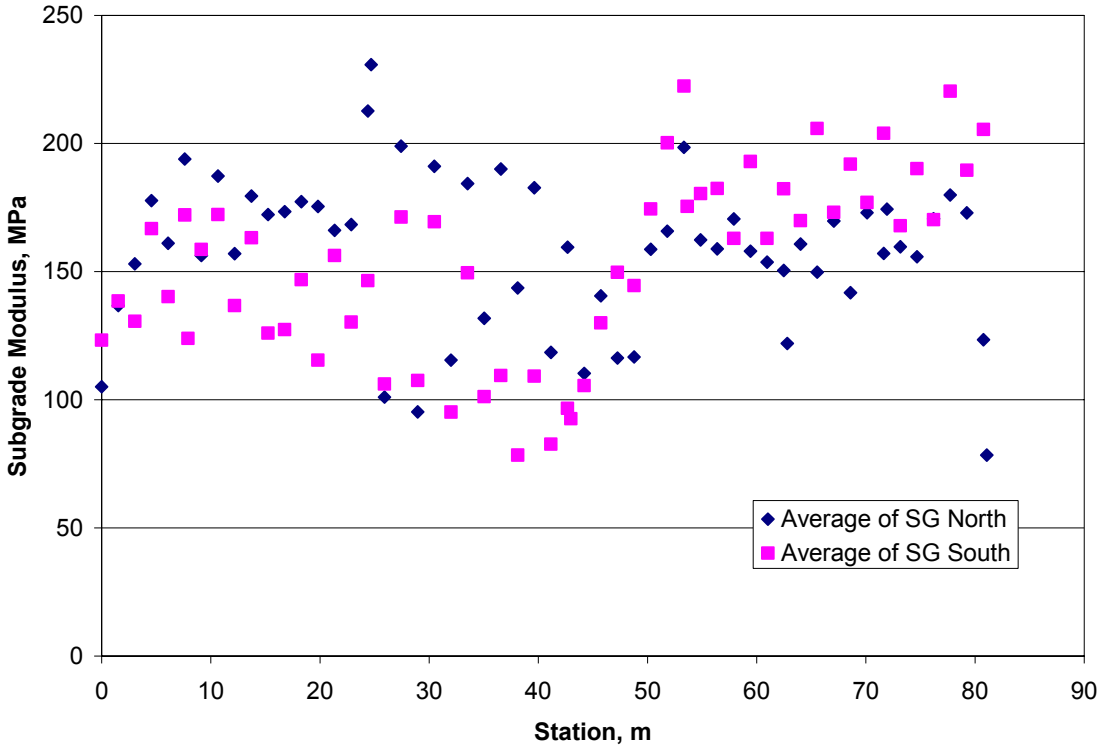

Figure 32. Average subgrade modulus along the pavement test section.

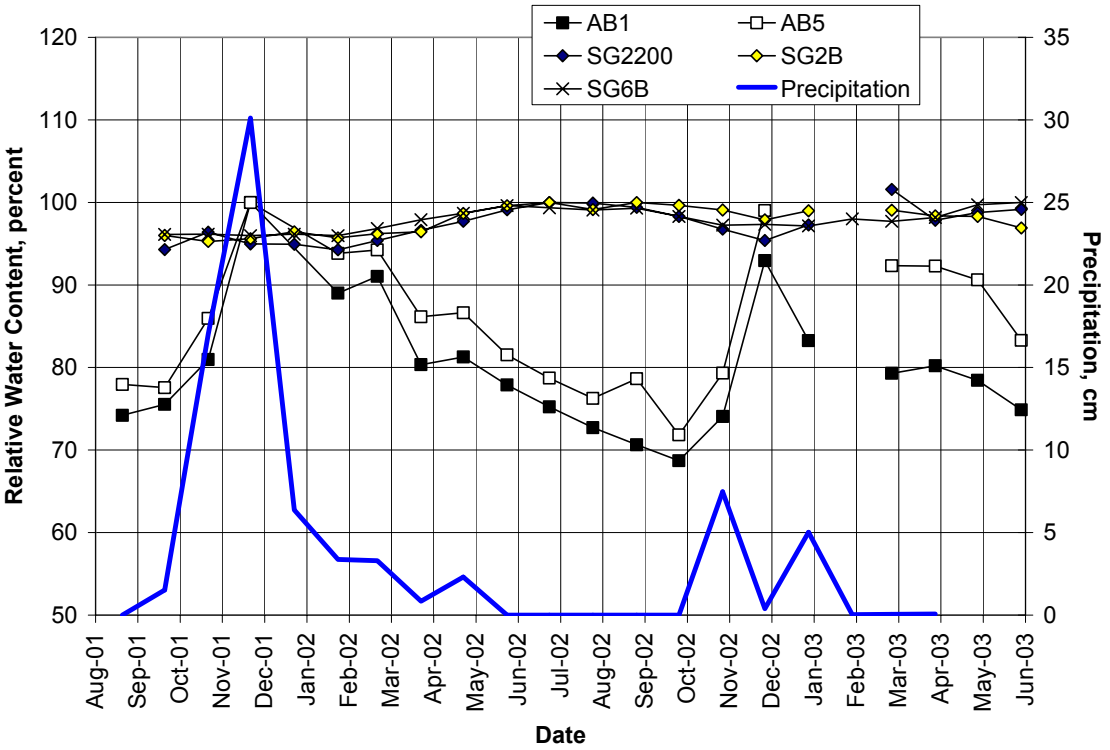

Figure 33. Variation of moisture content with precipitation over time.

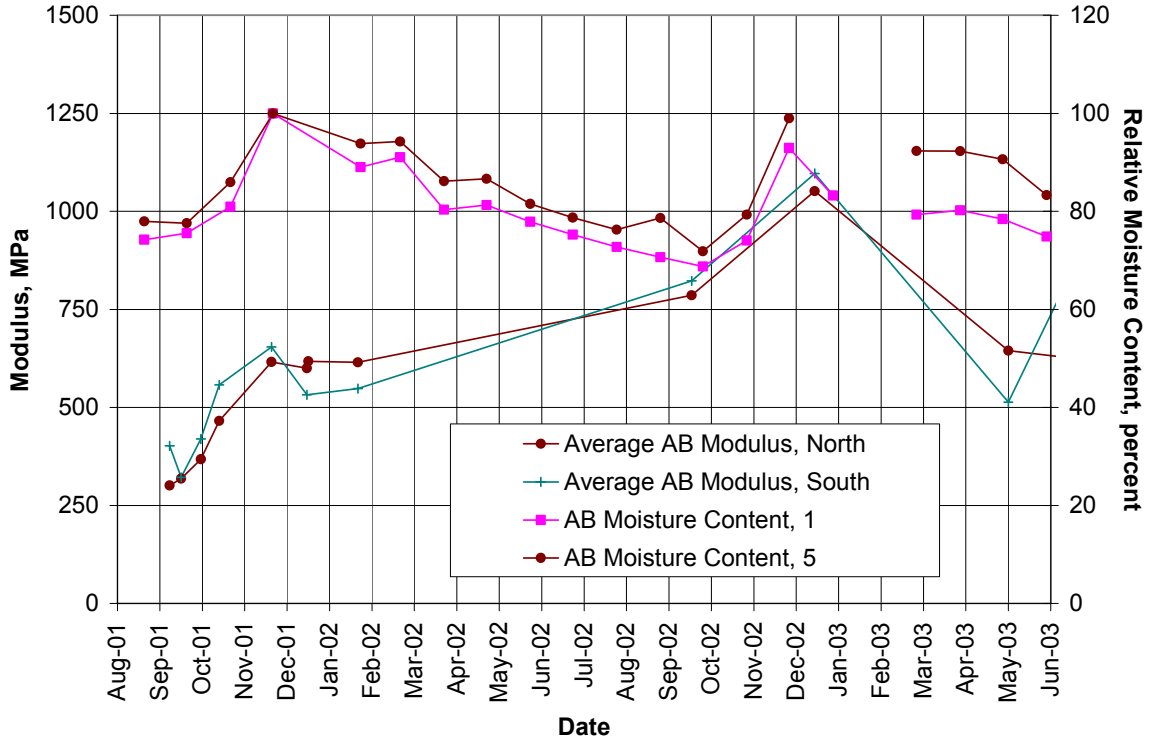

Figure 34. Variation of modulus with time as a function of moisture content for aggregate base.

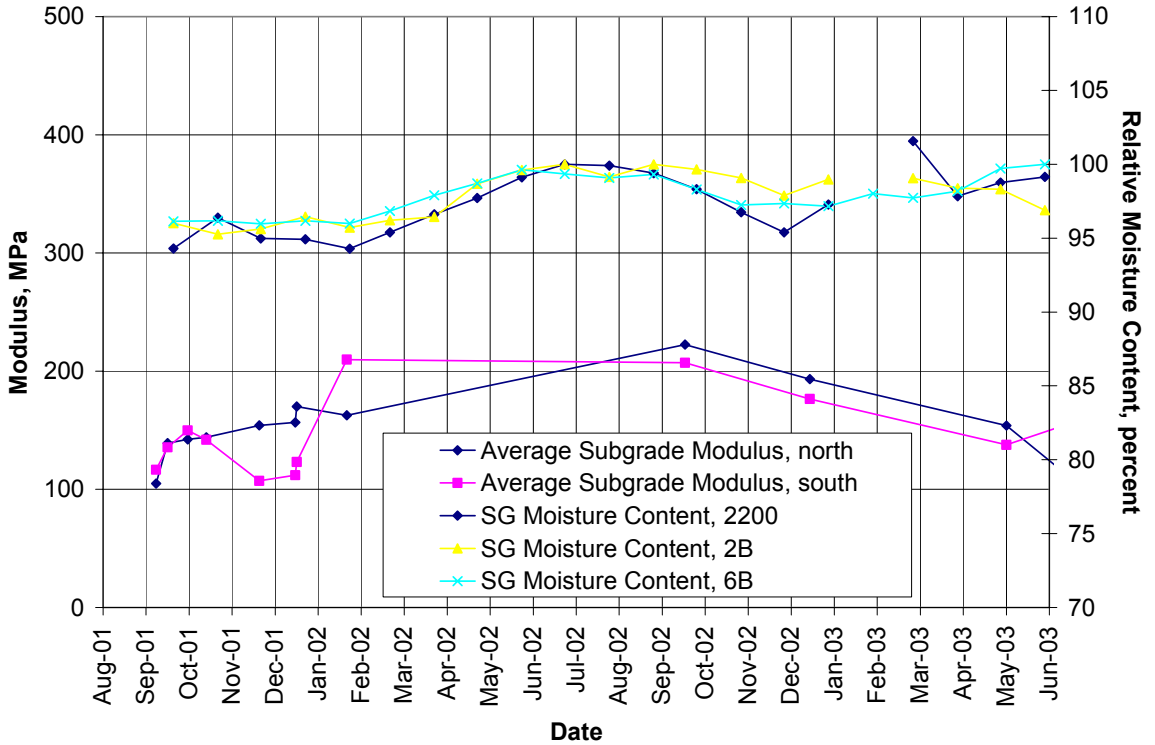

Figure 35. Variation of modulus with time as a function of moisture content for subgrade.

4.0 ACCELERATED PAVEMENT TESTING WITH THE HEAVY VEHICLE SIMULATOR

Accelerated pavement testing using the Heavy Vehicle Simulator was conducted on six-sub sections selected on the pavement test section. Locations are shown in Figure 2.

Actual layer thicknesses for each of the HVS test sections measured from nearby extracted cores and dynamic cone penetrometer tests are presented in Table 6.

Table 6 Layer Thicknesses on Each HVS Test Section

Layer	Design Thickness	Measured Layer Thicknesses in -HVS Test Section (mm)					
		567	568	569	571	572	573
AC, mm	90	78	80	81	82	78	76
AB, mm	410	352	349	337	352	349	337

4.1 Environmental Conditions of the Tests

The target temperature for each test section was established at 20ºC at a pavement depth of 50 mm. Trafficking was stopped if the surface temperature deviated more than ±2ºC from the target. The subgrade was in direct contact with the natural water table, resulting in changes in water content caused by seasonal variations. The water table is located at approximately 3.0 to 5.0 m below the surface of the pavement and fluctuates seasonally.

4.2 Traffic Loading

Each HVS test section was 8.0 m in length. Pavement performance in the one meter turnaround areas at the ends of the HVS wheelpath was not included in the performance evaluations. All trafficking had an established wander pattern across the 1.0-m width of the wheelpath.

All test sections were trafficked bi-directionally. Wheel speed was approximately 2.1 m/s (7.5 kph) in one direction and 1.9 m/s (6.8 kph) in the other direction.

Radial tires on 110-mm wide rims were used at a 720-kPa inflation pressure. A 40-kN traffic load on dual tires was used for each test section.

4.3 Failure Criteria

Failure criteria were established based on many factors including expected performance, previously collected data, Caltrans guidelines, and judgment of project staff. For analysis purposes the criteria utilized were:

- Cracking density of 2.5 m/m^2 or more, and
- Maximum surface rut depth of 12.5 mm or more.

4.4 Pavement Instrumentation and Methods of Monitoring

Details of the instrumentation are presented in Appendix B. Instrumentation of the test sections consisted of the following:

- Multi-Depth Deflectometers (MDD): used to measure elastic vertical deflections and permanent vertical deformations at various levels in the pavement structure, relative to a reference depth located in the subgrade. (N.B.: due to the saturated condition of the subgrade at the time of MDD installation, it was not possible to properly anchor the MDD).
- Road Surface Deflectometer (RSD): used to measure elastic vertical deflections at the surface of the pavement;
- Falling Weight Deflectometer (FWD): used to measure elastic vertical deflections at the surface of the pavement;

- Thermocouples: used to measure temperatures at various depths in the asphalt bound materials;
- Laser Profilometer and Straight Edge: used to measure the transverse profile of the pavement surface to determine surface rutting;
- Dynamic Cone Penetrometer (DCP): used to measure the relative shear resistance of unbound layers;
- Digital Crack Images: used to measure surface cracking;
- Time Domain Reflectometer: used to monitor the changes in water content in the unbound layers just outside the trafficked area during testing of the section, and
- Coring: used to determine pavement thicknesses and air-void contents of asphalt bound materials outside the trafficked area, and inside the trafficked area upon completion of testing.

Detailed description of the instrumentation used during accelerated pavement testing is presented elsewhere.(*6*)

4.5 Summary of HVS Test Data

4.5.1 Climate Conditions

The HVS test sections were tested in sequence at different periods during the year. The climate conditions under which each section was tested are critical for interpreting accelerated pavement test results. Figure 36 shows the sequence of HVS tests together with the average measured monthly air temperatures and precipitation amounts collected at a nearby weather station. Also in the figure are estimates of relative moisture content in the aggregate base and

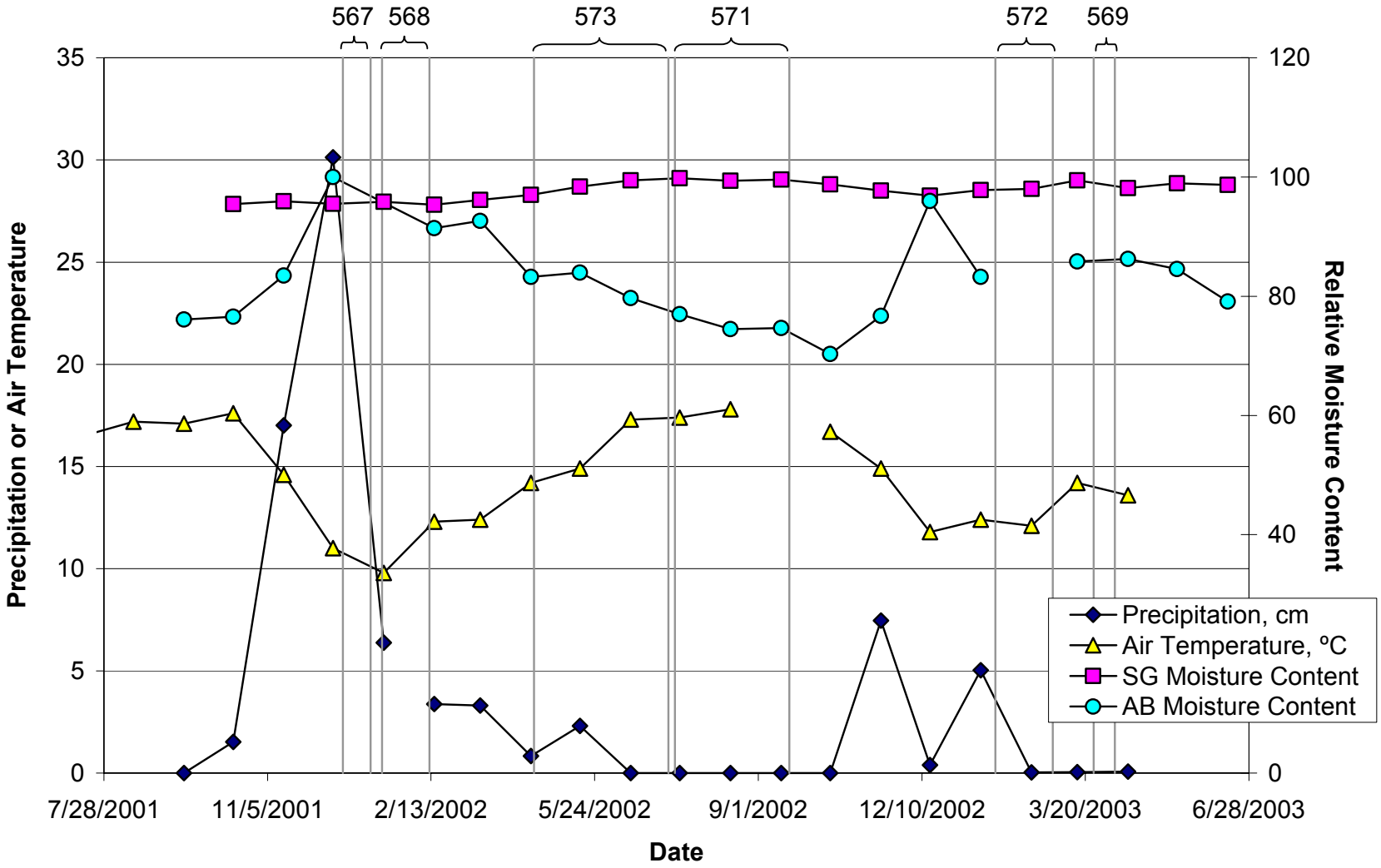

Figure 36. Sequence of HVS and climatic conditions during first stage of HVS testing.

subgrade layers. The figure shows that HVS Sections 567, 568, 573, 572, and 569 were tested during the rainy season. Sections 571 and 573 were tested when the air temperatures were the highest. In terms of moisture content, Figure 36 also shows that Sections 567, 568, 572 and 569 where tested when the aggregate base moisture content was relatively high (≥ 80 percent relative moisture content), and 571 and 573 when the aggregate base moisture content was comparatively lower (< 80 percent). Subgrade moisture varied little throughout testing on all HVS test sections.

4.5.2 Thickness and Air-void Content of Asphalt Concrete Layer

Layer thickness and air-void content significantly influence the fatigue performance of the asphalt concrete. Table 7 presents the estimated average thickness and air-void contents for each of the HVS test sections determined from asphalt concrete core samples obtained after construction. In general, greater thicknesses and lower air-void contents provide longer pavement lives, assuming all other conditions (e.g., mix design, climatic factors, etc.) remain constant. Based on this assumption, HVS sections 571 and 573 should have a shorter fatigue life than Section 569. However, in order to completely address the fatigue performance of the sections, the effect of the underlying layers must be considered because the sections were tested at different conditions of the aggregate base and subgrade.

Table 7 Air-void Content and Thickness of Asphalt Concrete Layer at HVS Test Sections

	Air-Void Content, percent		**Thickness, mm**	
Section	**Average**	**Standard Deviation**	**Average**	**Standard Deviation**
567	8.6	1.2	80.3	2.6
568	7.4	0.1	80.5	7.8
569	7.1	1.1	88.7	13.6
571	9.6	1.2	78.0	9.6
572	9.1	1.9	80.3	5.0
573	9.3	2.8	79.5	9.5

4.5.3 Surface Rutting

A summary of surface rutting data collected on the six HVS test sections is presented in Figure 37. HVS testing was continued beyond the 12.5-mm rutting failure criterion in order to provide more complete data for performance model development and calibration. The data show significant variability among the HVS tests. Sections 571 and 573 show less permanent deformation and a lower rate of rutting than the other sections. Based on the climatic and moisture content data presented, Sections 571 and 573 developed less surface rutting because they were tested when the aggregate base had lower moisture content values. Sections 567, 568, 572, and 569 experienced large rates of rutting believed to stem from plastic deformation in the aggregate base. Sections 572 and 567 had the largest rates of surface rutting. Although the average surface rutting for Section 569 was less than 6 mm, half of the sections exhibited surface rutting in the range of 12 mm.

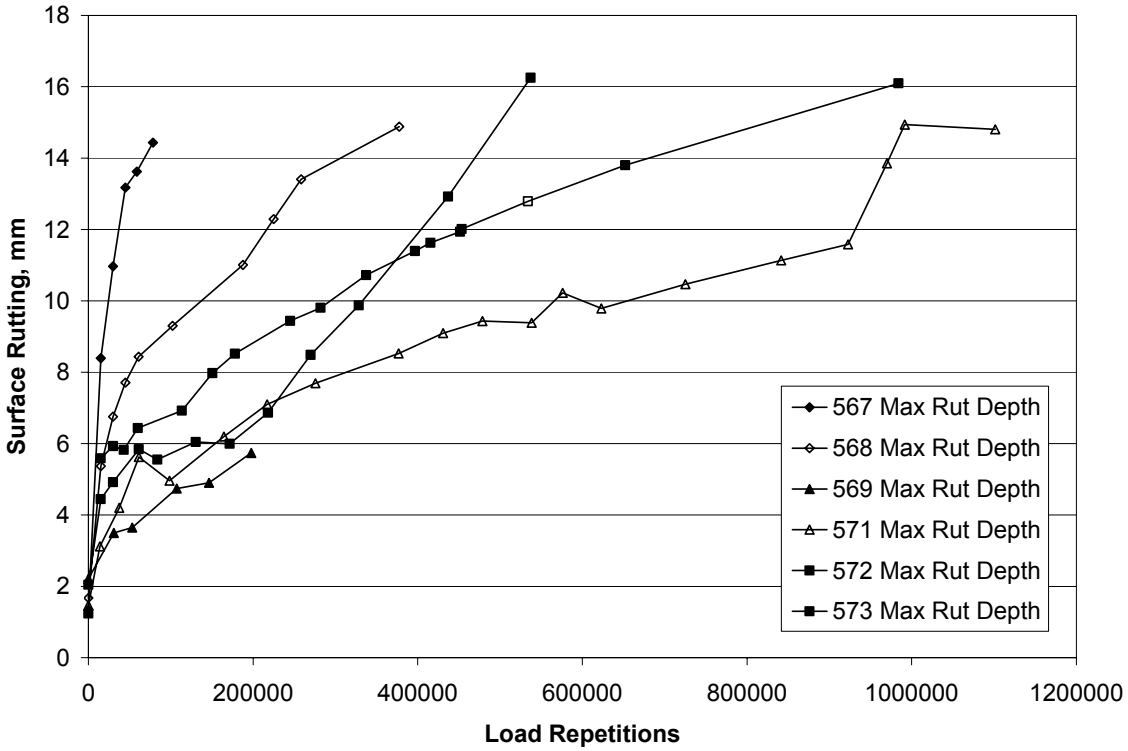

Figure 37. Summary of surface rutting performance.

4.5.4 Road Surface Deflectometer

Average surface deflections for each HVS test section measured by an RSD under a slow moving 40 kN wheel are presented in Figure 38. The trend of increasing surface deflection with higher number of load repetitions is similar to the one described for the surface rutting. Change in deflection with load repetitions is reduced for some sections. For example, for Sections 571 and 573, the deflections remain relatively constant in the range 200,000 to about 800,000 repetitions. As will be seen subsequently, this is also reflected in the crack density versus load repetitions data. For Section 571, for example, crack development occurs at a relatively slow rate up to about 800,000 repetitions and then increases, as do deflections (Figure 38).

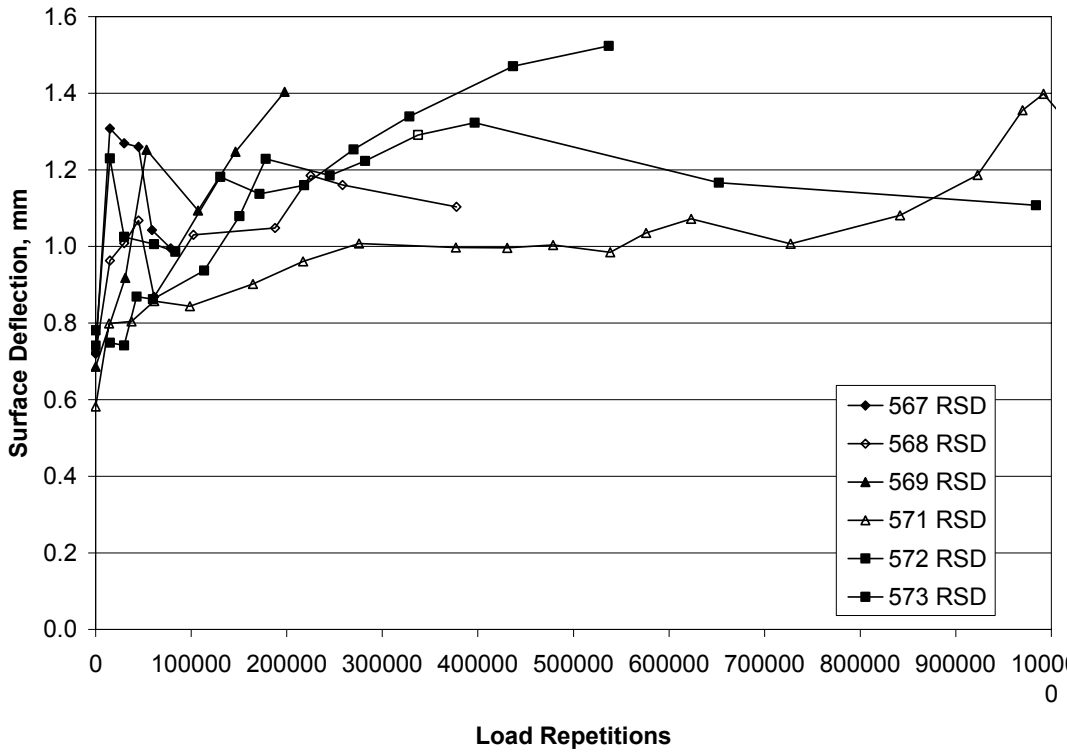

Figure 38. RSD surface deflections on HVS test sections.

4.5.5 Surface Cracking Measurements

Digital photographs of surface cracking were obtained at various time intervals during testing of each of the HVS test sections. These images were then processed to determine surface cracking at a given number of load applications. Figures 39 to 44 illustrate the surface cracks obtained at the end of HVS testing for each of the pavement sections. Surface crack patterns were different for each of the HVS sections: alligator cracks appeared in Sections 567 and 572; transverse cracks developed in Sections 568, 571, and 573; and a combination of alligator cracking, transverse cracking, and no cracking was observed in Section 569.

The type of crack pattern observed may be associated with the condition of the aggregate base and subgrade layers and is similar to patterns in surface rutting and surface deflection data. Sections 571 and 573 were tested during a dry summer season. A weaker foundation typically produces more alligator cracking as seen in the remaining test sections except for Section 568.

Figure 45 summarizes surface cracking measurements with number of load applications for each HVS test section. HVS testing was continued beyond the 2.5 m/m^2 crack density failure criterion because the rut limit had not been reached and additional data were desired for developing and calibrating performance models. Only one crack density point is shown for Sections 567, 569, and 573. The data show much lower crack density on Sections 571 and 573 than on the other sections. This observation is consistent with the drier aggregate base and subgrade when Sections 571 and 573 were tested. The effects of aggregate base and subgrade moisture conditions on the performance of the test sections conform with accepted pavement theory and practice.

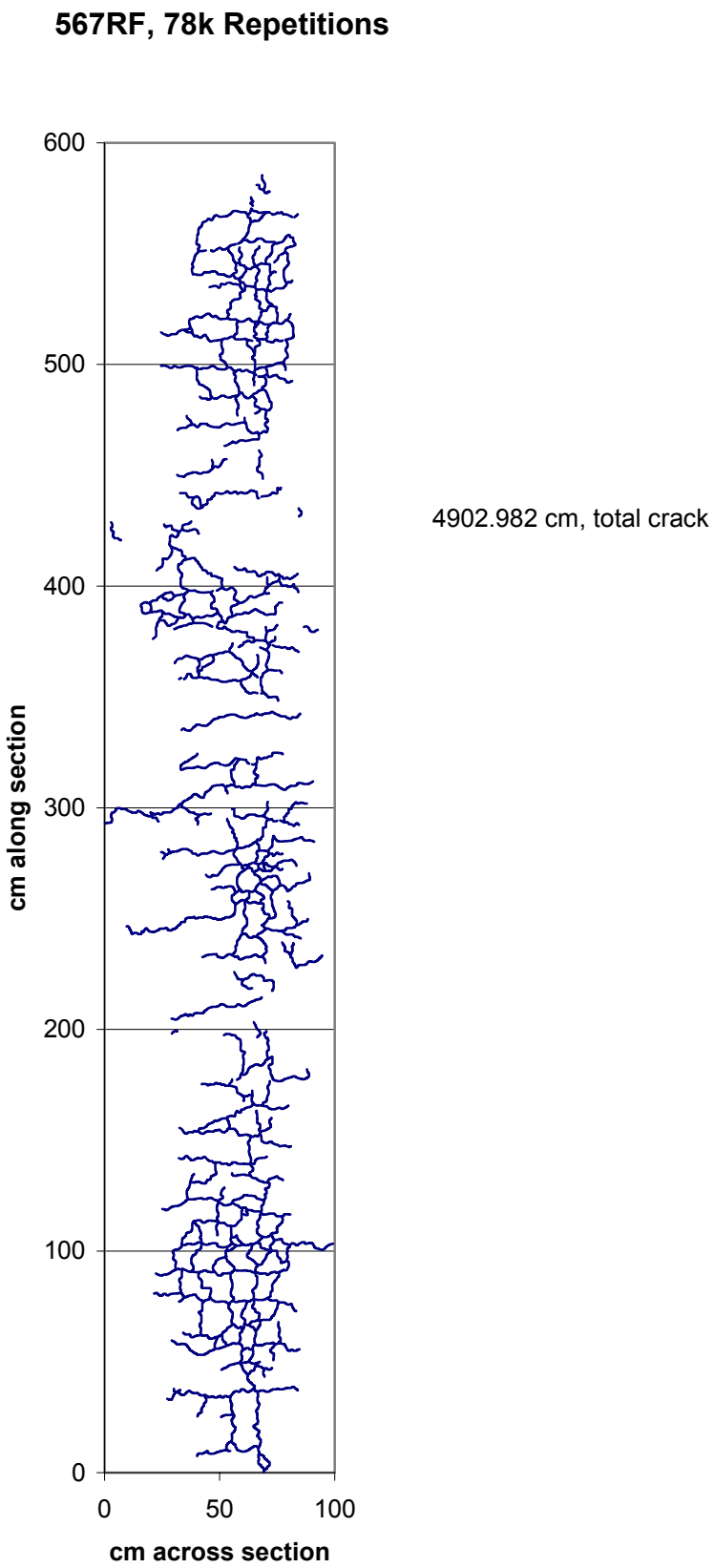

Figure 39. Crack pattern for Section 567.

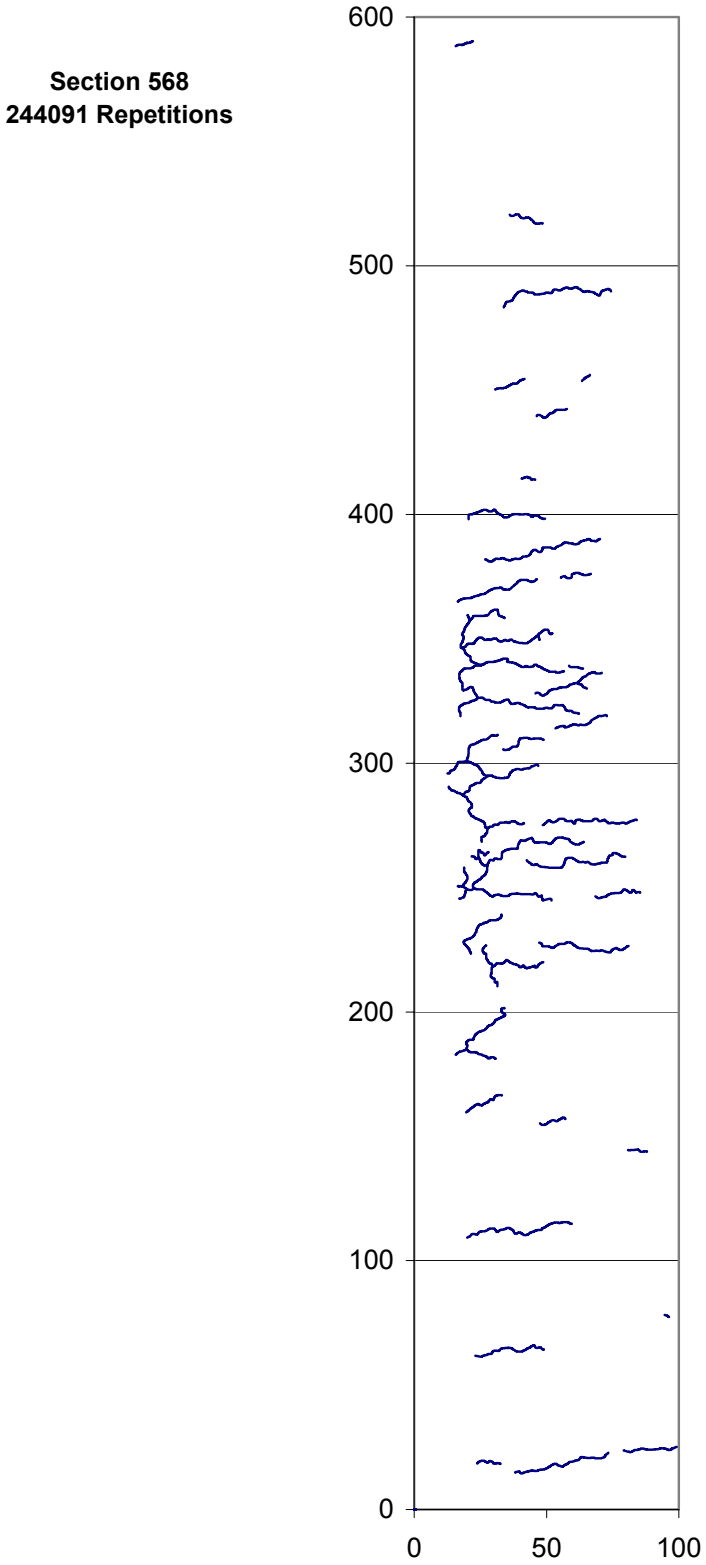

Figure 40. Crack pattern for Section 568.

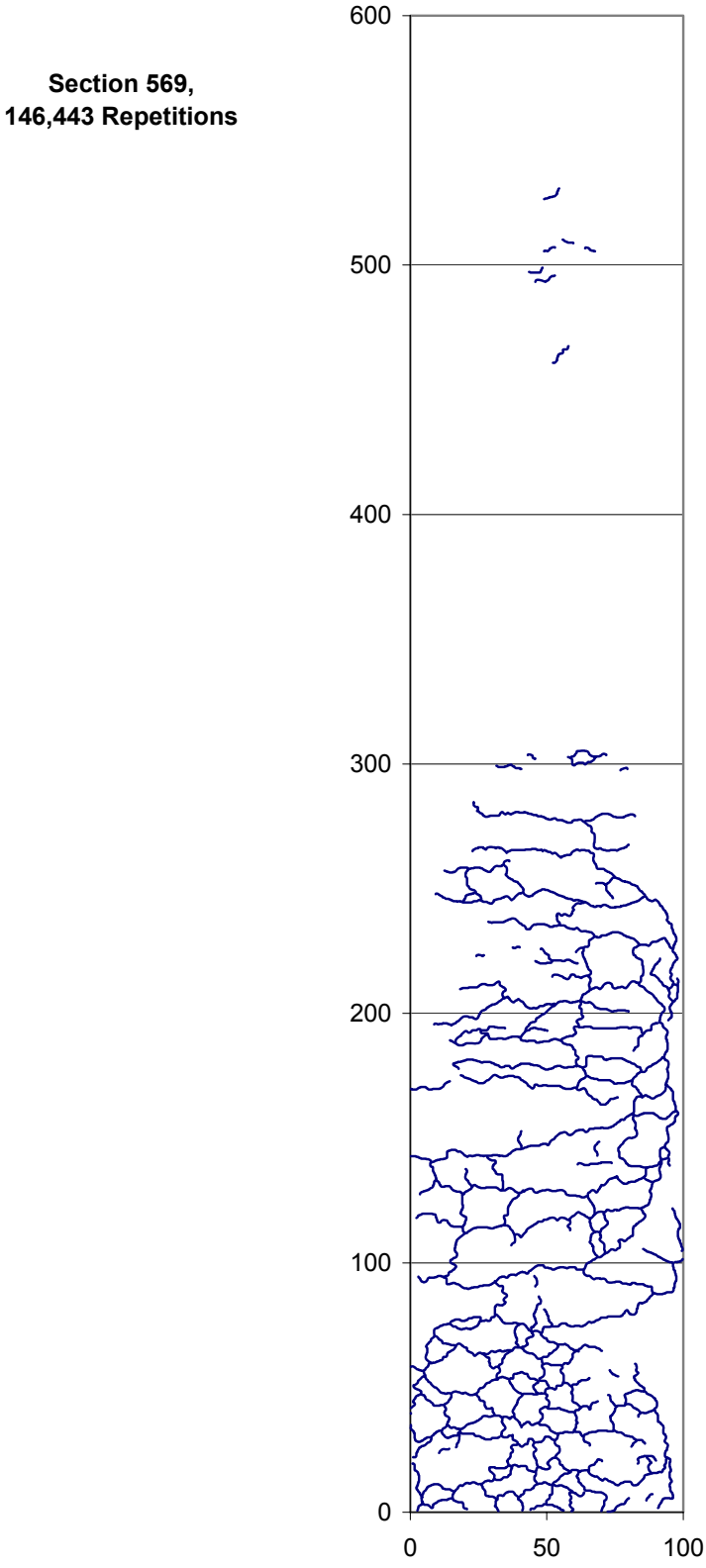

Figure 41. Crack pattern for Section 569.

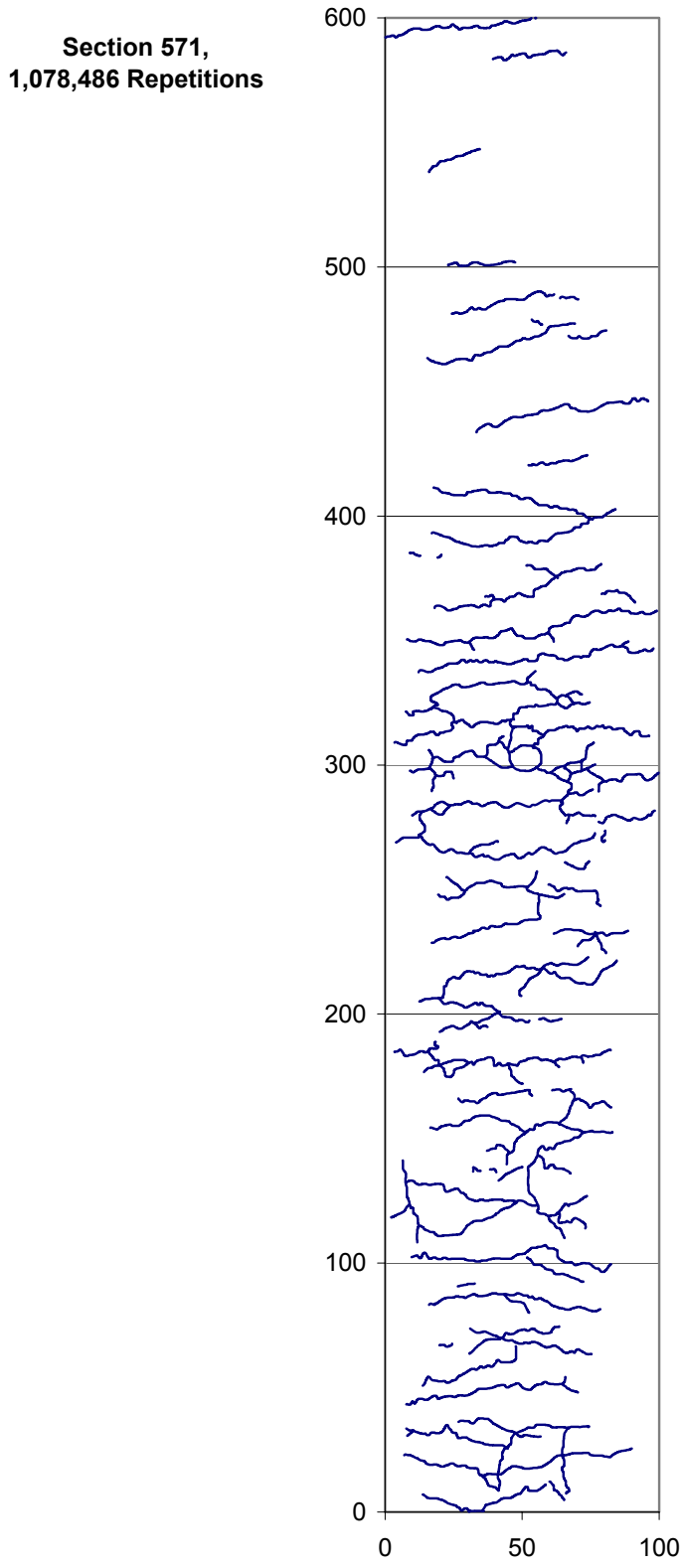

Figure 42. Crack pattern for Section 571.

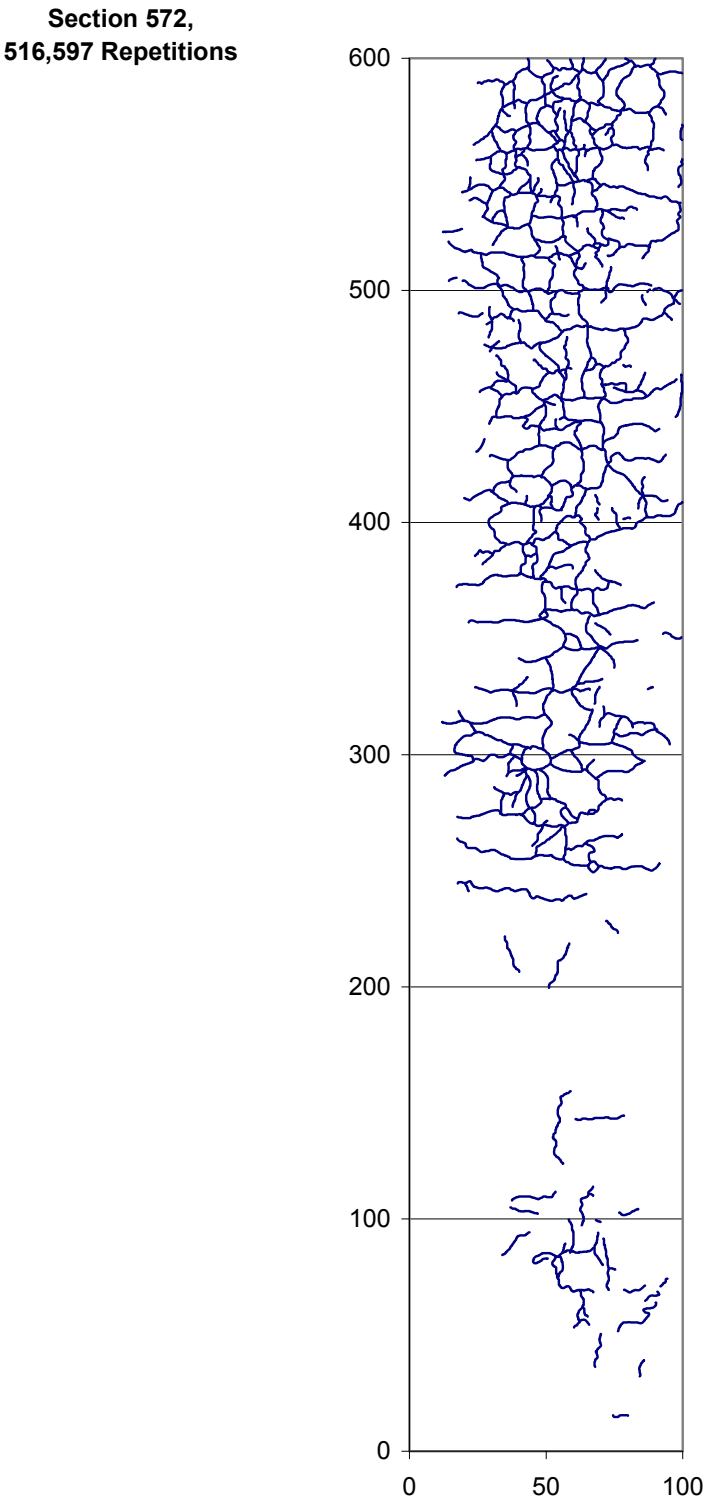

Figure 43. Crack pattern for Section 572.

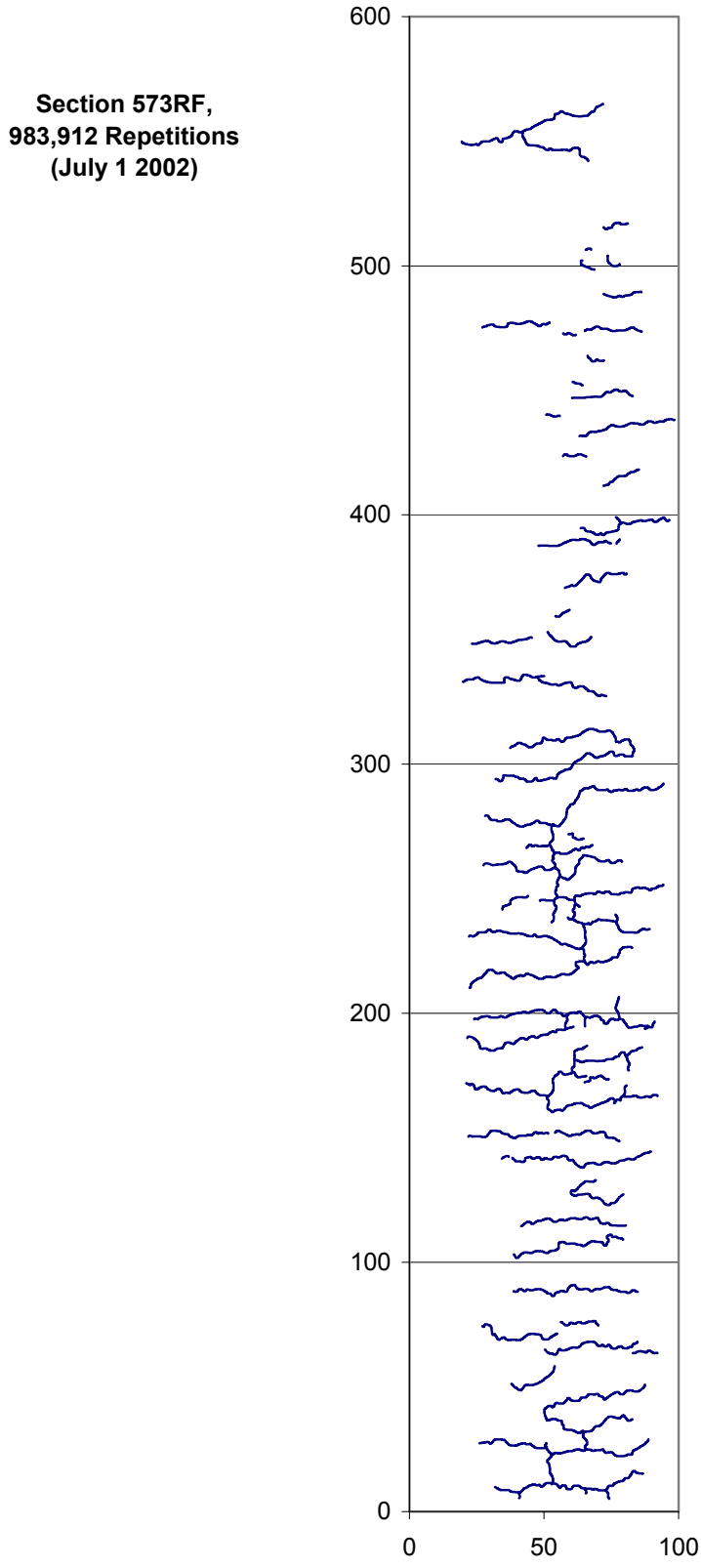

Figure 44. Crack pattern for Section 573

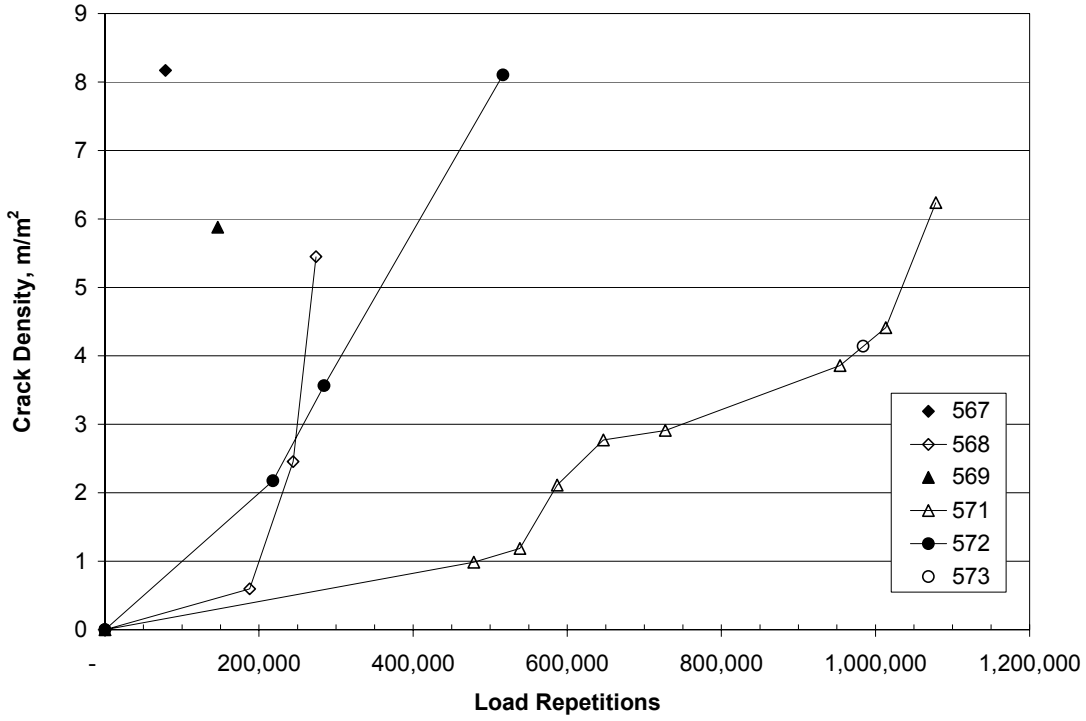

Figure 45. Surface cracking on HVS test sections.

4.5.6 FWD Testing

FWD testing was conducted on the sections before and after HVS testing to monitor changes in layer moduli. Figures 46 and 47 present modulus values back-calculated from: (1) FWD deflection data obtained from the individual test sections; and (2) the initial FWD deflection data presented in Section 5.3.4.2 and shown as "Intact" in the figures. In addition, the actual time intervals for the HVS tests are indicated in the figures. FWD testing before and after HVS testing was conducted several weeks before and after HVS tests. Modulus values for Section 567 are from FWD tests after HVS testing.

Figure 46 shows a clear reduction in asphalt concrete modulus after HVS testing for Sections 567, 568, 569, and 572 while Section 573 shows a slight reduction and Section 571 a slight increase in modulus. The reason for the increase or slight reduction in asphalt concrete

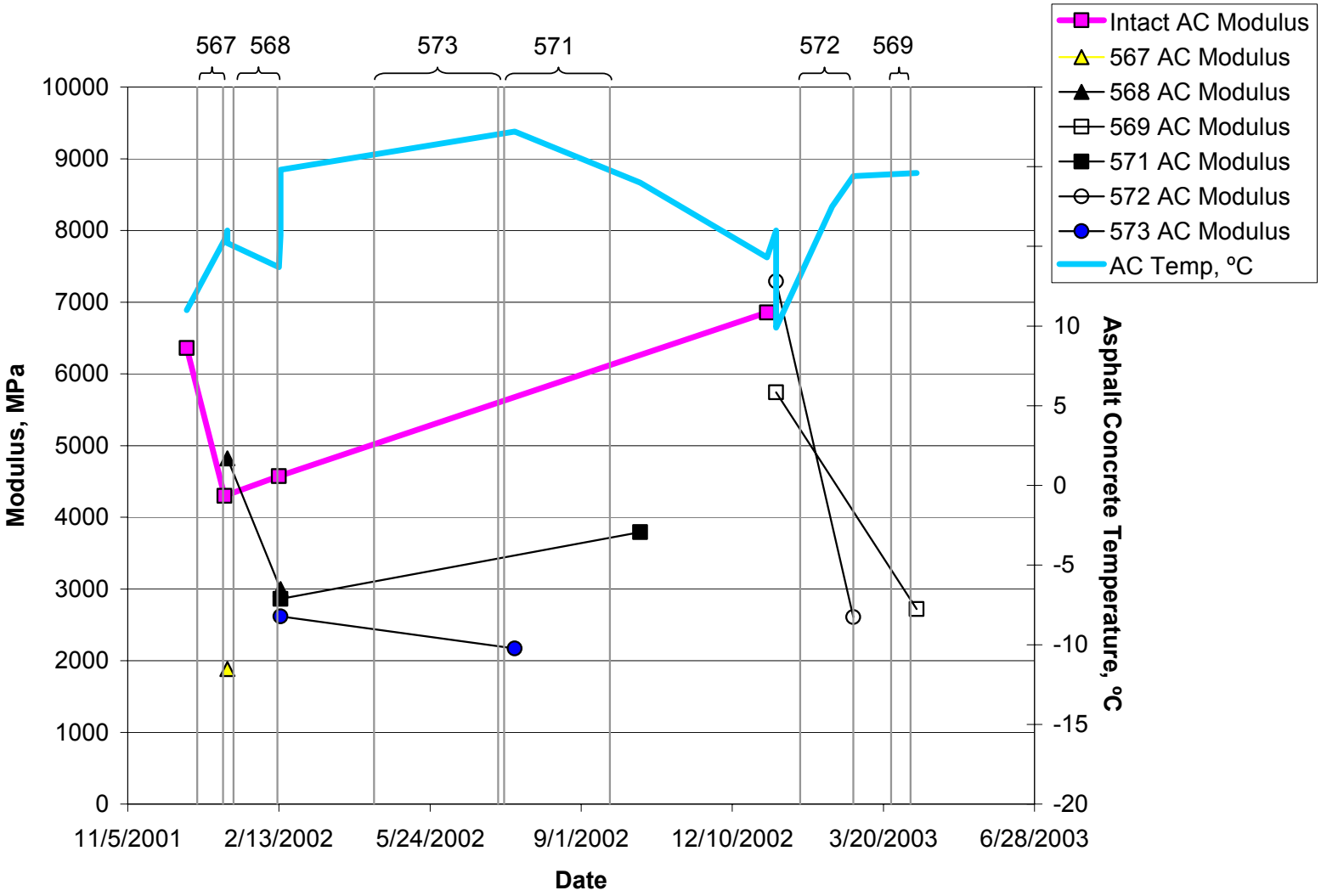

Figure 46. Back-calculated asphalt concrete moduli for HVS sections.

modulus after HVS testing is relates somewhat to the fact that the FWD test conducted after HVS testing was at a lower temperature than the one obtained before HVS testing. Data interpretation must account for these variations. Asphalt concrete modulus values were in the range of 4000 to 7000 MPa before HVS testing depending on temperature and from 2000 MPa to 4000 MPa after HVS testing. The performance measures described eaerlier realte reasonably to these changes.

Modulus values for aggregate base are shown in Figure 47. The data show a clear reduction in aggregate base modulus over time for all sections. Aggregate base modulus values were in the range of 500 MPa to 1100 MPa before HVS testing and between 100 MPa to 300 MPa after HVS testing. The agreement between intact modulus and modulus before HVS testing for each of the sections appeared reasonable.

Modulus reductions for subgrade are not as significant as those for the asphalt concrete and aggregate base layers; such variations in modulus can be due to changes in moisture content as seen in Figure 36.

Results for the aggregate base are less certain. FWD testing indicated higher modulus during the wet-cold periods, which may imply better resistance to deformation. However, sections tested by the HVS during wet-cold periods failed faster than those tested during the dry-warm periods. These results suggest care must be exercised in using such values to estimate performance since moisture content significantly affects asphalt concrete pavement behavior.

4.5.7 Summary of Performance Data and Overlay Design

Table 8 summarizes performance data for the pavement sections tested with the HVS. Data are shown in chronological order of HVS testing. Table 8 also presents an overlay design based on RSD and FWD deflections.

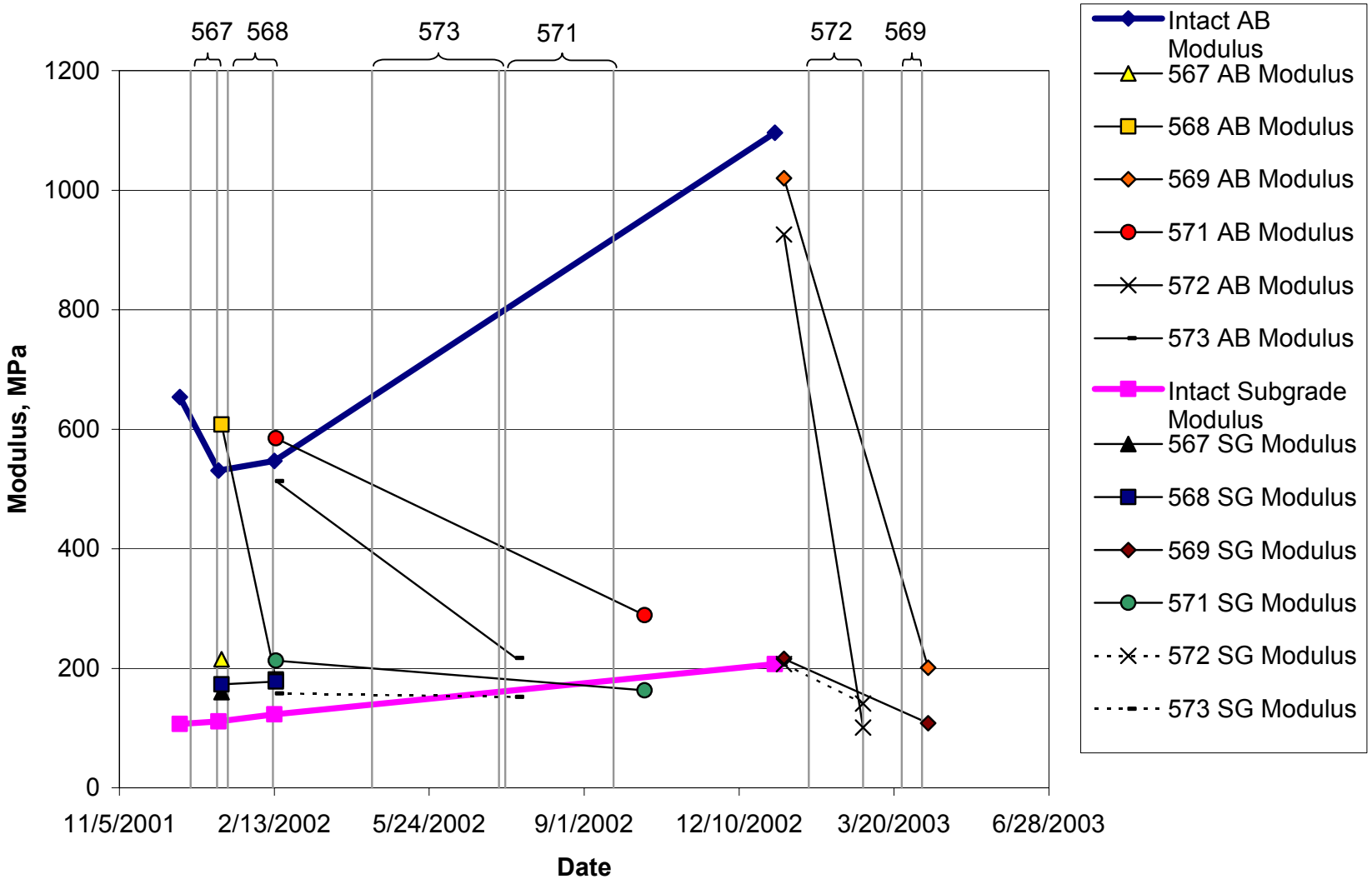

Figure 47. Back-calculated aggregate base and subgrade moduli for HVS sections.

Table 8 Summary of Performance Data and Overlay Design

	Test Section					
	567	**568**	**573**	**571**	**572**	**569**
	Thickness, mm					
Design AC	90	90	90	90	90	90
Design AB	410	410	410	410	410	410
As-built AC	80	80	80	78	80	89
As-built AB	352	349	337	352	349	337
	Traffic					
TI	7	7	7	7	7	7
	HVS Testing					
Start Date	12/21/2001	1/14/2002	4/17/2002	7/12/2002	1/24/2003	3/25/2003
Target AC Temperature, ºC	20	20	20	20	20	20
AB Condition	Wet	Wet	Dry	Dry	Wet	Wet
Load, kN	40	40	40	40	40	40
No. Reps	78500	377556	983982	969897	328416	197782
ESALs						
HVS Trafficking	Completed	Completed	Completed	Completed	Completed	Completed
	Performance					
Failure Mode	Fatigue & Rutting	Fatigue & Rutting	Fatigue & Rutting	Fatigue & Rutting	Fatigue	Fatigue
Cracking Denisty, m/m^2	8.1	5.5	4.1	6.2	8.1	5.9
Final Rut Depth, mm	13.7	14.2	15.3	14.1	8.8	3.8
	RSD Deflection & Overlay Design					
Measurement Date	1/7/2002	2/12/2002	7/8/2002	9/20/2002	2/28/2003	4/7/2003
Temperature, ºC	20	20	20	20	20	20
Load, kN	40	40	40	40	40	40
Average Deflection, mm	1.12	1.18	1.24	1.10	1.37	1.40
80 percentile, mm	1.16	1.22	1.28	1.21	1.42	1.89
80 percentile mils	45.8	48.0	50.5	47.6	55.9	74.4
Tolerable Deflection, mils	27.88	27.76	28.06	27.62	27.88	25.36
Percent to reach	39.1	42.1	44.4	41.9	50.1	65.9
Increase in GE, ft.	0.402	0.462	0.518	0.458	0.633	0.978
OL Thickness, ft.	0.21	0.24	0.27	0.24	0.33	0.51
OL Thickness, mm	64.5	74.1	83.1	73.5	101.5	156.9
OL Design: Full Depth, mm						
OL Design: ½ thickness, mm						
	FWD Deflections & OL Design					
80 percentile, mm	0.211	0.237	0.323	0.39	0.622	0.586
80 percentile, mils	8.3	9.3	12.7	15.4	24.5	23.1
Tolerable Deflection, mils	27.88	27.76	28.06	27.62	27.88	25.36
Percent to reach	0.0	0.0	0.0	0.0	0.0	0.0
Increase in GE, ft.	0	0	0	0	0	0
OL Thickness	Half thickness of existing AC 40 to 45 mm (Reflective Cracking Controls)					
OL Thickness, mm						

In summary, the ranking of HVS sections from worst to best performance is 567, 569, 572, 568, 571, and 573. The performance of the sections appears significantly influenced by the behavior of the aggregate base under conditions of high and low moisture content. Sections 571 and 573 were tested when the aggregate base was at lower moisture content than the other pavement sections. These sections showed less permanent deformation and less surface cracking than the other test sections. Overlay designs were developed after HVS testing and evaluation of surface deflections.

5.0 CONCLUSIONS

The construction, preliminary field and laboratory data, and accelerated pavement tests reveal several issues regarding the performance evaluation of asphalt concrete pavement cross section tested under the HVS.

During the construction process the following was observed and should be addressed by Caltrans.

1. Proper compaction of the subgrade and aggregate base layers is primarily affected by the water content in these layers. Current Caltrans specifications for subgrade and aggregate base compaction do not explicitly address this issue, and water content during compaction is left for the field engineer to decide. Water content based on optimum moisture content to reach the maximum wet density according to Caltrans specifications would produce a base/soil too wet to compact. Performance of the unbound layers can be detrimental if this issue is not addressed properly.
2. The compaction of the aggregate base layer is significantly affected by the support provided by the subgrade. Data indicated that low aggregate base moduli were obtained in locations where low subgrade moduli were observed.
3. The asphalt concrete layer has a significant effect on the behavior of the aggregate base and subgrade. In general, the asphalt concrete provided a confining pressure that increased the modulus of the aggregate base. In addition, it provided additional cover to the subgrade by reducing the subgrade vertical stresses which in turns increasing the subgrade modulus.

From the HWD and HVS tests the following can be concluded:

1. Modulus of the asphalt concrete was significantly affected by the asphalt concrete temperature. In general lower moduli were obtained during the hot summer months, and higher moduli during the cold winter months.
2. The performance of the HVS test sections was significantly influenced by the behavior of the aggregate base. Test sections that were tested during the dry months lasted longer both in fatigue and surface rutting than the test sections tested during the wet months.
3. Air-void contents and thicknesses were similar for the test sections; therefore, the effect of these variables could not be addressed.
4. FWD and HVS testing indicated that the modulus of the aggregate base can not be used as an indicator of aggregate base performance. Aggregate base moduli were higher during the cold/wet months but decreased rapidly when tested under the HVS. The aggregate base moduli of the sections during the dry/warm months were lower than those during the cold/wet months, but the sections tested during the dry period had longer pavement lives.

6.0 REFERENCES

1. California Department of Transportation. *Highway Design Manual.* Section 600. Sacramento, 1991.

2. Bejarano, M.O. *Subgrade Soil Evaluation for the Design of Airport Flexible Pavements.* Ph.D. Thesis, University of Illinois, Urbana, IL. 1999.

3. California Department of Transportation. *California Test Methods.* Division of Engineering Services. https://www.dot.ca.gov/hq/esc/ctms/

4. California Department of Transportation. *Construction Manual*. Division of Construction. http://www.dot.ca.gov/hq/construc/manual2001/

5. Dynatest, Inc. *ELMOD 5.0*. Software program. Dynatest International, Denmark.

6. Harvey, J.T. et al. *Initial Cal/Apt Program: Site Information, Test Pavements Construction, Pavement Materials Characterizations, Initial CAL/HVS Test Results, and Performance Estimates*. Pavement Research Center, Institute of Transportation Studies, University of California, Berkeley. 1996.

7. AASTHO T-166. AASHTO. "Bulk Specific Gravity of Compacted Bituminous Mixtures using Saturated Surface-Dry Specimens." *Standard Specifications for Transportation Materials and Methods of Sampling and Testing, Part II Tests.* Washington, D.C., latest edition.

APPENDIX A: BID DOCUMENTATION

INVITATION TO BID

1. Introduction

Attached are plans and specifications for the construction of a research pavement test section and associated work at the University of California Berkeley Richmond Field Station, CA. The test section is 125 m (410 ft) in length with a width of 8.8 m (28.9 ft). You are invited to submit a price proposal to perform this work. The site will be available for construction activities between 1 September and 1 October 2001.

2. Site Inspection

The owner's site representative is Mr. Ed Diaz (510) 231-5750, who can be contacted with regards to the site inspection. The site inspection will be held at 10:00 am on Thursday 16 August 2001. Clean copies of plans and specifications will be available at this time. Refer to attached map for directions to the Richmond Field Station.

3. Bid Due Date

All bids are due at 12:00 noon on Monday 27 August 2001. Bids submitted after this time will not be considered.

4. Submission of Bids

Submit bids to:

N.F. Coetzee Ph. D., P.E.
Dynatest Consulting, Inc.
165 South Chestnut Street
Ventura, California 93001
Fax +1 805 648-2231

Subject: Site Work for HVS Study Test Job (Goal 9)

Intent of Project:

The intent of the test section is to simulate actual freeway paving. This is crucial to ensure that the tests performed on the pavement duplicate as closely as possible the effects of trafficking on in-service pavements.

Site Conditions:

The site is located at the University of California Berkeley Richmond Field Station, at 1353 South 46th Street, Richmond, California. The site is located at the end of Lark Drive East of Building 280. The test section will extend along the existing Lark Drive from the intersection of Lark Drive and Avocet Way to the intersection of Lark Drive and the entrance road to Building 201 (EPA).

A line of trees is situated along the southern edge of the test section with amenities accommodated along the northern edge. Drainage is supplied in the form of drainage ditches along each shoulder, draining towards Building 280. A protected grassland extends the entire length of the test section and is situated approximately 15 m from the northern shoulder of Lark Drive.

Access to the Field Station is through the gate on Regatta Boulevard at the northwest corner of the Field Station. Access to the Field Station as well as the location of the construction site is illustrated in the attached figures.

Test Section Provisions

1. The test section will be constructed according to the description provided below. All work shall conform to the 1999 edition of the standard plans and specifications of the State of California Department of Transportation (Caltrans), except as modified or supplemented by the provisions included within this document.
2. Contractor shall remove existing AC and AB from the existing road. The AC and AB will be off-hauled.
3. Contractor shall rip and recompact the existing subgrade to the design elevation and grade. The subgrade will be graded with a uniform cross slope of 2% across the entire width of the road. The elevation graded shall be as given in the attached figures. Compaction shall be to standard Caltrans Specifications. Cut and fill may be required to maintain elevation and cross slope. Excess material shall be off-hauled. Full compensation shall be considered as included in various items of work and no additional payment allowed.
4. Unsuitable material encountered below the designated subgrade grade-line shall be excavated and off-hauled as directed by the owner. Unsuitable material is defined as per section 19-2.02 of the standard specifications, and includes any existing AB encountered in the existing pavement structure. Excavated areas shall be replaced with excess subgrade, graded and compacted to standard specifications. Full compensation for furnishing all labor, equipment, materials, tools, and other costs and items necessary shall be considered included in the unit cost paid for excavation and replacement of all unsuitable material below the designated subgrade grade-line.
5. Contractor shall construct drainage ditches along the edge of the southern and northern shoulders. The drainage ditches will be constructed using existing in-situ material. The existing 150 mm ∅ drainage pipe of length 12 m will be replaced with a 300 mm ∅ drainage pipe with a length of 12 m. Compaction in the vicinity of the new 300 mm ∅ drainage pipe shall be to Caltrans specifications
6. The contractor shall furnish and place Class 2AB. The compacted AB shall have a uniform thickness per standard specifications and shall maintain a 2% cross slope across the full width of the section and a longitudinal slope of 0.15 % as given in the attached figures.

   Compacted lift thicknesses for AB shall be as follows:

Lift 1: 150 mm
Lift 2: 150 mm
Lift 3: 110 mm

7. Compaction requirements are as specified in the Caltrans standard specifications.

8. All grading shall be completed with electronic control (i.e. laser/ cross slope stringline/ cross slope).

9. Contractor shall apply a prime coating to the AB at least 24 hours prior to paving. Application rate of the prime coat shall be 1.15 *L* per square meter.

10. Contractor shall pave dense graded asphalt concrete (DGAC) in two passes maintaining the 2% cross slope of the AB and the longitudinal grading of the AB across the full width and length of the test section. The asphalt mat width for any pass shall not be less than 3.53 m and not more than 3.67 m

11. The DGAC shall be compacted in two layers, each of 45 mm compacted thickness.

12. An asphaltic emulsion tack coat will be applied to the DGAC between lifts. The application rate of the tack coat is specified as 0.3 *L* (residual asphalt) per square meter of surface covered. The second DGAC lift shall not be applied until the asphaltic emulsion has broken. AR-4000 asphalt cement can be substituted for emulsion and, if substituted, shall be applied at 0.3 *L* per square meter of surface covered.

13. Contractor shall furnish dense graded asphalt concrete (DGAC) meeting Caltrans specifications for 19 mm maximum, medium grading, Type A dense graded asphalt concrete, with AR-4000 binder. The contractor must provide a copy of the Caltrans certified mix design (less than one year old) and have it approved by owner at least 3 days prior to paving.

14. Compaction of the DGAC shall not be as specified in the standard specifications. Compaction is specified in terms of Maximum Theoretical Relative Density (MTRD), AASHTO Method T209. The MTRD of the compacted DGAC shall be between 92% and 95% MTRD. The MTRD of the DGAC to be used shall be tested by the UC-Berkeley Pavement Research Center if the MTRD test results are not available for the chosen mix. If the MTRD results are not available a DGAC sample of 10 kg of loose mix shall be made available to UC Berkeley by the accepted bid party 3 days prior to construction of the DGAC layer. In all other circumstances, the cost of testing the MTRD of the DGAC will be borne by the contractor.

15. Contractor shall furnish samples of subgrade, AB and DGAC for lab testing at the time of construction. Contractor shall provide subgrade (100 kg), AB (150 kg) and DGAC (150 kg) to UC-Berkeley for research testing. Sampling shall be performed during construction as arranged between owner and contractor. Containers for the samples will be supplied by the owner.

16. Contractor shall make the necessary arrangements to ensure that all paving and rolling equipment is clean of dirt and mud and will not contaminate the DGAC paving.

17. Full compensation for furnishing all labor, equipment, materials, tools and other costs and items necessary for the complete placement of the aggregate base and dense graded asphalt concrete shall be considered included in the unit cost paid for the AB and DGAC.

18. Full compensation for costs of labor, equipment, material, tools, and other costs and items incurred due to delays caused by the owner performing sampling, testing and instrumentation other than inspection testing after the completion of the AB layer, shall be considered included in the unit cost of standby time and no additional payment shall be considered. Standby time will be calculated in minimum increments of 0.25 hours. Standby time shall not be paid except between the hours of 7:00 AM and 5:00 PM, Monday through Friday, and a maximum of 4 hours standby time shall be paid for any day.

19. A penalty shall be applied for each day after 1 October needed for completion of the project. This penalty will be based on the total bid amount and will constitute 1% of the total bid amount for every day late.

20. Inspection will be performed by owners representatives, which may include UCB, Caltrans, Contra Costa County, or other staff.

21. The contractor shall have in his possession at time of construction and during the construction period general liability insurance of in excess of $1 million for each occurrence and auto insurance of in excess of $1 million for each occurrence. This insurance shall include all operations, related to the construction, that occur on the premises of the Richmond Field Station. The contractor shall need to present proof of such insurance prior to the initiation of construction. The contractor shall furthermore possess Workman's Compensation insurance for all persons he employs in completion of the construction project.

Schedule of Quantities

Description of Activity	**Estimated Quantity (unit)**	**Cost per unit**	**Total Cost**
Excavate existing AB and AC	210 m3	/m3	
Rip, grade and recompact subgrade	1056 m2	/m2	
Install drainage ditch (drainage pipe included)	250 m	/m	
Furnish and place AB	820 tons (SG = 2)	/ton	
Tack coat	900 m2	/m2	
Priming coat	900 m2	/m2	
Furnish and place DGAC	210 tons (SG = 2.5)	/ton	
		TOTAL $	

Description of Activity	Cost/ (unit)
Clearing & Grubbing	/m^2
Excavate unsuitable material	/m^3
Standby Time	/hour

Amendments to Bid

Amendment to Provision 10

Contractor shall pave dense graded asphalt concrete (DGAC) in two passes maintaining the 2% cross slope of the AB and the longitudinal grading of the AB across the full width and length of the test section. *An asphalt paver, possessing a solid extendable screed and electronic slope control, shall be used to pave the DGAC*. The asphalt mat width for any pass shall not be less than 3.53 m and not more than 3.67 m. *The contractor shall ensure that the paving of the DGAC is continuous, and simulates paving operations for highway construction.*

Additional Provision (Provision 22)

The contractor shall furnish the owner with a complete list of all equipment and machinery that shall be used during the completion of the project. This list shall be submitted by the contractor as part of the bid.


MAPQUEST
0 4mi
0 4km
Oleum
Hercules
Nitro
Pinole
Christie
Glen Frazer
Muir
Vine Hill
San Pedro Rd
Santa Venetia
Fairfax
San Rafael
Rheem
San Pablo
Pleasant Hill
Richmond
Las Juntas
Stege
El Cerrito
Kensington
Corte Madera
El Campo
Albany
Berkeley
Lafayette
Orinda
Tamalpais Valley
Sausalito
Emeryville
Moraga
Pinehurst Rd
West Oakland
Oakland
Chinatown
Atlantic Ave
580
101
1
80
24
13
242
4
©2001 MapQuest.com, Inc.; ©2001 GDT, Inc.

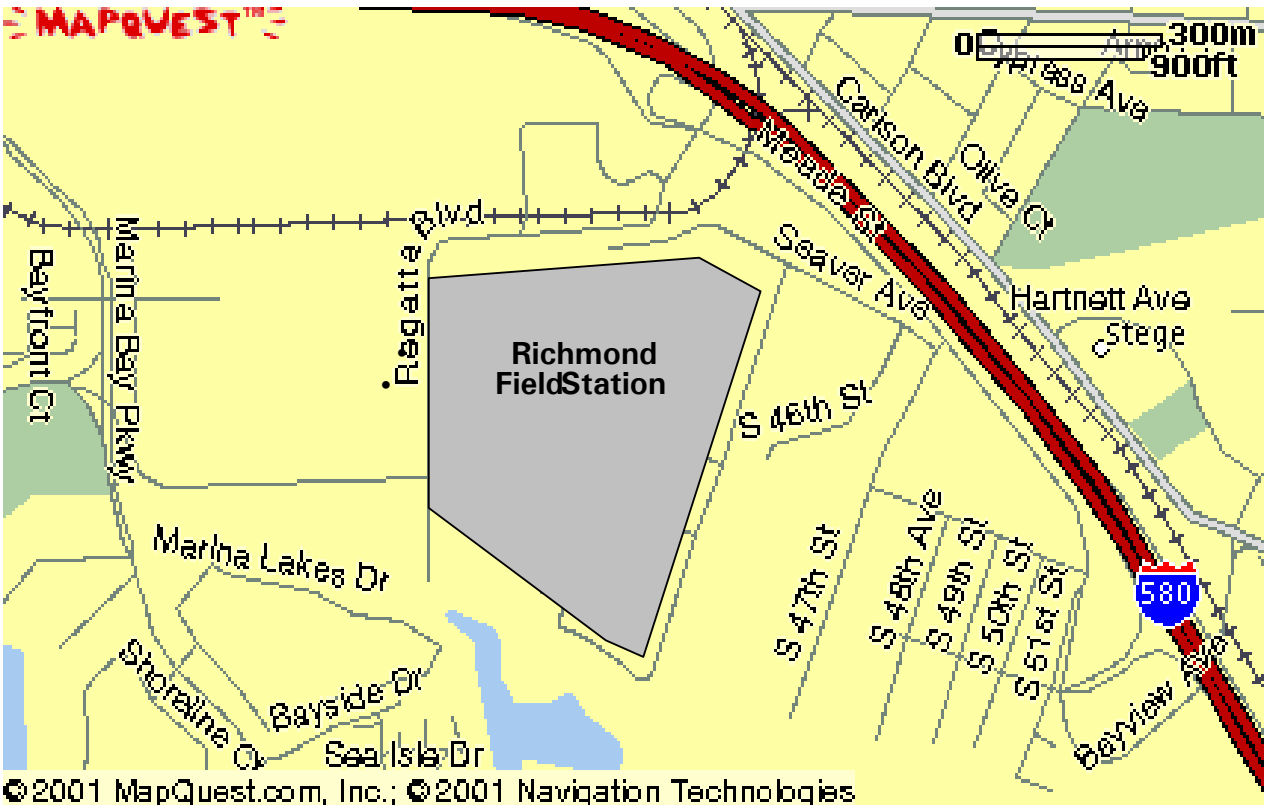
MAPQUEST
0 300m
900ft
Carlson Blvd
Olive Dr
Seaver Ave
Hartnett Ave
Stege
Regatta Blvd
Marina Bay Pkwy
Bayfront Ct
Richmond
FieldStation
S 46th St
S 47th St
S 48th Ave
S 49th St
S 50th St
S 51st St
Marina Lakes Dr
Shoreline Ct
Bayside Dr
Sea Isle Dr
Bayview Ave
580
©2001 MapQuest.com, Inc.; ©2001 Navigation Technologies

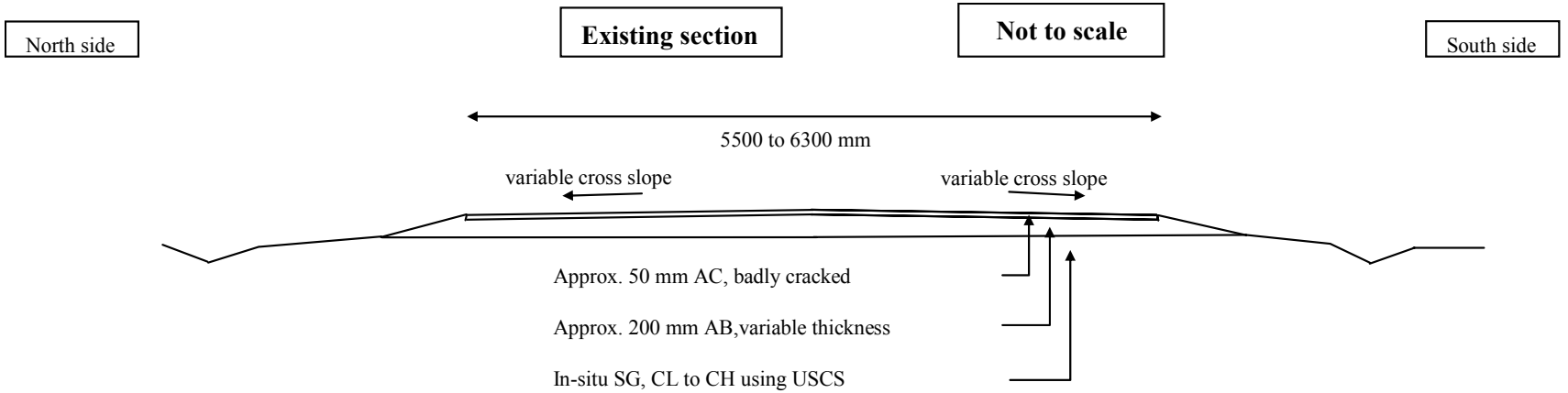
North side
Existing section
Not to scale
South side
5500 to 6300 mm
variable cross slope
variable cross slope
Approx. 50 mm AC, badly cracked
Approx. 200 mm AB,variable thickness
In-situ SG, CL to CH using USCS

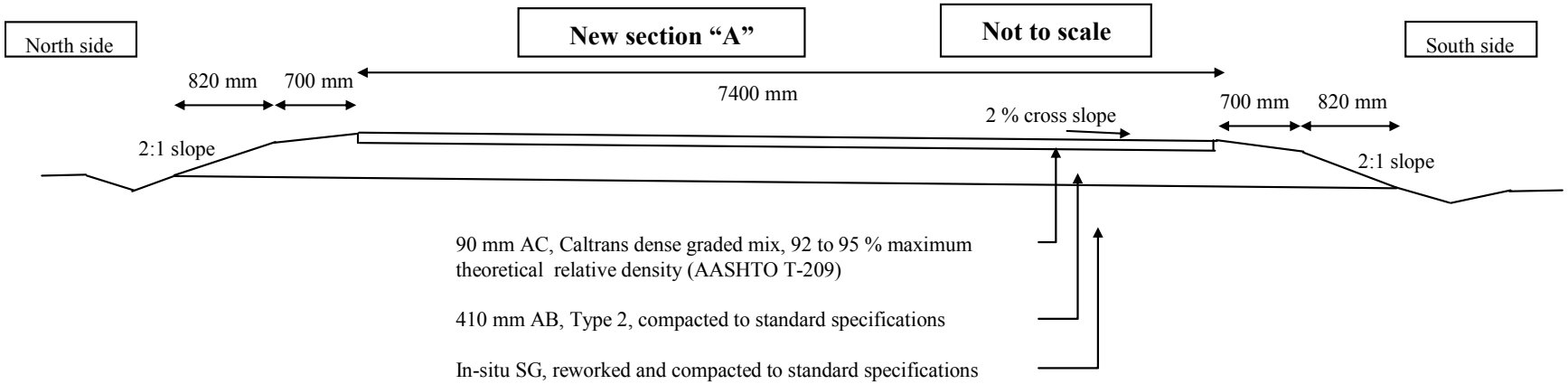
North side
New section "A"
Not to scale
South side
820 mm
700 mm
7400 mm
700 mm
820 mm
2 % cross slope
2:1 slope
2:1 slope
90 mm AC, Caltrans dense graded mix, 92 to 95 % maximum theoretical relative density (AASHTO T-209)
410 mm AB, Type 2, compacted to standard specifications
In-situ SG, reworked and compacted to standard specifications

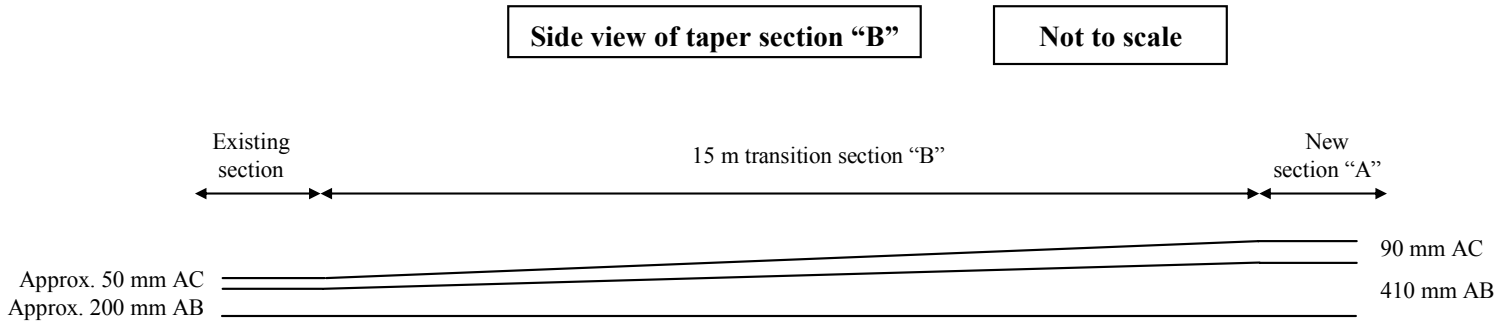
Side view of taper section "B"
Not to scale
Existing section
15 m transition section "B"
New section "A"
90 mm AC
410 mm AB
Approx. 50 mm AC
Approx. 200 mm AB

Plan view of existing conditions

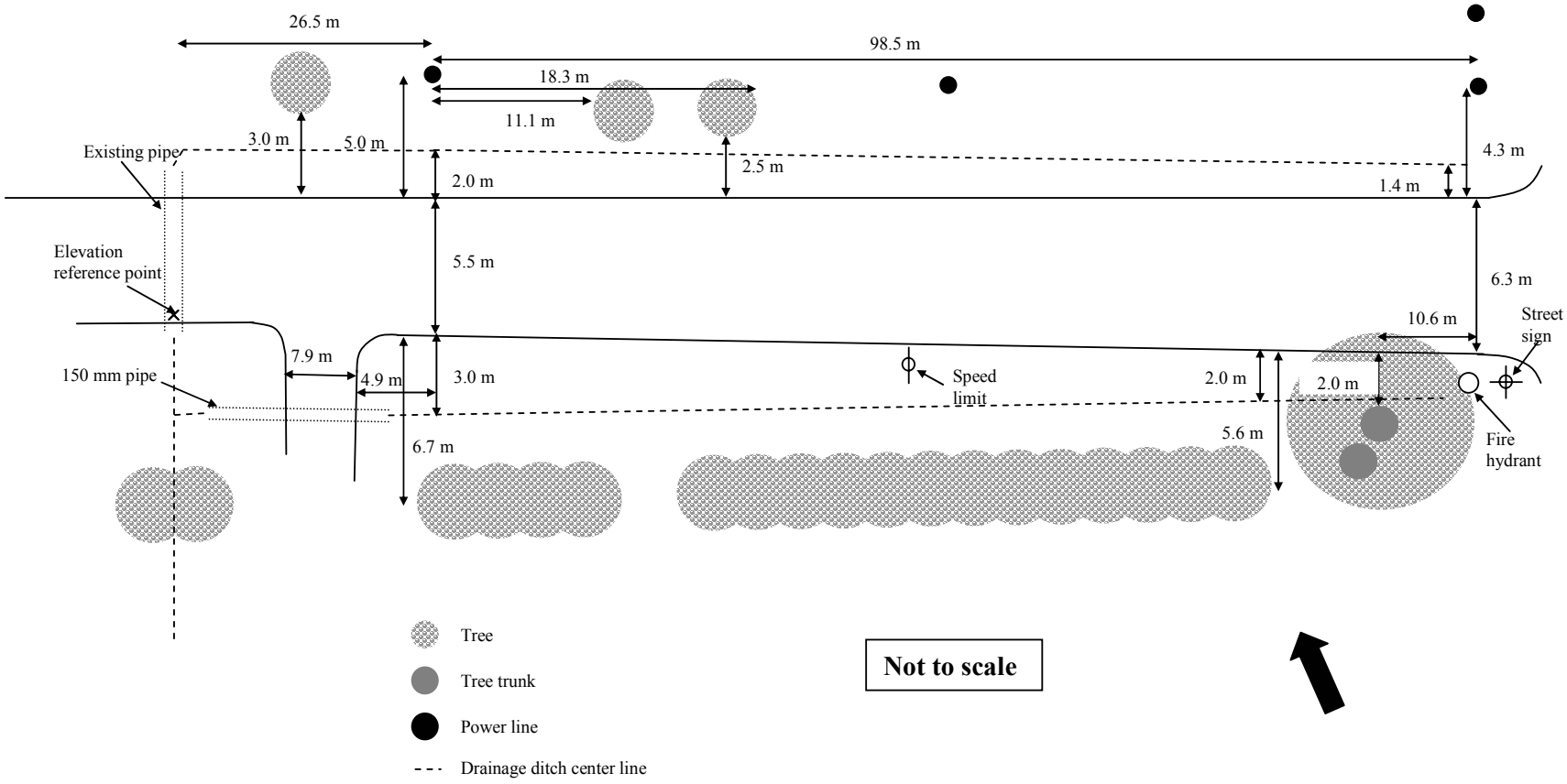

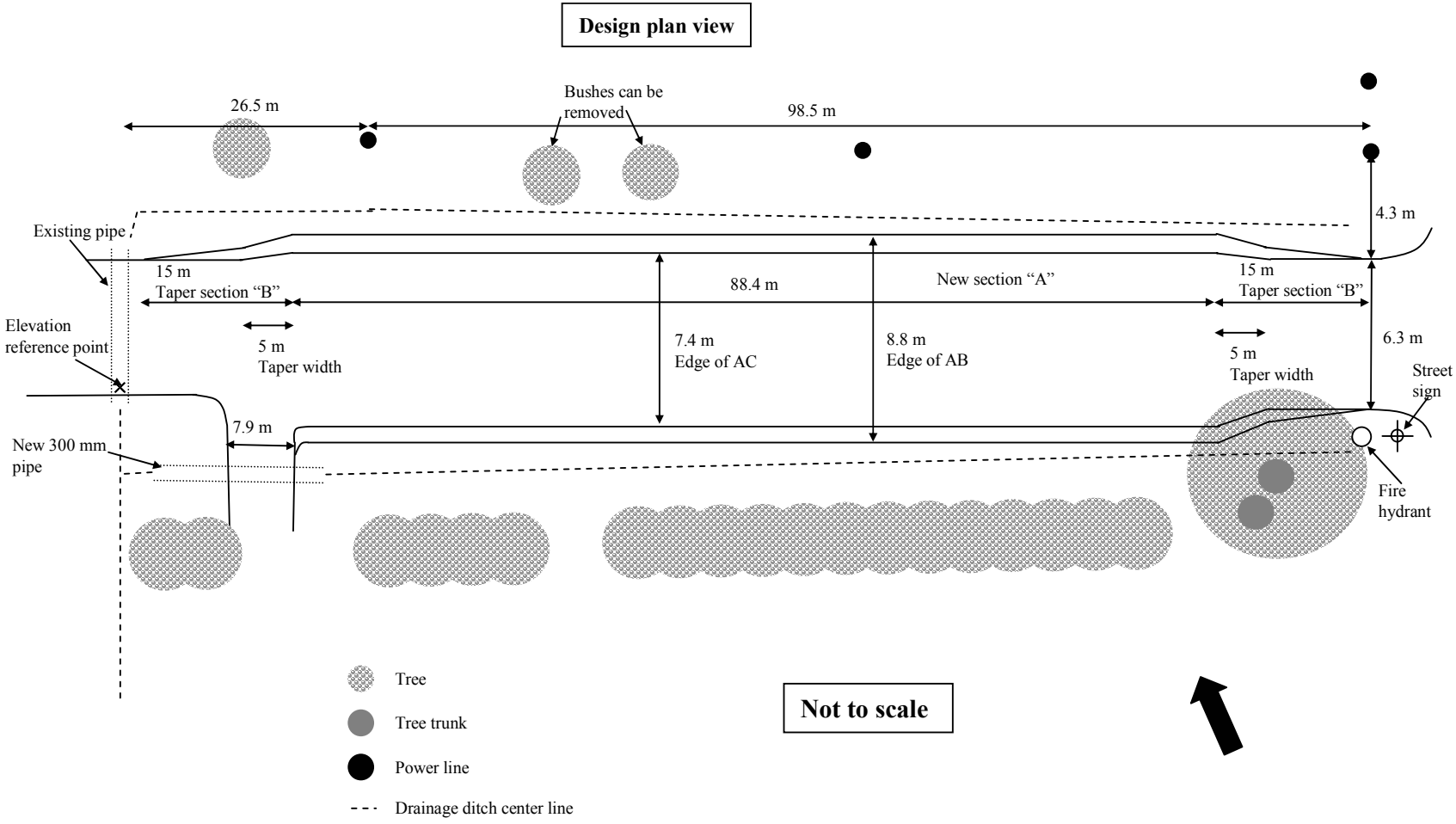
Design plan view
26.5 m
Bushes can be removed
98.5 m
4.3 m
Existing pipe
15 m
Taper section "B"
88.4 m
New section "A"
15 m
Taper section "B"
Elevation reference point
5 m
Taper width
7.4 m
Edge of AC
8.8 m
Edge of AB
5 m
Taper width
6.3 m
Street sign
7.9 m
New 300 mm pipe
Fire hydrant
Tree
Tree trunk
Power line
Drainage ditch center line
Not to scale

APPENDIX B: INSTRUMENTATION TYPES AND LOCATIONS ON TEST SECTIONS

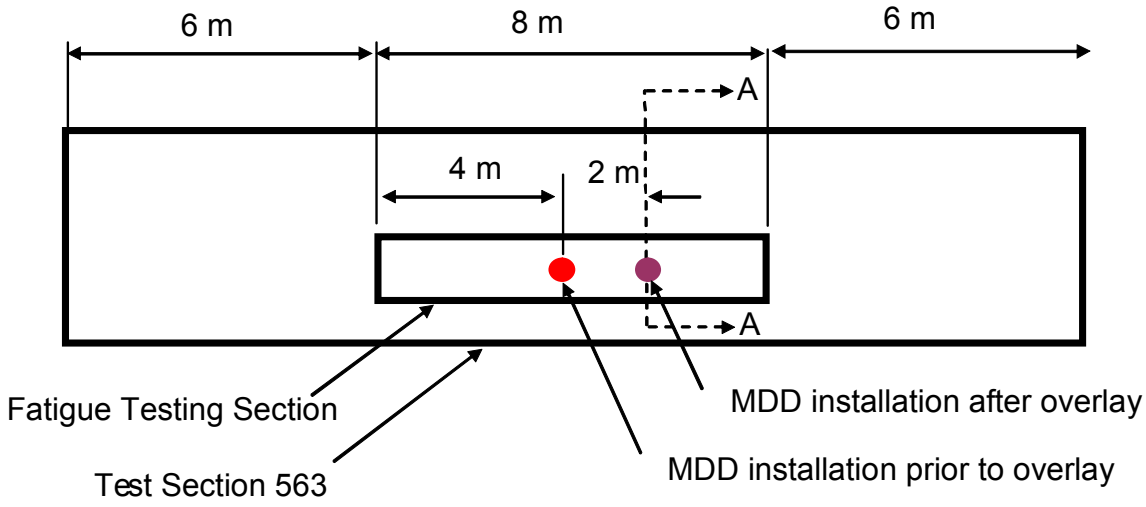

Plan View.

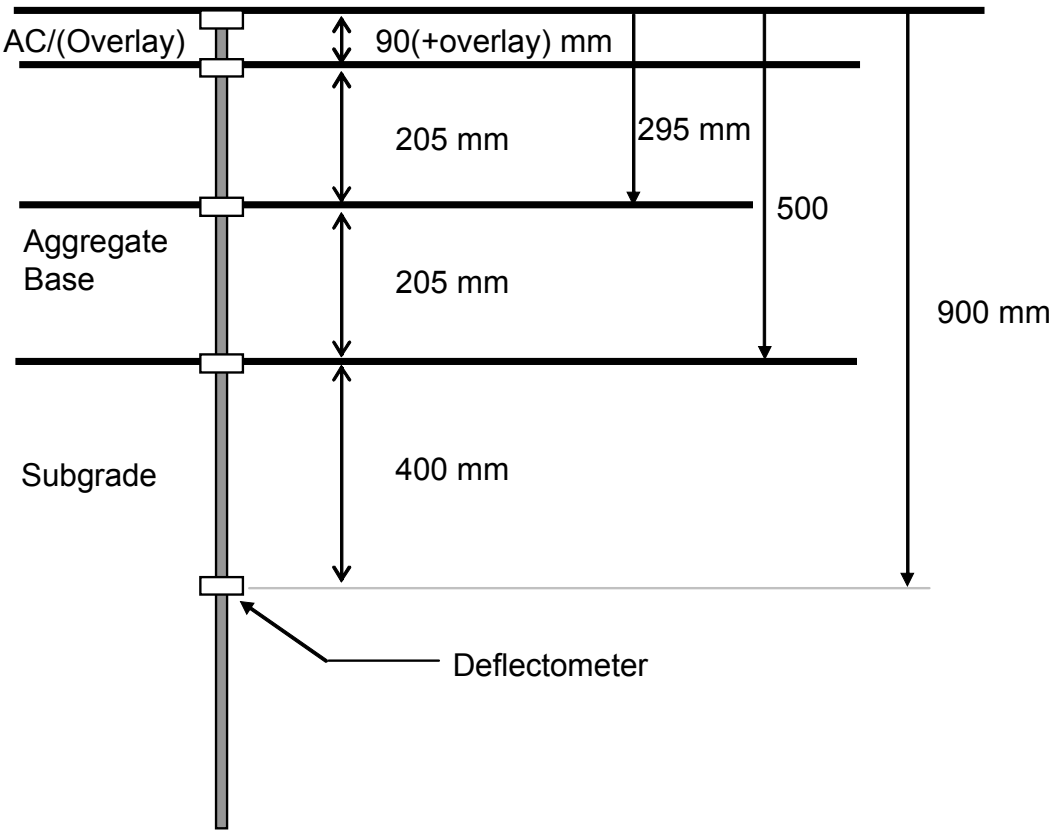

Section A-A.

Figure B1. Multi-Depth Deflectometer (MDD) placement.

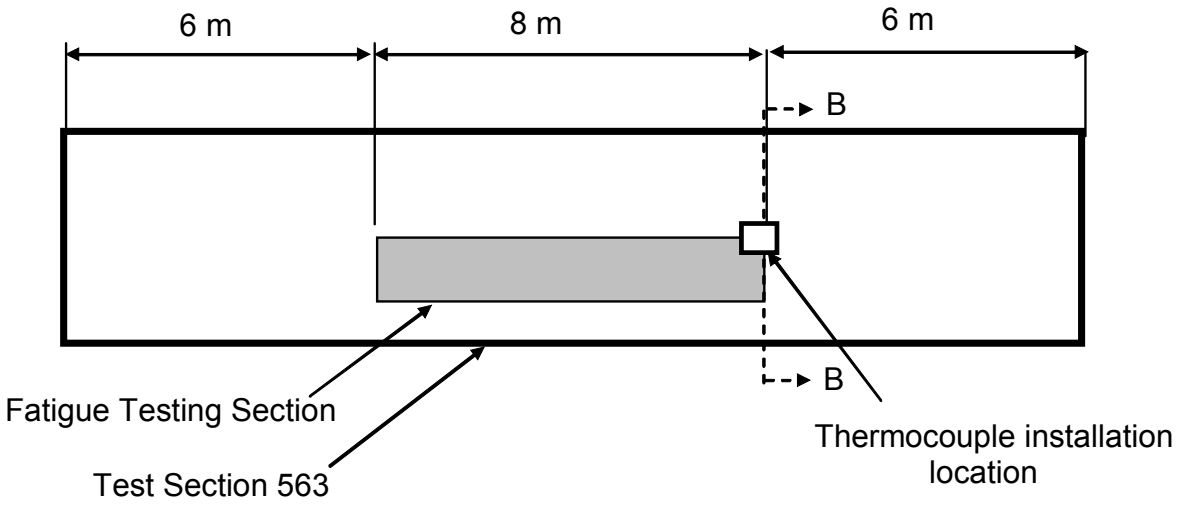

Plan View

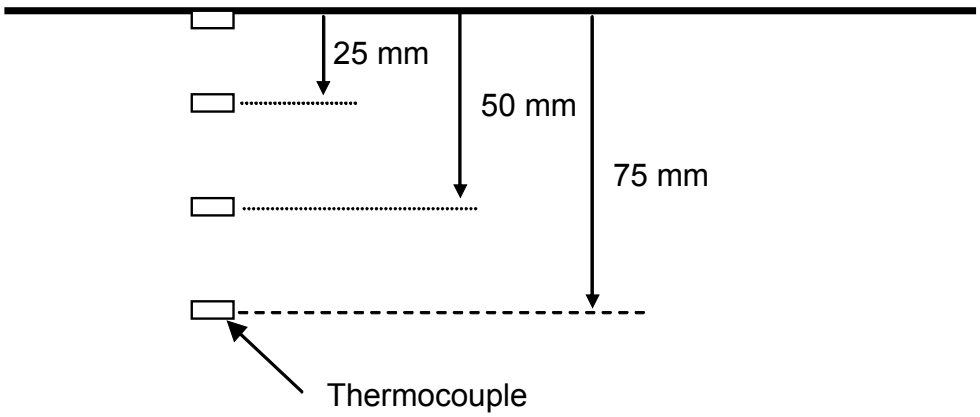

Section B-B.

Figure B2. Thermocouple placement.

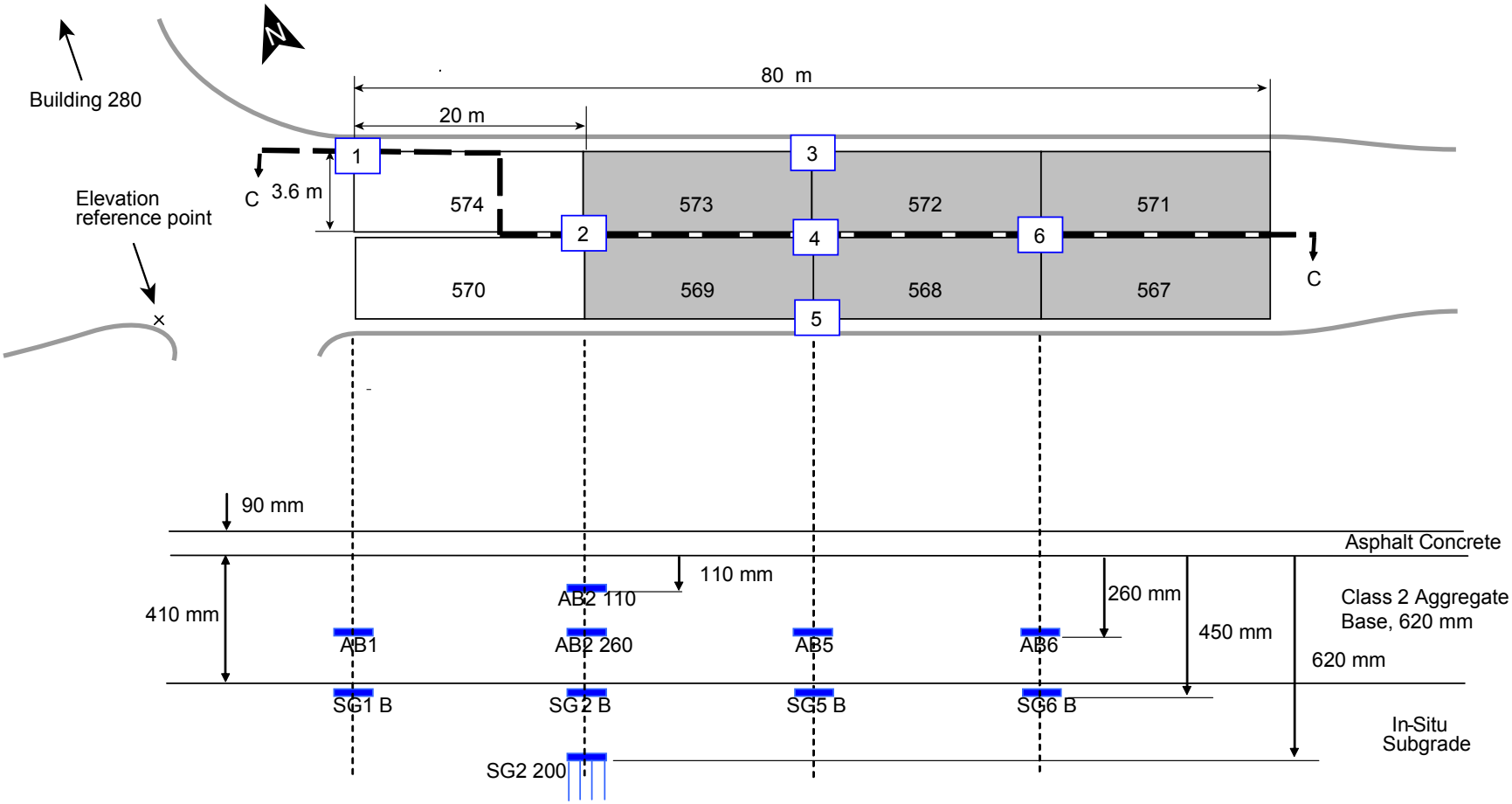

Figure B3. Time Domain Reflectometer (TDR) placement.